

INVESTIGATION OF NOVEL APPROACHES FOR THE TREATMENT OF HEAD AND NECK CANCER WITH COLD ATMOSPHERIC PLASMA

MSc by Research Thesis

Elena Alina Vochițu BSc (Hons)

December 2024

Biomedical and Life Sciences

Lancaster University

Biomedical &
Life Sciences

**Lancaster
University**



ABSTRACT

Head and neck squamous cell carcinoma (HNSCC) is an umbrella term for cancers that develop in the mucosal epithelium in the head and neck area. Current treatment options include surgical tumour removal, radiotherapy, chemotherapy, targeted therapy or immunotherapy. There is an urgent need for more effective treatments that enhance therapeutic efficacy and functional outcomes. Cold atmospheric plasma (CAP) has undergone multiple trials for applications in the medical field, including cancer treatment. We investigated the co-treatment of CAP with chemotherapeutics and DNA damage response inhibitors (DDRi) in A253 and FaDu cell lines using proliferation and spheroid growth assays and immunofluorescence. Data suggests an enhanced anti-proliferative effect on HNSCC in both 2D and 3D cultures. Our results indicate a possible synergistic effect between the combination of CAP and cisplatin or DDRi. We then progressed to testing cisplatin-loaded hydrogels as plasma-activated hydrogel therapy (PAHT). PAHT combines CAP with hydrogel material, which is made of sodium polyacrylate and poly(vinyl alcohol). It can be loaded with cationic drugs such as cisplatin and, when exposed to CAP, the hydrogel changes in ionic strength and pH, leading to the delivery of the drug deep into the tissue. The anti-proliferative effects of PAHT were measured using a cell proliferation assay and the results demonstrate that the combination led to enhanced cell death, although leakage of cisplatin from the gels in the absence of CAP was also noticed. This study demonstrates that CAP enhances the anti-proliferative effects of cisplatin and DDRi through both direct application and indirect PAHT treatment, emphasizing its potential to develop innovative therapies for HNSCC and highlighting PAHT's ability to aid in the locoregional treatment of this cancer.

ACKNOWLEDGEMENTS

This work results from the encouragement and support of many people, and I am sincerely grateful to each of them.

First and foremost, I would like to extend my deepest gratitude to Prof Sarah Allinson – for all the support she provided on the technical aspects of my work and for laying the foundation of my first experience working independently in a laboratory setting. I am a full-time overthinker and I have always struggled with impostor syndrome. Our regular Monday meetings were my weekly dose of reassurance. They have always given me the drive to keep going.

I sincerely thank Dr Panagiotis Kotsantis for providing critical feedback, thoughtful suggestions, and constant motivation throughout this research at our lab and Appraisal meetings. Their expertise and mentorship were invaluable in navigating challenges and improving the quality of this work.

I also deeply appreciate Dr. Nishtha Gaur's encouragement and assistance. I learned a lot when we worked together in the lab, and all the research I was able to conduct for this paper was due to her and Sarah's past hard work.

Charley and Ivo, our little chats at lunch and around the lab will always be a core memory for me. I will miss the long walks around campus late in the evening and quoting TikTok sounds at the most random moments. I will always remember the meetings in our BLS office and how we've struggled together with GraphPad, analysing spheroids, and the multi-channel pipette.

My best friend Michael, having coffee with you every day was, without a doubt, some sort of therapy. Thank you for always believing in me, sometimes even more than I think I have ever believed in myself.

Măriuca and Mihail – thank you for being my constants in a world full of drafts, deadlines, and caffeine.

However, this whole journey would not have been possible without my family. To my parents, you always say you are thankful for having me as your daughter. Truth is, I would not be the person I am today without you, and I am most thankful for that. To my little sister, thank you for all the calls and all the funny memes and videos you've sent me daily. The greatest gift our parents ever gave us was each other.

TABLE OF CONTENTS

Investigation of novel approaches for the treatment of head and neck cancer with cold atmospheric plasma	1
Abstract.....	2
Acknowledgements.....	3
List of Abbreviations	6
1. Introduction.....	9
1.1. Introduction to Head and Neck Squamous Cell Carcinoma.....	9
1.2. Risk factors and epidemiology.....	11
1.2.1. Tobacco use and HNSCC.....	11
1.2.2. Alcohol consumption and HNSCC.....	14
1.2.3. Human papillomavirus infection and HNSCC.....	17
1.2.4. Epidemiology and trends in incidence.....	22
1.3. Overview of Head and Neck Squamous Cell Carcinoma Development.....	24
1.3.1. DNA Damage and DNA Repair	24
1.3.2. Cancer Hallmarks and HNSCC.....	29
1.4. Diagnosis, treatments and clinical trials.....	41
1.4.1. Up-to-date diagnosis and treatment options.....	41
1.4.2. Clinical trials and cytotoxic agents.....	42
1.5. Emerging technologies: plasma-based treatments.....	45
1.5.1. Introduction to plasma	45
1.5.2. Plasma components and their role in DNA damage	49
1.5.3. Plasma pharmacokinetics: Implications for drug delivery	52
1.6. Conclusion and aims	54
2. Materials and Methods	55
2.1. Materials	55
2.1.1. Reagents	55
2.1.2. Antibodies.....	55
2.1.3. Buffers and Solutions	56
2.1.4. Spheroid Staining.....	56
2.1.5. Tissue culture.....	57
2.1.6. Cold Atmospheric Plasma Jet.....	57

2.1.7. Composite Hydrogels	58
2.2. Methods.....	59
2.2.1. Cell proliferation assay: Cisplatin and DDR inhibitors.....	59
2.2.2. Cell proliferation assay: Cold Atmospheric Plasma.....	60
2.2.3. Cell proliferation assay: Composite Hydrogels	60
2.2.4. For Immunofluorescence.....	61
2.2.5. Spheroid Treatment and Staining.....	62
2.2.6. Immunofluorescence.....	62
3. Co-treatment of HNSCC Cells with Cisplatin and Cold Atmospheric Plasma	64
3.1. Introduction.....	64
3.2. Mechanism of Action.....	66
3.3. Results and Discussion.....	69
3.3.1. Cisplatin: Cell Proliferation Assay	69
3.3.2. Cisplatin: Direct Plasma Treatment.....	71
3.3.3. Cisplatin: Immunofluorescence.....	76
3.3.4. Spheroid Testing.....	81
3.3.5. Indirect Plasma Treatment: Composite Hydrogels	89
4. Co-treatment of HNSCC cells with DNA Damage Inhibitors and Cold Atmospheric Plasma.....	94
4.1. Introduction.....	94
4.2. Inhibitors of the DNA Damage Response	102
4.3. Results and Discussion.....	108
4.3.1. Single Agent DDRi: Cell Proliferation Assay.....	108
4.3.2. DDRis in Combination with Direct Plasma Treatment	111
4.3.3. Phosphorylation of H2AX After Combination Treatment With CAP and DDRis	115
4.3.3.1. Direct CAP treatment and adavosertib (Wee1i)	117
4.3.3.2. Direct CAP treatment and olaparib (PARPi).....	123
4.3.3.3. Direct CAP treatment and ceralasertib (ATRi)	126
4.3.3.4. Direct CAP treatment and AZD1390 (ATMi)	130
5. Conclusions and Future Research.....	134
Reference List.....	140

LIST OF ABBREVIATIONS

5-FU – 5-Fluorouracil

ADH – Alcohol Dehydrogenase

AKT – Protein Kinase B

ALDH1 – Aldehyde Dehydrogenase 1

ATR – Ataxia Telangiectasia and Rad3-related

ATM – Ataxia Telangiectasia Mutated

BER – Base Excision Repair

BRCA1/2 – Breast Cancer Gene 1/2

CAP – Cold Atmospheric Plasma

CDKN2A – Cyclin Dependent Kinase Inhibitor 2A

CHK1 – Checkpoint Kinase 1

COX-2 – Cyclooxygenase-2

CPD – Cyclobutane Pyrimidine Dimer

CSMD1 – CUB and Sushi Multiple Domains 1

CT – Computed Tomography

CYP2A6 – Cytochrome P450 Family 2 Subfamily A Member 6

CYP2B6 – Cytochrome P450 Family 2 Subfamily B Member 6

DDR – DNA Damage Response

DISC – Death-Inducing Signaling Complex

DNA-PK – DNA-dependent Protein Kinase

DSB – Double-Strand Break

E2F1 – E2F Transcription Factor 1

EGF – Epidermal Growth Factor

EGFR – Epidermal Growth Factor Receptor

EMT – Epithelial-Mesenchymal Transition

ERK1/2 – Extracellular Signal-Regulated Kinases 1/2

HER1/2/3/4 – Human Epidermal Growth Factor Receptors 1/2/3/4

H2AX – H2A Histone Family Member X

H₂O₂ – Hydrogen Peroxide

HNC – Head and Neck Cancer
HNSCC – Head and Neck Squamous Cell Carcinoma
HPV – Human Papillomavirus
HR – Homologous Recombination
IF – Immunofluorescence
IR – Ionizing Radiation
KRAS – Kirsten Rat Sarcoma Viral Oncogene
MAPK – Mitogen-Activated Protein Kinase
MDM2 – Mouse Double Minute 2 Homolog
MGMT – O6-Methylguanine-DNA Methyltransferase
MMP – Matrix Metalloproteinase
MRI – Magnetic Resonance Imaging
MRN – MRE11-RAD50-NBS1 Complex
mTOR – Mechanistic Target of Rapamycin
MMR – Mismatch Repair
NHJE – Non-Homologous End Joining
NO – Nitric Oxide
NER – Nucleotide Excision Repair
NOTCH1 – Neurogenic Locus Notch Homolog Protein 1
OPSCC – Oropharyngeal Squamous Cell Carcinoma
PAA – Sodium Polyacrylate Particles
PAHT – Plasma-activated Hydrogel Therapy
PARP – Poly(ADP-ribose) Polymerase
PDK1 – 3-Phosphoinositide-dependent Protein Kinase-1
PET – Positron Emission Tomography
PI3K – Phosphatidylinositol 3-Kinase
PIKK – Phosphatidylinositol 3-Kinase-Related Kinase
PIK3CA – Phosphatidylinositol-4,5-bisphosphate 3-kinase catalytic subunit alpha
PLK1 – Polo-like Kinase 1
PTEN – Phosphatase and Tensin Homolog
PVA – Polyvinyl Alcohol
RAD51 – RAD51 Recombinase
RAR- β – Retinoic Acid Receptor Beta

RB – Retinoblastoma Protein
RNS – Reactive Nitrogen Species
RONS – Reactive Oxygen and Nitrogen Species
ROS – Reactive Oxygen Species
RPA – Replication Protein A
RTK – Receptor Tyrosine Kinase
SSB – Single-Strand Break
SSBR – Single-Strand Break Repair
STAT – Signal Transducer and Activator of Transcription
TGF- β – Transforming Growth Factor Beta
TLS – Translesion Synthesis
TP53 – Tumor Protein p53
VEGF – Vascular Endothelial Growth Factor
VLP – Virus-Like Particle
WEE1 – WEE1 G2 Checkpoint Kinase
XRCC1 – X-ray Repair Cross Complementing 1

1. INTRODUCTION

1.1. INTRODUCTION TO HEAD AND NECK SQUAMOUS CELL CARCINOMA

Head and neck squamous cell carcinoma (HNSCC) is an umbrella term for a heterogeneous group of malignancies that develop in the mucosal epithelium in the head and neck area, such as the larynx, the oral cavity (ie. floor of the mouth, lips, hard palate, buccal mucosa, anterior tongue, retromolar trigone), the oropharynx (ie. base of the tongue, soft palate, posterior pharyngeal wall, lingual tonsils, uvula and palatine tonsils), the nasopharynx, and the hypopharynx (Figure 1). HPV-associated HNSCC usually develops in the palatine and lingual tonsils of the oropharynx, while tobacco-related HNSCC mainly occurs in the larynx, the oral cavity, and the hypopharynx (Johnson et al., 2020).

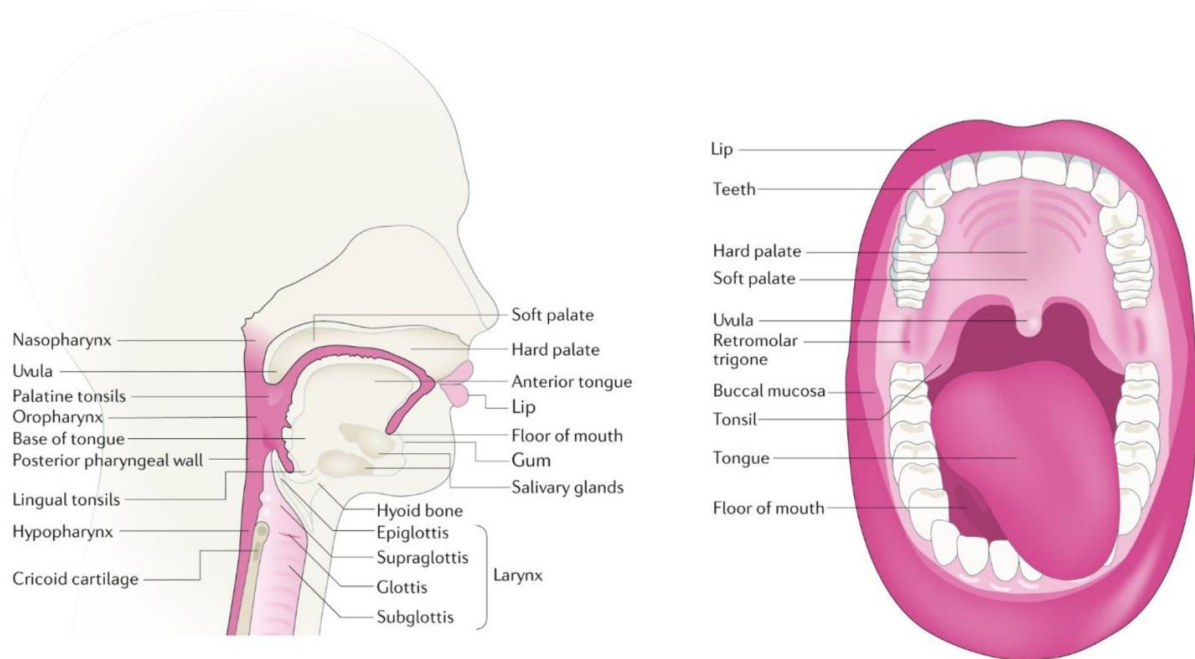


Figure 1: HNSCC anatomical sites (Johnson et al., 2020). HNSCC originates from the mucosal epithelium in various regions, including the oral cavity (e.g., tongue, floor of mouth), nasopharynx, oropharynx (e.g., tonsils, base of tongue), hypopharynx (lower throat), and larynx. The aetiology of HNSCC varies – human papillomavirus (HPV)-associated HNSCCs primarily occur in the oropharynx, while tobacco-associated HNSCCs commonly develop in the oral cavity, hypopharynx, and larynx. These distinctions highlight the influence of risk factors on the tumour's location and origin. Reprinted from Nature Reviews Disease Primers, Volume 6, Article number 92, Daniel E. Johnson et al, Head and neck squamous cell carcinoma, Copyright 2020, with permission from Springer Nature.

Oral squamous cell carcinoma (OSCC), by way of illustration, presents as a highly aggressive tumour with a prognosis that has seen minimal improvement over the past thirty years. Manifesting anywhere within the oral cavity, including the oral floor, buccal mucosa, the tongue, upper and lower gingiva, and palate, OSCC continues to pose significant challenges despite advancements in cancer detection and treatment (Sasahira and Kirita, 2018). In addition to this, OSCC of the tongue and gingiva tends to infiltrate deeper muscles and the jawbone, respectively. Moreover, due to the rich lymphatic network and numerous anastomoses in the oral cavity, OSCC frequently metastasizes to cervical lymph nodes (Raúl González-García et al., 2008). Its overall 5-year survival rate remains notably low, consistently below 50% over the past decades

(Kim et al., 2016), and it ranks among the leading causes of morbidity and mortality in regions including Central and Eastern Europe, Melanesia, and South-Central Asia (Torre et al., 2015).

1.2. RISK FACTORS AND EPIDEMIOLOGY

The main risk factors for HNSCC development are alcohol and tobacco consumption, environmental pollutants, occupational or radiation exposure, age, diet, underlying genetic predispositions (e.g. Fanconi anaemia – which leads to impaired DNA repair processes), or infections with certain viral agents such as human papillomavirus (most often type 16) and Epstein-Barr virus.

1.2.1. TOBACCO USE AND HNSCC

Globally, around 70 to 80% of HNSCC cases are linked to tobacco and alcohol use, the risk being ten times higher in smokers than in never-smokers (Khariwala, Hatsukami and Hecht, 2011). The carcinogenic agents in tobacco products, such as tobacco-specific nitrosamines (TSNA) and polycyclic aromatic hydrocarbons (PAH), can trigger adduct formations in the DNA, leading to disruptions in the DNA structure. DNA adducts form when carcinogens bind to and disrupt the double-helix structure of DNA. If not repaired, these adducts can lead to miscoding and permanent mutations, disabling tumor suppressor genes such as *TP53* and potentially activating oncogenes like *KRAS* (Khariwala, Hatsukami and Hecht, 2011).

4-(Methylnitrosamino)-1-(3-pyridyl)-1-butanone (NNK) and N-nitrosornicotine (NNN) are two well-known carcinogenic compounds found specifically in tobacco. When these compounds undergo bioactivation by phase I enzymes (such as cytochrome P450 enzymes in the liver), they become more reactive and can modify cellular macromolecules through a process called pyridyloxobutylation (Wang et al., 2019). Both DNA and protein adducts formed by these activated carcinogens release a compound called 4-hydroxy-1-(3-pyridyl)-1-butanone (HPB) upon hydrolysis. HPB is unique to TSNAs, so its presence is highly specific to tobacco exposure and the bioactivation of carcinogens from it. As a result, HPB can serve as a valuable biomarker, indicating both tobacco exposure and the occurrence of bioactivation, which links it directly to the carcinogenic processes associated with smoking (Wang et al., 2019).

A study by Jethwa and Khariwala (2017) quantified the level of DNA adduct formation found in the oral cavity of HNSCC patients who smoke by determining the level of 4-hydroxy-1-(3-pyridyl)-1-butanone (HPB)-releasing DNA adducts present at diagnosis. After analysing the DNA in buccal cells, the results indicate that DNA adduct levels are higher in smokers with HNSCC compared to cancer-free smokers. This result might suggest that the difference between smokers with HNSCC and cancer-free smokers is attributable to variations in DNA repair and carcinogen processing, which might differ in some smokers.

Beyond its carcinogenic effects, tobacco has been shown to negatively impact treatment outcomes in HNSCC patients, including reduced radiation effectiveness, poorer surgical results, and increased wound complications. Studies have shown that patients who continue smoking even after undergoing radiotherapy could develop

osteoradionecrosis, which leads to hospitalization during treatment, influencing both survival and local control (hazard ratio 1.7, respectively 1.5) (Zevallos et al., 2009).

In addition to this, smoking before surgery can lead to higher risks of anaesthetic complications and poor wound healing (Tang et al., 2014). Hatcher et al. (2015) studied 129 HNSCC patients scheduled for major surgery, considering demographic factors, history of smoking, and urinary cotinine levels. Cotinine is the primary metabolite of nicotine, formed in the liver through enzymatic metabolism.

When a person consumes nicotine (such as through smoking), it is rapidly processed in the liver, where approximately 70–80% of nicotine is converted to cotinine. This transformation is mainly catalyzed by the enzyme CYP2A6, and to a lesser extent, nicotine is also metabolized into another compound, nornicotine, with the help of both CYP2A6 and CYP2B6 enzymes (Kaprio, 2022). Cotinine has a longer half-life than nicotine, remaining in the bloodstream for 15–19 hours, compared to the 2–3-hour half-life of nicotine. This extended presence of cotinine in the blood results in relatively stable plasma concentrations of about 1–3 μM in regular smokers. Because of its stability and longer half-life, cotinine is often used as a reliable biomarker to assess nicotine exposure over a longer period, as it provides a more consistent measure than nicotine itself (Kaprio, 2022).

The results of the Hatcher et al. (2015) study showed that current or former smokers were six times more likely to experience complications, such as vascular, renal, and pulmonary acute blood anaemia, urinary tract infections, and delirium and had longer hospital stays compared to non-smokers. Moreover, it is believed that endothelial migration is negatively impacted by smoking, triggering luminal thrombosis,

while nicotine is known to increase vasoconstriction, affecting organ oxygen delivery (Marin et al., 2008).

According to Marron et al. (2009), HNSCC risk is reduced by 30% when quitting tobacco smoking for a short period (between one to four years), compared to individuals actively smoking. In addition to this, in laryngeal cancer, the risk is reduced by 60% after 10 to 15 years, and in oral cavity cancer, the risks go down to a never-smoker level after 20 years (Marron et al., 2009).

1.2.2. ALCOHOL CONSUMPTION AND HNSCC

Alcohol is the second major risk factor for HNSCC. Alcohol toxicity results from ethanol and its metabolic byproducts, involving the oral microbiota and oxidative stress. Alcohol may increase epithelial cell exposure to carcinogens, leading to DNA damage, epigenetic changes, and impairments in the DNA repair processes, including the formation of DNA adducts, similar to tobacco consumption (Ferraguti et al., 2022).

Acetaldehyde, the main oxidative metabolite of alcohol, is a tumor initiator which binds to DNA and disrupts the double helix. Other carcinogenic compounds released when ingesting alcohol are the reactive oxygen species (ROS) (i.e. hydroxyl radicals, superoxide, and hydrogen peroxide) formed during alcohol biotransformation involving alcohol dehydrogenase (ADH), catalase, and cytochrome P-450 2E1 (CYP2E1) (Boccia et al., 2009), the major alcohol-metabolizing enzyme in the brain.

CYP2E1 is associated with oxidative damage, and it can cause disruptions in mitochondria (Jin et al., 2013). When ROS are generated, the intracellular redox state is

negatively affected, leading to a high increase in oxidative stress and neuronal cell death due to the oxidation of lipids, DNA, and proteins (Miller-Pinsler and Wells, 2014).

Various mutations can be triggered by the production of ROS, such as single and double-strand breaks, oxidized bases, and the formation of exocyclic adducts, promoting clonal expansion and cellular immortalization, which are directly linked to cancer development (Ferraguti et al., 2022).

A myriad of genetic modifications can be triggered by alcohol consumption, leading to somatic copy-number alterations in oncogenes and tumor suppressors commonly encountered in HNSCC, such as *CDKN2A*, *FHIT*, the 11q13 region, *HER2*, 3q25-qter, and *CSMD1*. However, unlike tobacco, *TP53* mutations are not as frequent (Urashima et al., 2013).

Moreover, aldehyde dehydrogenase 1 (ALDH1) is an enzyme that plays a critical role in the primary pathway of alcohol metabolism, converting the byproducts of alcohol breakdown into less harmful substances that can be further processed by the body (Ferraguti et al., 2022). The gene encoding ALDH1 is located on chromosome 9q21.13. In the context of head and neck cancer, ALDH1 has gained attention as a highly selective prognostic marker. Studies have shown that cells positive for ALDH1 (ALDH1+ cells) tend to exhibit resistance to radiotherapy and could initiate and sustain tumour growth. This makes ALDH1 a marker of interest for predicting tumour aggressiveness and treatment resistance in HNC (Ferraguti et al., 2022).

However, determining the exact impact of alcohol on cancer and other health conditions is challenging. Unlike some toxins that have a clear dose-response relationship (a "threshold effect" where harm only begins above a certain level of exposure), alcohol does not have a clearly defined threshold. This means that even low

levels of alcohol consumption may still contribute to neoplastic and non-neoplastic diseases, adding complexity to understanding and assessing alcohol-related health risks (Ferraguti et al., 2022).

Incidentally, compounds derived from fermentation (e.g. ethyl carbamate), often found in alcoholic drinks, are known to be carcinogenic to humans (IARC Working Group on the Evaluation of Carcinogenic Risks to Humans, 2010; Boffetta and Hashibe, 2006). Moreover, studies have shown that certain microorganisms found in the oral microbiota, play an important role in interfering with the carcinogenic effect of alcohol consumption (Salaspuro, 2020). Genus *Neisseria*, which is often found in the human oral microbiota, has high ADH activity and has been proven to generate high amounts of acetaldehyde when cultured *in vitro* in the presence of ethanol. Similarly, *N. subflava* and oral streptococci, such as *Streptococcus salivarius*, *Streptococcus intermedius*, and *Streptococcus mitis* display the same ADH activity and capability to produce acetaldehyde from ethanol (Ferraguti et al., 2022).

Individuals that continue alcohol consumption even after the start of their treatment experience a significant negative impact on survival, with a hazard ratio of 1.28 (Fortin, Wang and Vigneault, 2009), and poorer quality of life (Potash et al., 2009). Cessation of alcohol consumption is necessary for individuals who must undergo surgery and involves screening all patients for excessive alcohol consumption with questionnaires such as the Fast Alcohol Screening Test (Parker, Marshall and Ball, 2008).

1.2.3. HUMAN PAPILLOMAVIRUS INFECTION AND HNSCC

HPV-16 infection is actively increasing in prevalence as a causative agent for HNSCC, mostly in oropharyngeal and oral squamous cell carcinoma (Shaw and Beasley, 2016). Human papillomaviruses (HPVs) are DNA viruses that target various epithelial tissues in the body. There are two main categories of HPVs based on their tissue tropism: **cutaneous types** that infect the skin (epidermis) and **mucosotropic types** that infect mucosal linings, such as those in the upper respiratory system and anogenital tract (Humans, 2007). HPVs are further classified into low-risk and high-risk types based on their potential to cause cancer. High-risk HPVs (HPV 16, 18, 31, 33, 35, 39, 45, 51, 52, 56, 58, and 59) have been shown to promote cancer through their ability to disrupt cellular control of growth and genome stability, leading to unchecked cell division and genomic instability (Humans, 2007). This cancer-causing potential is primarily due to two viral proteins, **E6** and **E7**, which interfere with tumor suppressor pathways and other cellular processes that control proliferation and apoptosis (Humans, 2007).

HPVs specifically target keratinocyte progenitor cells, which are early-stage cells that mature into keratinocytes. These progenitor cells are encountered in the basal layer of stratified squamous epithelia, directly attached to the epithelial basement membrane. This membrane is essential for the integrity of the epithelial layer and, for HPVs to initiate infection, it must reach these basal cells (Faraji et al., 2017). Experimental models have shown that HPVs need access to the basement membrane to establish infection, and this access is often facilitated by micro-abrasions or tiny tears in the epithelial surface, allowing the virus to bypass the protective outer layers (Kines et

al., 2009). Once the HPV reaches the basal layer, it can infect the progenitor keratinocytes, starting a cycle of infection that could lead to cellular changes and contribute to cancer development for high-risk HPV types (Faraji et al., 2017).

In the head and neck, specifically in the oropharynx, HPV can establish infection without the presence of epithelial abrasions. This infection mechanism in the oropharynx is attributable to the presence of a specialized structure of the tonsillar tissues in Waldeyer's tonsillar ring, which includes the lingual, tubal, palatine, and adenoid tonsils (Faraji et al., 2017). The tonsillar structures are made out of a specific type of epithelium combined with lymphoid tissue called reticulated squamous epithelium (Figure 2). Compared to the continuous basement membrane most epithelial tissues have, this specific tissue has a fenestrated basement membrane (Faraji et al., 2017).

These natural gaps allow the immune cells to move between lymphoid tissue and epithelium, providing them access to potential pathogens encountered in the oral cavity (Faraji et al., 2017). However, these gaps are the entry points of HPV infection to the basal keratinocytes of the tonsillar epithelium. This distinctive feature of Waldeyer's ring may explain the higher susceptibility of the palatine and lingual tonsils to HPV-related cancers, such as oropharyngeal squamous cell carcinoma (Westra, 2012).

Viral oncoproteins E6 and E7, whose expression is induced in the keratinocytes after HPV infects the basal cells, are known to inactivate tumour suppressor proteins, such as p53 and Rb (Retinoblastoma Protein), promoting abnormal cell growth, genomic instability, and disruption of keratinocyte differentiation (Faraji et al., 2017). The infection leads to disrupted cell differentiation in the basal layer, with the involvement of genes like *E2F1*, which regulates cell cycle progression. As cells grow

abnormally, mutations in genes like *TRAF3*, *FHIT*, and *PTEN* contribute to the early stages of carcinogenesis by altering cellular signaling and promoting uncontrolled growth (Faraji et al., 2017). When the infection reaches the carcinoma in situ stage, mutations in genes on chromosome 3q26/28 are encountered and cells become cancerous but have not yet invaded the surrounding tissues. Additional mutations in genes such as *PIK3CA*, *SOX2*, and *TP53* drive the transition to invasive carcinoma, where cancer cells penetrate the basement membrane and spread to surrounding tissues (Figure 2) (Faraji et al., 2017).

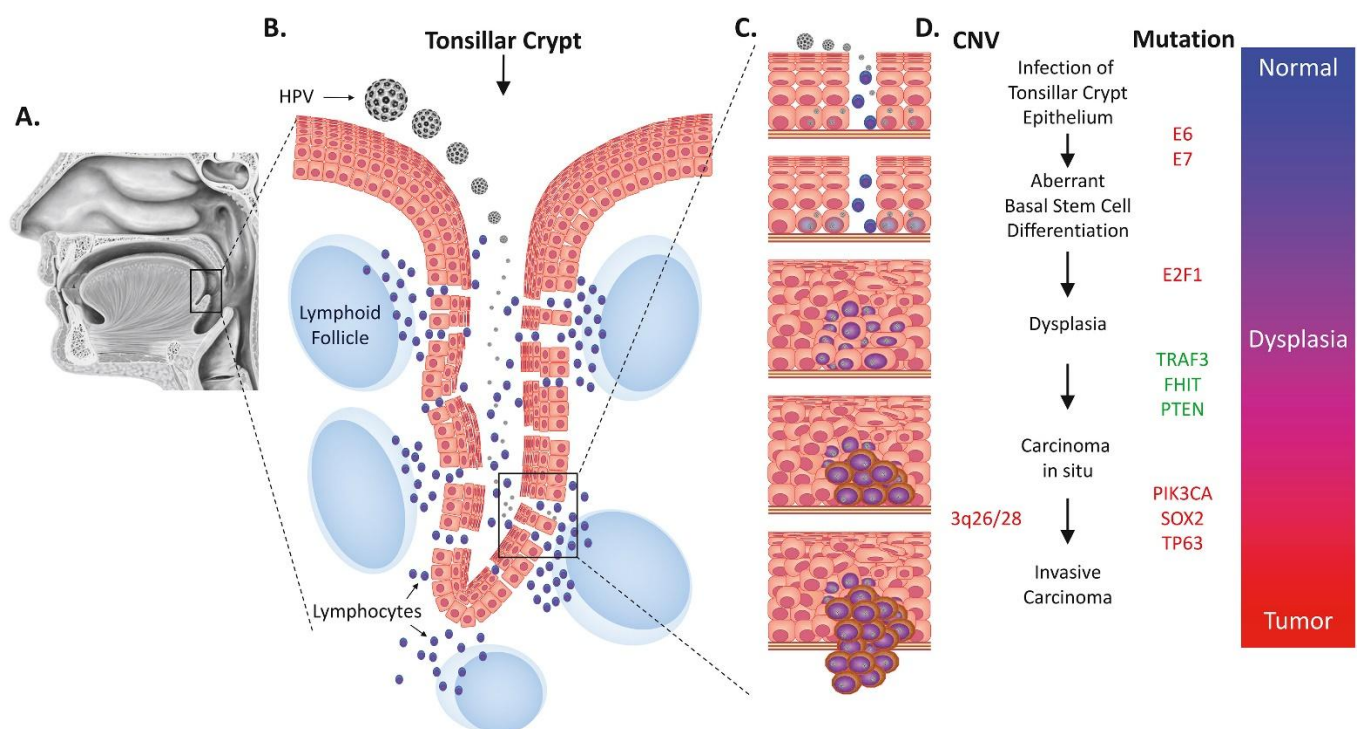


Figure 2: Progression of HPV infection to invasive carcinoma in HNC (Faraji et al., 2017). HPV infects the tonsillar crypts, bypassing the typical epithelial barrier due to the crypt's unique structure. HPV infection leads to progressive genetic and cellular changes, resulting in dysplasia and eventually invasive carcinoma. This model demonstrates the molecular steps involved in HPV-induced cancer in the tonsils, specifically showing the roles of viral proteins (E6, E7) and the accumulation of host mutations. The colour gradient on the right indicates the stages of transformation, from **normal** cells (blue) to **dysplasia** (purple), and finally to **tumour** (red) as the cells progress through the stages of HPV-induced carcinogenesis. Reprinted from *Microbes and Infection*, Volume 19, Issues 9-10, Farhoud Faraji et al (2017), Copyright 2017, with permission from Elsevier.

Worldwide, over 80% of young adults have an HPV infection at some point during their lifetime, but most cases are spontaneously cured by the immune system within two years (Tanaka and Alawi, 2018). If the infection is not cleared, pre-malignant or malignant lesions could be triggered by chronic HPV infections, which can appear in multiple anatomical sites, such as the oropharynx (Fakhry and D'Souza, 2013). A study by D'Souza et al. (2014) has shown that HPV-16 DNA is, in most cases, not detected in the partners of OPSCC patients, highlighting the uncertainty behind chronic HPV infections and why certain individuals can clear the infection while some do not.

In the United States, approximately 70% of oropharyngeal cancer (OPSCC) cases are HPV positive, while there is lower HPV prevalence in other HNSCC sites, due to the oropharynx being particularly susceptible to HPV persistence (D'Souza et al., 2007). Based on risk profiles and demographics, there are significant dissimilarities between HPV-related and HPV-unrelated oropharyngeal cancer. For example, individuals with HPV-related OPSCC are significantly younger, male, and of white race, and have heightened numbers of lifetime oral sex partners, but reduced tobacco and alcohol usage, and improved dentition, compared to HPV-negative OPSCC patients (Zhou, Jou and Cohen, 2021).

Vaccine development for HPV infections started back in the 1990s, using virus-like particles (VLPs) from the major papillomavirus capsid protein L1 through a process of recombinant protein expression in yeast and bacteria (Zhou, Jou and Cohen, 2021). Nowadays, three HPV vaccines passed clinical trials and provide protection against nine types of HPV. Multiple studies highlight the effectiveness of the vaccines, which is

highest in individuals vaccinated before the first sexual contact (Castle and Maza, 2015). In addition to this, there has been a significant decrease in the prevalence of HPV infections in girls aged 13 to 19 (83%), and those aged 20 to 24 (66%), 5 to 8 years after vaccination (Drolet et al., 2019). Another study, that focused on over 2600 men and women (18-33 age range), concluded that the prevalence of oral infections with four different types of HPV has a decline of 88% for the individuals that received at least one dose of 4vHPV vaccine, compared to those not vaccinated (Chaturvedi et al., 2018).

Despite all studies confirming the effectiveness of the HPV vaccine, global access is still hard to achieve, influenced by multiple factors such as healthcare infrastructure, costs, education, and geographical location (Roden and Stern, 2018). In 2019, it was estimated that globally, 15% of girls and 4% of boys received the full course of the HPV vaccine, with an additional 20% of girls and 5% of boys receiving at least one dose (Bruni et al., 2021). Regionally, Australia and New Zealand had the highest HPV vaccine coverage (77%), followed by Latin America (61%), and Europe and North America (35%). In contrast, Northern Africa, Asia, and Oceania (excluding Australia and New Zealand) had low coverage rates. In Sub-Saharan Africa, despite only one-third of countries including HPV vaccination in their national schedules, coverage reached nearly 20% (Bruni et al., 2021).

While 55% of countries globally have introduced the HPV vaccine, 70% of eligible girls still live in countries without a national HPV program. This gap is largely due to 7 of the 10 most populous countries (China, India, Nigeria, Pakistan, Indonesia, Bangladesh, and Russia) either not having introduced the vaccine or only offering it sub-nationally (Bruni et al., 2021). Consequently, global coverage reached only 15% in 2019. Of the 30% of girls aged 9 to 15 who live in countries with an HPV vaccine program, just

over half (53%) completed the final dose. Global coverage has been gradually increasing, but this is primarily due to more countries introducing the vaccine rather than improvements in vaccination rates within existing programs (Bruni et al., 2021).

Additionally, The COVID-19 pandemic in 2020 has significantly disrupted HPV vaccination programs worldwide. Due to school closures and interruptions in routine immunization services, HPV vaccine delivery has been halted in most countries, affecting coverage for other vaccines as well. By August 2020, approximately 70 countries reported that their immunization programs had been interrupted as a result of the pandemic (Bruni et al., 2021).

1.2.4. EPIDEMIOLOGY AND TRENDS IN INCIDENCE

According to the latest GLOBOCAN estimates (2020), HNSCC accounts for approximately 890,000 new cases and 450,000 deaths worldwide, which makes HNSCC the sixth most common type of cancer, accounting for 4.5% of cancer diagnoses and deaths (Figure 3) (Barsouk et al., 2023). The highest incidence rates of HNSCC are encountered in South and Southeast Asia, predominantly in India, where tobacco, with or without areca nut use, accounts for around 80% of all HNSCC cases (Cheong et al., 2017; Gormley et al., 2022). In the Indian subcontinent and Taiwan, around 50% of oral cancer cases are linked to betel quid chewing.

Chewing areca nut (a main component of betel quid) is a significant risk factor for oral cancer. Studies show that individuals who chew betel quid have a considerably higher risk of developing oral cancer compared to those who have never used it

(Warnakulasuriya and Chen, 2022). One of the primary alkaloids in areca nut is arecoline, strongly linked to carcinogenic properties, as shown in studies using human primary cells and other experimental systems (Gupta et al., 2020).

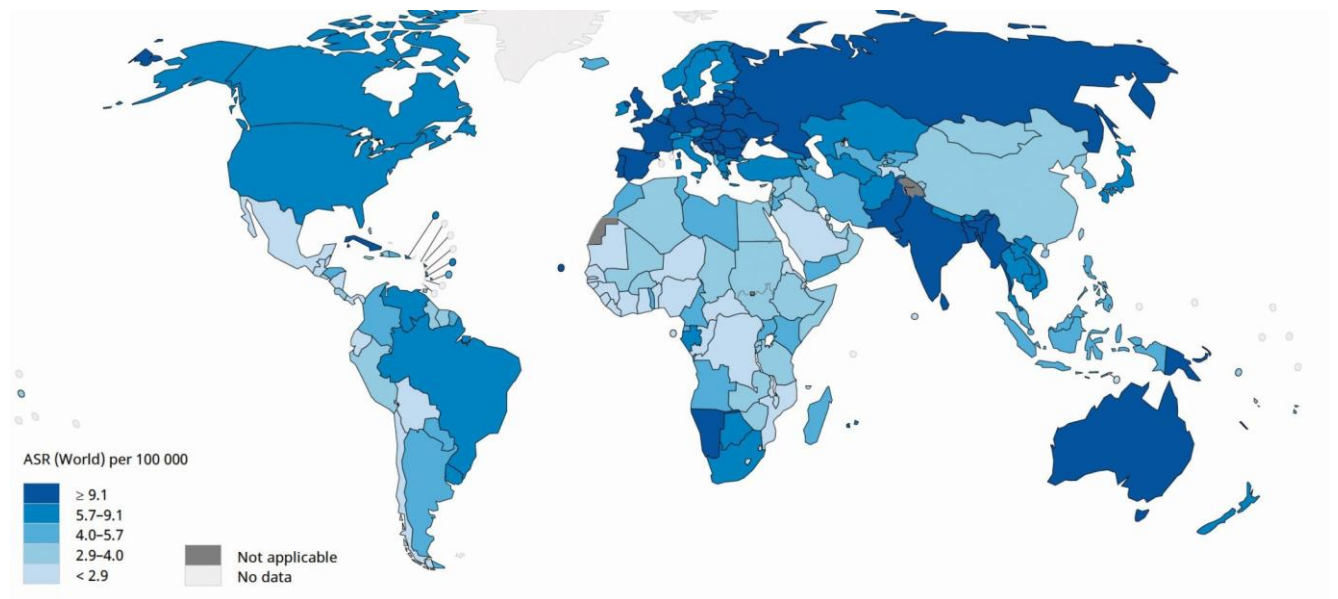


Figure 3: The global incidence of HNSCC, reprinted from International Agency For Research On Cancer, 'Cancer today (Gormley et al., 2022) – Data visualization tools for exploring the global cancer burden in 2020'. The map displays the lip, oral cavity, larynx, hypopharynx and oropharynx cancer sites, showing the estimated age-standardised rates of HNSCC incidence for both sexes.

The global incidence of HNSCC is rising in many countries, especially among younger populations, with a projected 30% annual increase by 2030 (Sung et al., 2021). HPV infection is expected to surpass tobacco as the main cause of HNSCC worldwide, leading to a higher incidence of oropharyngeal cancer compared to oral cancer. Additionally, laryngeal cancer cases have risen by 23% over the past decade (Fitzmaurice et al., 2017). In the United Kingdom, the incidence of oropharyngeal cancer

has risen by 6.5% among women, and 7.3% among men, while oral cancer has increased by 3.0% in women, and 2.8% in men, with the most significant growth occurring in individuals of disadvantaged socioeconomic backgrounds (Louie, Mehanna and Sasieni, 2015).

Every year in the United Kingdom, approximately 12,759 new cases of HNSCC are diagnosed, which averages out to 35 new cases every day between 2017 and 2019. Unfortunately, this number is expected to rise, with incidence rates predicted to increase by 3% from 2023-2025 to 2038-2040, potentially reaching around 16,300 new cases annually by 2038-2040, according to Cancer Research UK (2024). HNSCC ranks as the 13th most common cancer in women and the 5th most common in men, with the highest rates observed in individuals aged 65 to 69. Despite advancements, the survival rate for HNSCC varies widely, ranging from 19% to 59% for patients diagnosed between 2009 and 2013. Notably, 46% to 88% of HNSCC cases are preventable, highlighting the importance of early detection and prevention strategies (Cancer Research UK, 2024).

1.3. OVERVIEW OF HEAD AND NECK SQUAMOUS CELL CARCINOMA DEVELOPMENT

1.3.1. DNA DAMAGE AND DNA REPAIR

The average DNA molecule faces persistent attacks from a myriad of internal and external genotoxic agents, with estimates suggesting that each cell encounters up to 10^5 spontaneous or induced DNA lesions daily (De Bont and van

Larebeke, 2004). Despite this, all living organisms bear the responsibility of safeguarding their genome and accurately passing it on to subsequent generations (De Bont and van Larebeke, 2004).

DNA damage is known to be a causative factor in cancer development. DNA lesions, acquired from exogenous (environmental sources) or endogenous factors (cellular metabolic sources) have the potential to modify the fundamental structure of the double helix, consequently impacting transcription and replication processes. Exogenous factors include ultraviolet (UV) and ionizing (IR) radiations, and other chemical agents, while endogenous factors are oxidation, hydrolysis, alkylation, and mismatch of DNA bases in the double helix. The aberrant repair or replication of these lesions can result in mutations within the genome, which may be passed down to daughter cells, posing detrimental effects on an individual's health (Torgovnick and Schumacher, 2015).

In healthy cells, DNA damage repair mechanisms are able to withstand DNA damage and ensure that the cell continues to undergo division properly. Genome instability, one of the key hallmarks that aid in cancer development, arises from aberrations and deficiencies in the DNA damage response (DDR) network (Li et al., 2023). Therefore, neoplastic cells often have mutations in DDR genes or experience replicative stress, which leads to an inability to effectively repair DNA. As a result, these cells accumulate genetic mutations, contributing to tumorigenesis (Li et al., 2023). Targeting the DDR processes in cancer cells could be the future of therapeutic strategies, as interfering with their ability to repair DNA can induce excessive DNA damage that cancer cells will not be able to repair, ultimately leading to apoptosis (Li et al., 2023).

DDR proteins can be broadly categorized into two groups: caretakers and gatekeepers (Li et al., 2023). Caretakers are responsible for maintaining genome integrity by directly repairing DNA damage. They play a crucial role in ensuring that DNA is repaired accurately to prevent mutations that could lead to cancer or other diseases. On the other hand, gatekeepers regulate the repair process by coordinating it with other cellular events, such as the cell cycle and cell death, ensuring that DNA repair occurs at the appropriate time and in the proper context to maintain cellular function (Matthews, Bertoli and de Bruin, 2021).

Together, caretakers and gatekeepers work cooperatively to safeguard the genome. Different types of DNA damage activate specific DDR pathways tailored to repair the particular type of damage (Li et al., 2023). A very important characteristic of these DDR pathways is that they often exhibit redundancy, meaning multiple pathways can repair the same type of damage (Setton et al., 2021). This redundancy may help explain why synthetic lethal interactions, where inhibiting two DDR proteins leads to cell death, are common (Nijman, 2010). Essentially, if one repair pathway is defective, another pathway can often compensate, but if two related pathways are inhibited simultaneously, the cell may not be able to repair its DNA, leading to cell death (Li et al., 2023).

Damage sensors, signaling/mediator proteins, and effectors are part of the caretakers' category, collectively ensuring DNA damage is properly repaired (Brown et al., 2016). For example, one of the simplest DNA damages, UV-induced cyclobutane pyrimidine dimers (CPDs), can be repaired by photolyase proteins through a process known as photoreactivation, where light activates the repair enzyme to reverse the damage (Ramírez-Gamboa et al., 2022). Moreover, small modifications in the DNA

bases, which are usually caused by oxidants, UV, or alkylating agents are fixed by direct reversal repair enzymes without the need for additional proteins (Li et al., 2023). A good example is O⁶-methylguanine DNA methyltransferase (MGMT), which removes methyl groups from O⁶-methylguanine lesions through a mechanism where the methyl group is transferred to MGMT itself, resulting in its degradation (Mishina, Duguid and He, 2006).

Another DNA repair mechanism that is triggered when DNA bases undergo modifications is base excision repair (BER) (Dianov and Hübscher, 2013). When the BER process starts, DNA glycosylases detect and remove damaged bases (e.g. 5-hydroxycytosine), leaving behind AP sites (abasic sites). These sites are further processed by AP endonuclease 1 (APE1), which generates a single-strand break (SSB). The subsequent repair pathways for SSBs overlap with those for single-strand break repair (SSBR), with PARP1 playing a vital role in recognizing and signaling the break (Caldecott, 2022).

For more complex DNA damage, such as crosslinks that distort the DNA helix structure or bulk DNA adducts, nucleotide excision repair (NER) is activated to remove these larger lesions (Marteijn et al., 2014). Very similar to BER and NER, mismatch repair (MMR) is a DNA repair pathway that specifically attends to aberrations created during DNA replication, such as single nucleotide mismatches and small deletions or insertions, through a 'cut and patch' process (Li, 2007).

A more error-prone mechanism is translesion synthesis (TLS), which provides an alternative approach to dealing with DNA lesions, allowing replication to continue past damaged DNA without breaking the DNA strand (Sale, 2013). Due to the lack of 3' to 5' exonuclease activity, the mechanism that corrects errors in high-fidelity

polymerases. TLS lacks proofreading and employs low-fidelity polymerases; therefore, it increases the likelihood of mistakes in the DNA repair process and could boost the mutation rate (Goodman and Woodgate, 2013).

These DDR mechanisms highlight how various caretaker proteins collaborate to detect and repair DNA damage, preventing genomic instability and potential tumorigenesis. Triggering aberrations in the DNA repair processes of neoplastic cells is believed to be one of the targetable hallmarks of cancer (Pilié et al., 2018). When cancers have to over-rely on their remaining pathways for genome stability, they become vulnerable to DNA damage-induced cell death if the remaining pathways are pharmacologically disrupted (Al-Bedeary, Getta and Al-Sharafi, 2020).

Following this strategy, the first DNA repair inhibitor, olaparib, a PARP (Poly (ADP-ribose) polymerase) inhibitor, was approved in 2014 for the treatment of ovarian cancer with BRCA gene deficiencies (Deeks, 2015). Since then, at least six additional PARP inhibitors have been developed and approved worldwide, expanding their use to other cancers, including pancreatic, breast, and prostate cancers (Curtin and Szabo, 2020). The development strategy for PARP inhibitors has evolved, with a focus on selectively inhibiting PARP1, which maintains therapeutic efficacy while aiming to reduce side effects (Ngoi et al., 2021).

In addition to PARP inhibitors, other DNA damage response (DDR) checkpoint proteins have emerged as potential targets for cancer therapy. These include WEE1 (WEE1 G2 checkpoint kinase), ATR (ATM and Rad3-related), ATM (Ataxia-Telangiectasia Mutated), and PLK1 (Polo-like kinase 1). Inhibitors targeting these proteins are being tested in clinical settings, with some showing promising preliminary responses in certain cancer types. These DDR inhibitors aim to exploit the cancer cells'

vulnerabilities in repairing DNA, offering new therapeutic avenues for cancer treatment (Li et al., 2023).

1.3.2. CANCER HALLMARKS AND HNSCC

The growth signals of normal, healthy cells are meticulously regulated through both soluble and membrane-bound growth factors. In contrast, cancer cells exhibit autonomous and erratic growth patterns due to disrupting these regulatory signals (Keshavarzi et al., 2017). The concept of the hallmarks of cancer was introduced to describe a set of functional abilities acquired by human cells during their transition from healthy to neoplastic states, specifically traits essential for the development of malignant tumors, which serve as a framework for understanding the complexity of cancer (Hanahan, 2022).

These hallmarks encompass key traits such as sustaining proliferative signaling, promoting angiogenesis, resisting cell death, evading growth suppressors, achieving replicative immortality, and facilitating invasion and metastasis. These traits are underpinned by genome instability, which accelerates the acquisition of genetic alterations, and inflammation, which supports various hallmark functions (Figure 4) (Hanahan and Weinberg, 2011).

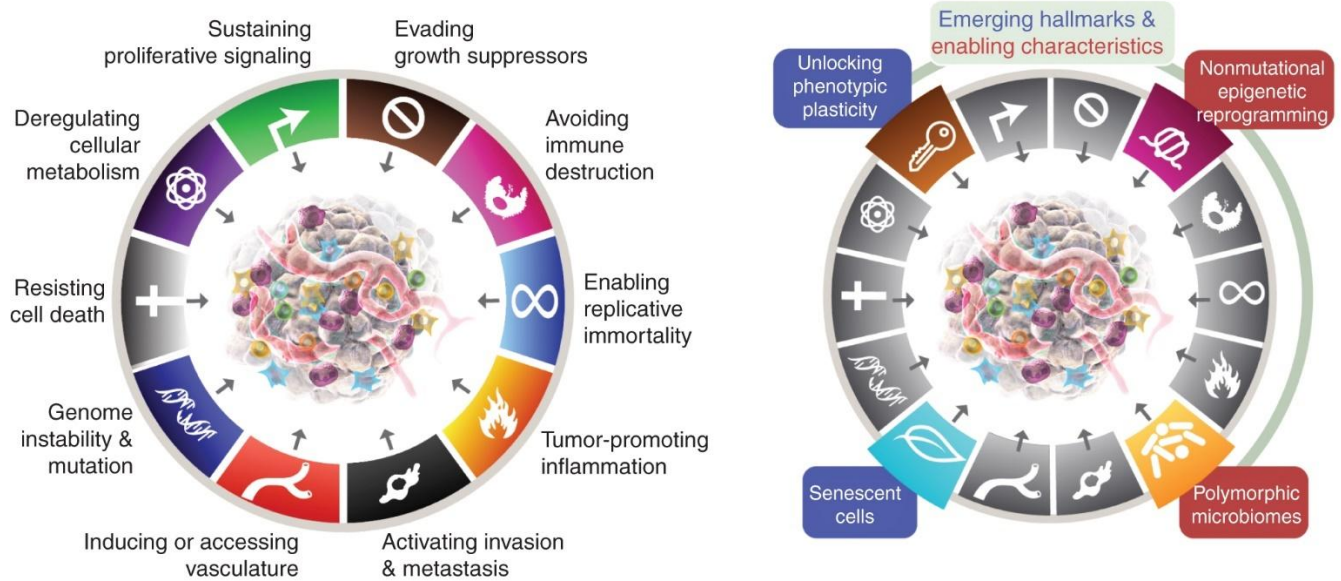


Figure 4: The hallmark traits commonly exhibited by most cancers (Hanahan, 2022). The 2022 Hallmarks of Cancer (left) now include eight core capabilities and two enabling characteristics. In addition to the six original hallmarks from 2000, two emerging hallmarks introduced in 2011—reprogramming cellular metabolism and avoiding immune destruction—are now considered core features. On the right, recent proposals include emerging hallmarks, such as senescent cells, epigenetic reprogramming, phenotypic plasticity, and polymorphic microbiomes. Reprinted (or adapted) from *Cancer Discovery*, 2020, 12 (1), 31-46, Douglas Hanahan, *Hallmarks of Cancer: New Dimensions*, with permission from AACR.

The most fundamental characteristic of cancer cells lies in their ability to sustain **proliferation**. Healthy tissues meticulously regulate the production and dissemination of growth-promoting signals, orchestrating cell entry and progression through the growth and division cycles. This regulation ensures the maintenance of a balanced cell population and the preservation of normal tissue structure and function. Neoplastic cells disrupt this delicate balance by deregulating these signaling pathways, granting themselves autonomy over their growth (Hanahan and Weinberg, 2011).

These enabling signals primarily stem from growth factors that bind to receptors on the cell surface, often containing intracellular tyrosine kinase domains. The family of

transmembrane tyrosine kinase receptors known as the epidermal growth factor (EGF) family encompasses epidermal growth factor receptor (EGFR) or human epidermal growth factor receptor 1 (HER1), HER2, HER3, and HER4 (Bernardes et al., 2010). Subsequently, these receptors instigate intricate intracellular signaling cascades that control cell cycle advancement and cellular growth, including augmentation in cell size. These signals often exert influence over other vital cellular processes, such as survival and energy metabolism (Hanahan and Weinberg, 2011).

In addition, the availability of growth factors undergoes intricate regulation through processes like sequestration in the pericellular space and the extracellular matrix, as well as through the actions of a sophisticated network of enzymes, including proteases and sulfatases. These enzymes modulate the liberation and activation of growth factors in a highly specific and localized manner, introducing another layer of complexity to our comprehension of the regulation of cell proliferation in both health and disease (Hanahan and Weinberg, 2011).

Mitogenic signaling pathways in cancer cells are comprehensively understood. Cancer cells can develop the capacity to maintain proliferative signaling through diverse alternative pathways. For example, they might generate their own growth factor ligands, enabling them to react to these self-produced signals by expressing corresponding receptors, consequently inducing autocrine proliferative stimulation (Lemmon and Schlessinger, 2010; Witsch, Sela and Yarden, 2010).

Alternatively, cancer cells can emit signals that stimulate normal cells within the surrounding tumor-associated stroma, inducing these cells to release various growth factors that support cancer cell proliferation (Cheng et al., 2008). Moreover, cancer cells may disrupt receptor signaling by increasing the levels of receptor proteins present on

their surfaces, rendering them hypersensitive to even low levels of growth factor ligands. Similar outcomes may arise from structural alterations in receptor molecules that enable ligand-independent activation (Bhowmick, Neilson and Moses, 2004).

Independence from growth factors can also arise from the constitutive activation of components within signaling pathways downstream of these receptors, bypassing the need for ligand-mediated receptor activation. Since multiple distinct downstream signaling pathways originate from a receptor stimulated by a ligand, the activation of one of these pathways, such as the Ras signal transducer pathway, may only replicate a portion of the regulatory instructions transmitted by the activated receptor (Hanahan and Weinberg, 2011).

Apart from their ability to induce and sustain growth-promoting signals, cancer cells must also evade robust mechanisms that negatively regulate cell proliferation, many of which are governed by **tumor suppressor genes**. Many tumor suppressors have been identified through their characteristic inactivation in animal or human cancers, with many validated through gain- or loss-of-function experiments in mice. Among these, the RB and p53 proteins serve as prototypical tumor suppressors, acting as central control points within two critical cellular regulatory pathways. These pathways dictate whether cells proceed with proliferation or, conversely, activate apoptosis or senescence (Hanahan and Weinberg, 2011).

Numerous studies have identified a significant correlation between the expression levels of EGFR, phosphorylated EGFR (pEGFR), HER2, or HER4 and the poor prognosis of patients with OSCC. Elevated levels of cyclin D1, a cell-cycle regulator governing the transition from the G1 to S phase, have also been linked to diminished survival rates (Monteiro et al., 2013; Silva et al., 2014). Furthermore, the presence of c-

Met, another transmembrane tyrosine kinase receptor, has been associated with unfavourable outcomes in OSCC patients due to its activation of matrix metalloproteinase (MMP)-1, -2, and -9 (Lim et al., 2012). Additionally, a study by Macha et al. (2011), focusing on the cytoplasmic transcription factors belonging to the signal transducer and activator of transcription (STAT) family, suggests that OSCC cases displaying expression of phosphorylated STAT3 (pSTAT3) are correlated with the poorest prognosis.

Various tumor-suppressor genes responsible for anti-growth signals undergo inactivation through the processes of mutation, methylation, and deletion that arise in cancerous cells, leading to loss of heterozygosity. Such an example is **p53**, which is widely recognized as the guardian of the genome, playing a crucial role in regulating the cell cycle, apoptosis, DNA repair, and cellular differentiation (Choi and Myers, 2008). Somatic mutations in the *TP53* gene are identified in approximately 60% of cases of HNSCC and approximately 10% of early oral dysplasia cases (Keshavarzi et al., 2017). For the rest of HNSCC cases, *TP53* regulation is negatively affected by interaction with different proteins, such as E6, the oncoprotein produced by HPV-16. E6 can interfere with the p53 protein, leading to its degradation. This happens in about 20% of cases of HNSCC (Boudewijn J.M. Braakhuis et al., 2004). In the other 20% of cases, the *TP53* gene might not be mutated, but other proteins in the p53 signaling pathway could be disrupted. A good example is the overexpression of MDM2, a key protein which regulates p53 by promoting its degradation (Bernstein et al., 2012). In 80% of HNSCC cases, this protein is overexpressed, leading to accelerated degradation of p53, therefore contributing to tumour development (Valentin-Vega et al., 2007).

Additionally, p53, can promote apoptosis (Levine and Oren, 2009) by inducing the expression of pro-apoptotic proteins like Noxa, Puma, and Aip1, aiding in triggering cell death. The p53 protein also represses the expression of antiapoptotic proteins, such as Bcl-2, which normally work to prevent apoptosis. This ensures that, when necessary, damaged cells undergo apoptosis (Bernstein et al., 2012).

In HNSCC, the presence of *TP53* mutations in a premalignant lesion is a strong predictor of progression to carcinoma, with a positive predictive value of 86% (Bernstein et al., 2012). This means that if a *TP53* mutation is found in a precancerous lesion, there is a high likelihood that the lesion will develop into cancer. Studies have also shown that mutant *TP53* is present in 29% of hyperplastic lesions (early, benign changes in tissue), 46% of dysplastic lesions (abnormal tissue growth that could progress to cancer), and 58% of HNSCC (cancerous lesions) (Bernstein et al., 2012).

Taking all this into account, a grading system for p53 mutations has been developed in head and neck cancers, including OSCC, categorizing mutations into low-risk missense mutations, high-risk missense mutations, and other mutations (Sandulache et al., 2018; Neskey et al., 2015). Subgroups with high-risk p53 mutations are associated with reduced sensitivity to cisplatin, increased risk of distant metastasis, extranodal extension, and poorer prognosis (Osman et al., 2015). Overall survival rates are notably lower in OSCC patients with p53 mutations compared to those with wild-type p53 (De Oliveira, Ribeiro-Silva and Zucoloto, 2007). A study by Poeta et al. (2007) analyzed 420 patients with HNSCC, including OSCC cases, and their results show that patients with any TP53 mutation had a 40% increased risk of death compared to those with wild-type TP53 (Hazard Ratio [HR] 1.4; 95% Confidence Interval [CI] 1.1–1.8).

According to the same study, disruptive TP53 mutations were associated with a 70% increased risk of death (HR 1.7; 95% CI 1.3–2.4).

Multiple studies so far highlighted that a significant correlation exists between decreased expression levels of the cell-cycle regulators p16 or p21 and poor prognosis in OSCC patients (Zhang Mingbin et al., 2013), (Padhi et al., 2017). The tumor suppressor phosphatase and tensin homolog (PTEN) acts by negatively regulating the phosphoinositide 3-kinase (PI3K)–Akt–mammalian target of rapamycin (mTOR) pathway and inhibiting insulin signaling by indirectly suppressing the mitogen-activated protein kinase (MAPK) phosphorylation and blocking insulin receptor substrate 1 (IRS-1) phosphorylation (Khalid et al., 2017). The lack of PTEN expression in OSCC serves as an indicator of a poor prognosis (Zhao et al., 2017). Additionally, PTEN inactivation can occur through gene methylation, as evidenced by the restoration of PTEN mRNA expression post-treatment with 5-aza-2'-deoxycytidine (5-Aza-dc), a demethylation agent, in human OSCC-derived cells (Kurasawa et al., 2008).

In addition to this, the presence of PIP3, which is the result of PIP2 being denatured by PI3K in the plasma membrane, activates a cascade of signaling events. PDK1 (3-phosphoinositide-dependent protein kinase 1) is recruited to the membrane by PIP3 and activates AKT (protein kinase B) (Vanhaesebroeck, Stephens and Hawkins, 2012). AKT is a key protein that regulates various cellular processes, including promoting cell survival, by phosphorylating a variety of target proteins. In HNSCC, PI3K is overexpressed in 37% of cases, and AKT is overexpressed in 17% of cases (Bernstein et al., 2012). Interestingly, similar alterations in the PI3K/AKT pathway are sometimes seen in the surrounding mucosa (healthy tissue near the tumour), indicating that these

changes might occur early in tumour development and are frequent targets in the process of tumour formation (Bernstein et al., 2012).

Besides the loss of tumour suppressor genes, HNSCC can evade growth suppression through the transforming growth factor- β (TGF- β) pathway, the NOTCH1 pathway and the retinoic acid receptor- β (RAR- β) pathway. TGF- β is a signaling molecule that normally suppresses cell growth by inhibiting the activity of Ras, a small protein (GTPase) that promotes cell division. In HNSCC, mutations that cause a loss of function in TGF- β receptors, combined with overexpression of Ras, can lead to uncontrolled cell proliferation and the development of typical HNSCC, as demonstrated in a mouse model (Lu, 2006).

This suggests that loss of TGF- β signaling and Ras activation can contribute to cancer development. NOTCH1 is a signaling pathway that plays a role in regulating cell fate and proliferation. In HNSCC, NOTCH1 signaling is often downregulated, which reduces its ability to suppress tumour growth (Bernstein et al., 2012). This downregulation may be caused by the overexpression of EGFR (epidermal growth factor receptor), which is commonly elevated in many cancers, including HNSCC (Kolev et al., 2008). Additionally, about 15% of HNSCC cases show a loss-of-function mutation in the *NOTCH1* gene, further impairing its tumor-suppressive role (Stransky et al., 2011; Agrawal et al., 2011).

Last but not least, RAR- β is a receptor activated by retinoids (vitamin A derivatives) that generally suppresses cell growth. In HNSCC, RAR- β expression is suppressed, often due to hypermethylation, which is a process where excessive methyl groups are added to the gene's promoter region, silencing its activity. This suppression

allows the cancer cells to bypass the growth-restraining effects of RAR- β (Bernstein et al., 2012).

Another hallmark of cancer is the ability of neoplastic cells to resist cell death. Apoptosis is a protective mechanism that occurs in response to various stress signals, such as DNA damage or the activation of oncogenes. Apoptosis serves as a defense mechanism by eliminating damaged or abnormal cells, preventing them from becoming cancerous (Bernstein et al., 2012). However, for cancer to develop and progress, cells must resist apoptosis. Neoplastic cells acquire resistance to apoptosis through the inactivation of pro-apoptotic factors (proteins that promote cell death) or the overactivation of apoptotic inhibitors (proteins that prevent cell death). This allows cancer cells to survive despite the presence of DNA damage or other forms of stress (Bernstein et al., 2012).

Another method neoplastic cells use to escape apoptosis involves EGFR (epidermal growth factor receptor) signaling. One of the key downstream effectors of EGFR signaling is STAT3, a transcription factor that regulates many cellular processes, including the suppression of apoptosis. When EGFR signaling is increased, it activates STAT3, which in turn inhibits apoptosis, allowing cancer cells to survive and proliferate (Grandis et al., 2000).

Replicative senescence is a process which allows normal cells to have a limited number of cell divisions. The telomeres, the protective end of chromosomes, get shorter after every cell division process (Bernstein et al., 2012). The cells stop dividing when they enter the senescence stage, and apoptosis is triggered if the telomeres continue to shorten beyond the critical point. The telomerase enzyme can counteract the shortening of telomeres by adding new telomeric repeats to the chromosome ends. This allows

cells to bypass the normal limit on the number of divisions, effectively extending their lifespan (Bernstein et al., 2012).

Telomerase is active during embryonic development, but it is typically inactive in somatic cells in adults. In many cancers, however, telomerase is reactivated, allowing cancer cells to maintain their telomeres and divide indefinitely, making them effectively immortal (Bernstein et al., 2012). This reactivation of telomerase is also observed in HNSCC, with 78% of HNSCC cases showing telomerase activation, as well as 85% of precancerous tissue and 53% of adjacent normal tissue (Bernstein et al., 2012).

Angiogenesis is the process that precedes the activation of metastasis. Tumours require a blood supply to grow and remove waste products (Bernstein et al., 2012). To achieve this, the tumour stimulates the formation of new blood vessels, a process known as angiogenesis. This is the sprouting of new vessels from existing blood vessels, which increases the blood supply to the tumour. Hypoxia, or low oxygen levels, occurs in the centre of growing tumours due to the rapid proliferation of tumour cells surpassing the formation of blood vessels (Bernstein et al., 2012).

In response to hypoxia, the tumour increases the production of pro-angiogenic factors, which promote the formation of new blood vessels. These pro-angiogenic factors are fibroblast growth factors (FGF 1 and 2), platelet-derived growth factor (PDGF), interleukin-8 (IL-8), and vascular endothelial growth factor (VEGF) (Bernstein et al., 2012). VEGF is one of the most important pro-angiogenic factors. It binds to receptors on endothelial cells, which are the cells that line the inside of blood vessels. VEGF binding to these receptors triggers endothelial cell proliferation (cell growth) and migration (movement), which are crucial steps in the formation of new blood vessels during angiogenesis (Bernstein et al., 2012).

High expression of VEGF has been observed in HNSCC, and it plays a significant role in the disease's progression by promoting angiogenesis (Caponigro et al., 2005). Studies have shown that the expression of VEGF or its receptors is increased in 50% of premalignant lesions and 75% of malignant oral and laryngeal lesions. This suggests that VEGF is an important factor in the development and progression of HNSCC, contributing to the tumour's ability to recruit blood vessels and sustain growth (Bernstein et al., 2012).

The process of metastasis involves the detachment of cancer from the primary tumour and the invasion of surrounding healthy tissue and distant sites. The mechanisms of this process heavily rely on changing shape and adhesion properties. A key event in this process is the epithelial to mesenchymal transition (EMT), in which epithelial cells, which are connected and stationary, lose their characteristics and gain mesenchymal traits, such as increased motility and the ability to invade surrounding tissues. EMT is a critical step in cancer metastasis (Fang and Kang, 2021).

E-cadherin is a cell adhesion protein that plays a crucial role in holding epithelial cells together at the adherens junctions, which are structures that mediate cell-cell adhesion (Petrova, Schecterson and Gumbiner, 2016). The protein complex that forms at these junctions includes E-cadherin and two catenins (α -catenin and β -catenin). These proteins help link the E-cadherin molecules to neighbouring cells, maintaining cellular cohesion and preventing detachment. During the transition to a mesenchymal phenotype (such as during EMT), the expression of E-cadherin and the catenins is downregulated. This downregulation weakens the attachment between cancer cells, facilitating their detachment and ability to migrate to other areas (Petrova, Schecterson and Gumbiner, 2016; Fang and Kang, 2021).

In HNSCC, the downregulation of E-cadherin occurs in 59% of cases, and the downregulation of catenins α and β occurs in 72% of cases (Tanaka et al., 2003). This downregulation is significant because it contributes to the loss of cell-cell adhesion, which is necessary for cancer cells to detach and invade surrounding tissues. Additionally, the downregulation of these proteins is linked to the presence of lymph node metastases, meaning that cancers with reduced E-cadherin and catenin expression are more likely to spread to nearby lymph nodes (Bernstein et al., 2012).

Cancer develops due to a complex interplay of genetic and environmental factors that occur over time. Over a long period, the accumulation of genetic changes and environmental damage results in the phenotypic variations seen in different cancers (Langie et al., 2015). Genome instability is generated by the intensification of mutations within the genome, and it allows genetic alterations to accumulate, aiding in cancer development. Genomic instability is considered an enabling characteristic of cancer because it facilitates the acquisition of the hallmarks of cancer by providing the genetic variations necessary for neoplastic cells to adapt and develop (Langie et al., 2015).

Another enabling characteristic of cancer is tumour-promoting inflammation, which is often encountered in HNSCC. Chemokines recruit immune cells (macrophages, mast cells, dendritic cells, lymphocytes, granulocytes) to the site of tumours, which paradoxically exploit the immune response to enhance their growth. Moreover, immune cells release reactive oxygen species, which increase genomic instability due to being mutagenic (Bernstein et al., 2012).

One inflammatory factor known as COX-2 produces inflammatory prostaglandins and has been linked to cancer progression. In HNSCC, COX-2 is overexpressed in 71% of cases, correlating with the production of VEGF. This combination may contribute to a

more aggressive disease with lymph node involvement (Bernstein et al., 2012). Furthermore, chronic oral infections like periodontitis have been linked to more aggressive oral cancers, and poor dental hygiene may play a role in the connection between cigarette smoking and HNSCC (Tezal et al., 2009). This highlights how inflammation, often driven by immune cells, can act as a facilitator of tumour growth and progression.

Overall, the myriads of mutations that could be involved in the development of HNSCC remain a largely unexplored area. Following the hallmarks of cancer, further studies on these mutations could aid in enabling more personalized therapies tailored to the specific genetic makeup of individual tumours.

1.4. DIAGNOSIS, TREATMENTS AND CLINICAL TRIALS

1.4.1. UP-TO-DATE DIAGNOSIS AND TREATMENT OPTIONS

Oral tumors often avoid detection until they have reached advanced stages, despite the oral cavity's accessibility for examination. Recently, non-invasive imaging techniques have emerged as valuable tools for detecting molecular and cellular alterations in living organisms. Technologies such as computed tomography (CT), positron emission tomography (PET), and magnetic resonance imaging (MRI) offer promise in screening patients, particularly those with oral squamous cell carcinoma, during the early phases of the illness (Keshavarzi et al., 2017).

The treatment so far requires a multidisciplinary approach, including medical, surgical, and radiation oncology, pathology, and radiology. The backbone of HNSCC

treatment is surgery, followed by definitive concurrent chemoradiation (CRT), adjuvant radiation therapy, chemotherapy, targeted therapy or immunotherapy (Anderson et al., 2021). When developing a treatment plan, the goal is to pursue the most curative approach possible while also preserving the patient's functional abilities, such as speech and swallowing (Johnson et al., 2020).

1.4.2. CLINICAL TRIALS AND CYTOTOXIC AGENTS

Despite the application of various treatment modalities for HNSCC patients, including chemoradiotherapy, targeted therapy, and immunotherapy, overall clinical outcomes have not shown a significant therapeutic advantage. Individuals with metastatic HNSCC typically face a poor prognosis, as the disease is often considered incurable at this stage (Goel et al., 2022). Currently, only a limited number of therapeutic approaches have demonstrated the ability to improve progression-free survival (PFS) or overall survival (OS) (Marur and Forastiere, 2016).

Although included in the standard treatment regimen, some of the therapies used in treating cancer can have a negative impact on the patient's quality of life. Radiotherapy, for example, requires different techniques, doses, fractionation schemes, and fields based on the specific condition of the patient. Radiotherapy complications, however, are very common in HNSCC patients. Modern techniques of radiotherapy, such as image-guided radiotherapy or intensity-modulated radiotherapy, alleviate the extent of the side effects due to the reduction of radiation delivered to the surrounding healthy tissue while also precisely covering the targeted area (Yeh, 2010).

Chemotherapy's effectiveness, for example, is usually evaluated using several prognostic markers, which help to predict clinical outcomes. Among these, previous treatments (such as chemotherapy, radiotherapy, surgery, or other interventions) and the cancer stage at diagnosis are the most critical factors affecting treatment response (Colevas, 2006). Despite these limitations, several pharmacological agents, particularly monoclonal antibodies, have exhibited significant potential in treating HNSCC, and many are currently being evaluated in clinical trials (Kozakiewicz and Grzybowska-Szatkowska, 2018).

A substantial number of clinical studies have confirmed the therapeutic efficacy of various treatments, including chemotherapy, radiation, immunotherapy, and targeted therapy (Moreira et al., 2017; Samra et al., 2018). Among these treatment options, a combination regimen of docetaxel, cisplatin, and 5-fluorouracil (5-FU) has emerged as particularly promising. Furthermore, these three drugs are the most frequently utilized medications in clinical trials globally (Goel et al., 2022). However, recent advancements in immunotherapy and targeted therapy have highlighted the potential for monoclonal antibody-based treatments. Drugs such as nimotuzumab, nivolumab, zalutumumab, pembrolizumab, panitumumab, and cetuximab, are among those that could play significant roles in future HNSCC management (Kozakiewicz and Grzybowska-Szatkowska, 2018).

Findings from various clinical trials have shown the efficacy of multi-combinational therapy. A combination of docetaxel with cisplatin and 5-fluorouracil (5-FU), followed by chemoradiotherapy (with weekly carboplatin), has led to improved three-year overall survival (OS) rates compared to a combination of only cisplatin and 5-FU (Posner et al., 2007). The main adverse effect observed in these treatments was

grade 3/4 neutropenia (a significant drop in white blood cell count), which was frequently reported. Despite its benefits, the docetaxel with cisplatin and 5-fluorouracil regimen also raised toxicity concerns, with 25.8% of patients experiencing grade 3-4 neutropenia and 7% experiencing treatment-related deaths (Lionnel Geoffrois et al., 2016). This underlines the critical issue of chemotherapy-induced toxicity in HNSCC treatment (Fayette et al., 2016).

Another potential therapy in the current treatment landscape for HNSCC is molecular-targeted therapy, with clinical trial results indicating a shift toward more tailored therapeutic approaches (Kozakiewicz and Grzybowska-Szatkowska, 2018). This type of therapy focuses on targeting molecules directly involved in the growth, progression, and spread of cancer, interfering with specific biological pathways or proteins more prominent or sometimes unique in cancer cells (Min and Lee, 2022). Some key molecular targets are Epidermal Growth Factor Receptor (EGFR), which is a protein that promotes cell growth and division when activated and it is often overexpressed in many cancers, including HNSCC, Vascular Endothelial Growth Factor (VEGF), which is a signal protein that stimulates the formation of blood vessels, therefore, targeting VEGF can inhibit tumour growth by restricting its blood supply, and Phosphatidylinositol 3-kinase (PI3K), which is an enzyme involved in cellular functions such as growth, proliferation, and survival. Abnormal PI3K signaling is linked to cancer progression (Goel et al., 2022).

Accounting for all of these aspects, while there are a variety of therapeutic strategies currently used in treating HNSCC, the complexity and variability of HNSCC is still a challenge when trying to achieve consistent treatment success. Ongoing research,

particularly in targeted therapies, immunotherapy, and the identification of biomarkers, is essential to improve outcomes for patients with HNSCC (Goel et al., 2022).

1.5. EMERGING TECHNOLOGIES: PLASMA-BASED TREATMENTS

1.5.1. INTRODUCTION TO PLASMA

The concept of plasma in medicine has been actively developing at a high pace in the last two decades, going from initial discovery to *in vivo/in vitro* pre-clinical trials and clinical trials that highlight its beneficial application in wound healing, tissue regeneration, disinfection, and even cancer treatment due to its anti-tumoral effects (Braný et al., 2020).

The surge of studies focusing on this innovation in the medical field emphasizes the vast prospects plasma promotes in developing novel approaches to treating different diseases, with supposedly fewer side effects or with an enhanced effect when used in combination therapy. Moreover, plasma research requires a multidisciplinary approach, and all the results so far have come to fruition due to the collaboration between the plasma physics community, chemists, and multiple health experts in life sciences and clinical medicine (Laroussi, 2020).

The beginning of plasma science started back in 1879, with William Crookes, which ionized gas in an electrical discharge tube after applying a high voltage through a voltage coil, and the result was firstly called 'radiant matter' and later, in 1927, Irving Langmuir changed the term to 'plasma' (Langmuir, 1928; Braný et al., 2020). Therefore,

plasma, the fourth state of matter, could be described as an ionized gas formed through the disintegration of polyatomic gas molecules or the discharge of electrons from monatomic gas shells (Adhikari and Khanal, 2013).

There are also three rules an ionized gas needs to follow in order to correctly be referred to as 'plasma', and these rules focus on plasma frequency, macromolecular neutrality, and Debye shielding. The macromolecular neutrality that characterises plasma is attributable to the fact that the net resulting charge of the ionized gas is zero, which means that plasma has essentially the same density of electrons (negative charge) and protons and other heavy particles (positive charge). The motion of these particles in plasma triggers the formation of electric fields and the further development of magnetic fields. Debye shielding, made of all the charged plasma particles, plays an important role in shielding the electrostatic fields formed inside the ionized gas. Finally, yet importantly, the plasma frequency helps plasma go back to its neutral charge if external factors are affecting its equilibrium conditions (Chaudhary, Imam and Ali, 2017; Adhikari and Khanal, 2013).

Considering temperature, plasma can be high temperature (10^8 K, the same temperature found in the solar core), thermal (2×10^4 K), and non-thermal (between 300 and 1000K in artificial conditions). The difference between the three groups stands in the electron density, with high-temperature and thermal plasma having higher ionization and electron density than non-thermal (cold) plasma.

In plasma with low ionization, such as cold plasma, which has ionization only up to 1%, the neutrally charged interactions between particles trigger multiple coulomb interactions, which lead to particle collisions. Particle collisions, such as electron-electron, have higher temperatures than ions and neutrons when they reach

thermodynamic equilibrium, but this type of collision cannot transfer kinetic energy to bigger particles (Chaudhary, Imam and Ali, 2017).

Regarding pressure, cold plasma can be triggered at both low and atmospheric pressure, and their benefits are diverse. The first studies on low-pressure cold plasma concluded that treating surfaces with plasma is more effective than conventional sterilisation (Fiebrandt, Lackmann and Stapelmann, 2018), while cold atmospheric plasma (CAP) has been proven to reduce microbial load (Napp et al., 2015).

This discovery is of high relevance due to the health concerns the world is facing nowadays with accentuated antibiotic resistance against certain bacteria strains, such as *Clostridium difficile* (C-diff) and Methicillin-Resistant *Staphylococcus aureus* (MRSA), and the difficulties encountered when treating chronic wounds, which are susceptible to bacterial infections, such as diabetic foot ulcers, venous ulcers or ischemic ulcers (Laroussi, 2020).

Alongside this, CAP has emerged as a promising tool in modern medicine, demonstrating significant potential across various therapeutic applications. It has already been successfully used in the clinical treatment of chronic wounds and skin disease, where it has shown the ability to promote healing and reduce inflammation (Braný et al., 2021).

In laboratory research, CAP has exhibited remarkable effects, including a selective decrease in the viability of tumour cells, which raises its potential as a cancer treatment. Furthermore, the synergy between CAP and standard pharmaceuticals is an exciting area of exploration, as studies suggest that combining plasma treatment with

conventional drugs may enhance their effectiveness and improve overall treatment outcomes (Braný et al., 2021).

Overall, the unique properties of CAP present a wide range of opportunities for advancing medical treatments, and ongoing research is essential to fully realize its benefits for patients (Figure 5).

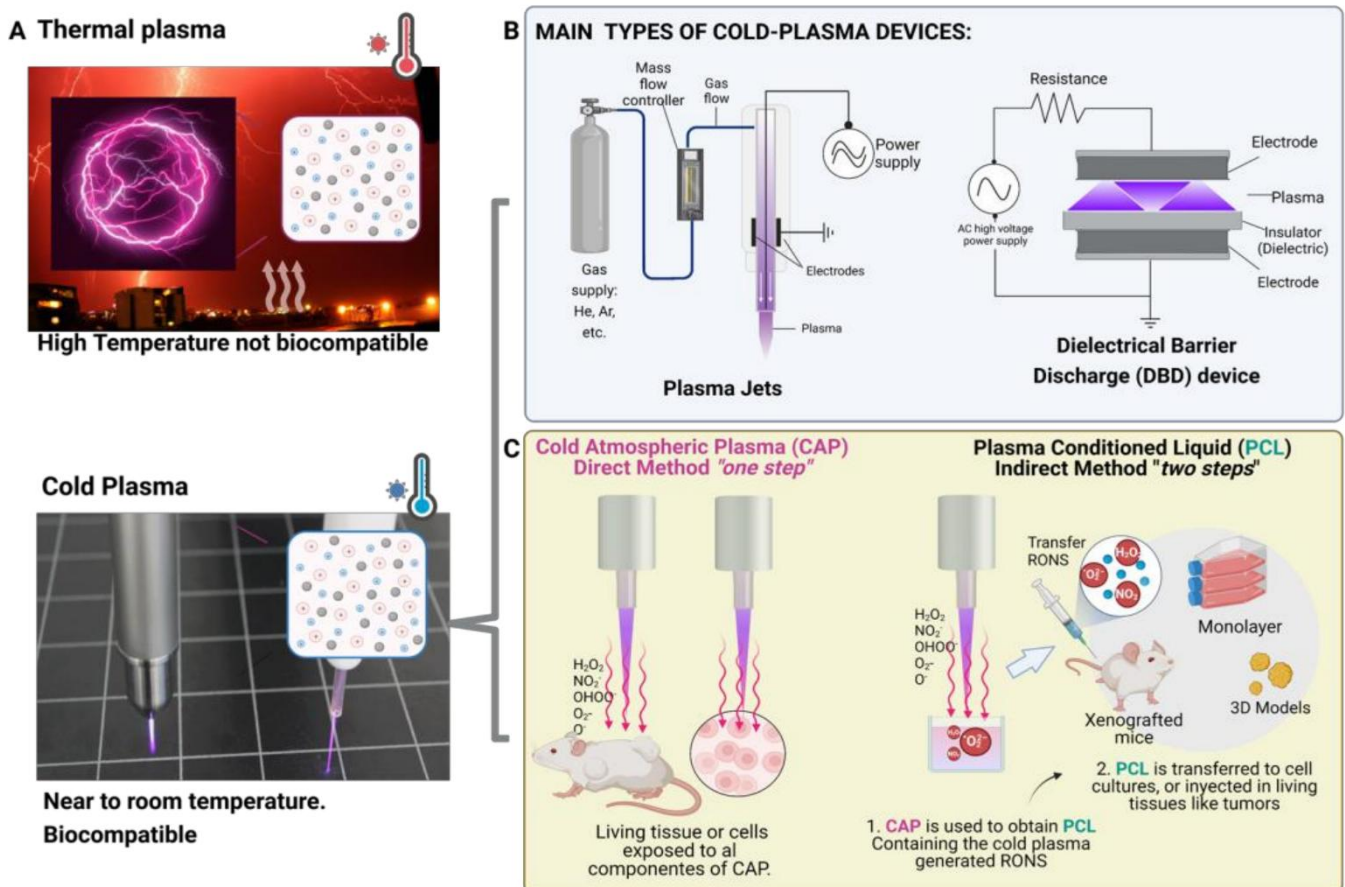


Figure 5: Introduction to cold atmospheric plasma (CAP) (Murillo et al., 2023). A – Atmospheric plasma can be thermal (functional at very high temperatures) or cold (appropriate for biomedical applications due to functioning at room temperature). B – types of CAP delivery devices used in cancer research: plasma jet and dielectric barrier discharge. C – types of applications in tissue or cell culture. The direct application involves the plasma itself being applied directly to the tissue or cells. All the components of plasma come into contact with the target, affecting the tissue or cells directly. For the indirect application, plasma is used to treat a liquid (creating the PCL), which contains the cytotoxic components generated by plasma. This liquid is then applied to the tissue or cells.

1.5.2. PLASMA COMPONENTS AND THEIR ROLE IN DNA DAMAGE

Over the past two decades, research on cold atmospheric plasma (CAP) has focused largely on its anti-cancer properties, which are primarily linked to CAP's ability to generate reactive oxygen species (ROS) and reactive nitrogen species (RNS) (Braný et al., 2021). These reactive species are highly significant in cancer treatment due to their potential to induce oxidative stress that can selectively harm tumour cells. Additionally, studies have explored CAP's influence on nitric oxide (NO) production, as NO plays a critical role in stimulating stem cell proliferation, which is vital for regenerative processes (Laroussi, 2020; Semmler et al., 2020).

Interestingly, healthy cells can activate their antioxidant defences to counter ROS and RNS, enabling them to survive CAP exposure with minimal damage (Snezhkina et al., 2019). By contrast, cancer cells already have elevated ROS levels and altered redox regulation mechanisms, making them particularly vulnerable to further increases in ROS and RNS triggered by CAP (Woedtke et al., 2019; Aggarwal et al., 2019).

This differential response allows CAP to target cancer cells more effectively while sparing healthy cells. Another reason tumour cells are thought to be more susceptible to CAP is their high replication rate. Attributable to this fact, they enter the S phase of the cell cycle, when DNA is unwound and thus more vulnerable, more frequently. Tumour cells are especially sensitive to CAP's ROS and RNS effects when this process takes place (Van der Paal et al., 2017).

Nonetheless, the response of cancer cells to CAP-generated reactive species varies with concentration. For example, at lower concentrations, hydrogen peroxide

(H₂O₂) can promote cell growth, while at higher concentrations, it can induce programmed cell death (apoptosis) (Thannickal and Fanburg, 2000). Similarly, nitric oxide (NO) has concentration-dependent effects: at low levels, NO can protect cells by reducing protein and lipid oxidation, stabilizing cell membranes, and limiting apoptosis; at higher concentrations, however, NO becomes cytotoxic, leading to cell damage (Kong et al., 2009). This concentration-dependent response of cancer cells to CAP highlights the complexity and the potential for precise modulation in CAP-based therapies.

Another strong interaction CAP could have with cells involves lipid peroxidation. In this process, a chain reaction in which oxidants and free radicals damage the lipids within the cell membrane is triggered. Most affected lipids in this process are the ones with carbon double bonds (e.g. polyunsaturated fatty acids) (Ayala, Muñoz and Argüelles, 2014; Gaschler and Stockwell, 2017). When low levels of lipid peroxidation are generated in healthy cells, the antioxidant defense mechanism of said cells is triggered, leading to increased production of antioxidant proteins that aid in counteracting oxidative stress, allowing cells to repair mild oxidative damage. Despite that, when the levels of lipid peroxidation are excessive, those defence mechanisms can no longer be able to perform their essential function. This would lead to apoptosis or even necrosis if the damage is extensive (Ayala, Muñoz and Argüelles, 2014; Gaschler and Stockwell, 2017).

Moreover, lipid peroxidation can disrupt the structure of lipids in the cell membrane, negatively affecting the membrane stability. High levels of peroxidation can generate pores in the membrane, which in turn allow reactive species and radicals to penetrate more easily into the cell (Ayala, Muñoz and Argüelles, 2014; Gaschler and Stockwell, 2017). Tumour cells, in particular, often have a unique lipid composition and

altered cholesterol levels in their membranes, which can make them more vulnerable to this peroxidation process (Szlasa et al., 2020; Preta, 2020; Semmler et al., 2020). As reactive species enter through these pores, they can interfere with critical cellular signaling pathways, causing signaling disruptions that may lead to cellular dysfunction or even cell death (Redza-Dutordoir and Averill-Bates, 2016; Zhang et al., 2016). This vulnerability in tumour cell membranes can potentially be used in targeted therapies, as it allows for selective damage to cancer cells while sparing healthier ones.

Besides reactive species and radicals, CAP also generates ultraviolet (UV) radiation, another factor that could negatively interact with cells. CAP-generated UV radiation can trigger the formation of pyrimidine dimers, damaging cellular DNA. These pyrimidine dimers are aberrant covalent links between adjacent pyrimidine bases in DNA. The generation of pyrimidine dimers increases cytotoxicity and cell mutagenicity (Goto et al., 2015).

The two most encountered types of pyrimidine dimers generated by UV radiation are pyrimidine (6-4) pyrimidone photo-products, formed due to a single covalent bond between the carbon at the 6 position on one ring and the carbon at the 4 position on the neighbouring ring, and cyclobutane pyrimidine dimers (CPDs), which form when two adjacent pyrimidine bases (e.g. thymine or cytosine) become directly bonded, generating a cyclobutane ring (Goto et al., 2015). The normal DNA structure and function are negatively affected by the increased number of CPDs and 6-4 photo-products, raising the probability of mutations and cell death. Since CAP can emit UV radiation across variable wavelengths that can drive pyrimidine dimer formation (Jiang et al., 2009), this poses a potential safety risk, particularly if exposure is too intense or prolonged.

Thus, while CAP holds therapeutic promise, it must be applied in carefully controlled dosages and under regulated conditions to minimize the risk of unintended cellular damage (Braný et al., 2021).

1.5.3. PLASMA PHARMACOKINETICS: IMPLICATIONS FOR DRUG DELIVERY

Conventional, up-to-date anti-cancer treatments frequently cause side effects due to the high and repeated doses of drugs required to achieve a therapeutic impact. This need for potent dosing often leads to toxicity, impacting not only cancer cells but also healthy cells, resulting in adverse effects for the patient (Pucci, Martinelli and Ciofani, 2019).

To address this, current research worldwide is focused on strategies that could generate the same therapeutic outcomes with lower drug dosages, therefore reducing side effects. Emerging research suggests that CAP may help meet this goal by enhancing the effectiveness of cancer treatments when used in combination with chemotherapeutic and pharmaceutical agents. CAP has shown potential in synergistic therapies, meaning that, when combined with conventional drugs, it could allow for effective cancer cell targeting at lower doses, reducing the likelihood of side effects and improving the overall safety of treatment (Braný et al., 2021).

While medical CAP devices have undergone stringent safety testing, there are possible issues regarding their use on tissues due to the potential effects of CAP-generated hydroxyl radicals. Although they may hold therapeutic promise for treating conditions such as cancers, their delivery carries potential mutagenic risks that warrant

careful evaluation (Sabrin et al., 2024). In addition to this, another challenge plasma medicine faces when using CAP as a therapy option is the precise delivery and control of clinically relevant doses of reactive oxygen and nitrogen species (RONS) in the millimolar range. Most CAP sources produce these RONS only in the micromolar range, making therapeutic concentrations hard to achieve (Sabrin et al., 2024).

Plasma-activated hydrogel therapy (PAHT) is a cutting-edge technology designed to address chronic diseases, including wounds and cancer while mending the side effects of hydroxyl radicals triggered by CAP and the limitation of clinically relevant doses (Sabrin et al., 2024). Research has shown that using a hydrogel film between CAP and the target tissue effectively blocked all hydroxyl radicals from reaching the target without affecting the passing of RONS. This finding suggests that hydrogels can serve as a protective barrier to minimize the potentially harmful cytotoxic effects of short-lived radicals while preserving the therapeutic benefits of CAP by delivering beneficial RONS to the target tissue (Sabrin et al., 2024). Moreover, PAHT can trigger the generation of higher RONS doses through electrochemical methods. Advanced sensor technologies paired with PAHT could allow for real-time, *in situ* monitoring of key parameters, promising a solution for precise control when administered to patients (Sabrin et al., 2024).

The potential of PAHT is currently being investigated across various medical applications, offering promising prospects for novel therapeutic approaches in wound healing and diseases such as cancer. Integrating PAHT with antimicrobial or chemotherapeutic agents represents a potential advancement in addressing diverse medical challenges, including HNSCC.

1.6. CONCLUSION AND AIMS

A diagnosis of head and neck squamous cell carcinoma (HNSCC) is often associated with a poor prognosis and complex symptomatology, highlighting the urgent need for more effective therapeutic strategies that enhance treatment efficacy and functional outcomes. The integration of conventional treatment approaches with innovative therapies represents a promising avenue for advancing HNSCC management. Emerging technologies such as cold atmospheric plasma (CAP) and plasma-activated hydrogel therapy (PAHT) show significant potential in diverse applications, including blood coagulation, disinfection, tissue regeneration, wound healing, and cancer treatment.

In the next chapters, we will discuss whether or not the anti-proliferative effects of chemotherapeutics (e.g. cisplatin) or DDR inhibitors such as adavosertib, olaparib, ceralasertib, and AZD1390 may be boosted by the co-treatment with CAP, in both 2D and 3D cultures of two HNSCC cell lines, A253 and FaDu. The anti-proliferative effects of the co-treatment will be evaluated through cell proliferation assays, spheroid growth assays, and the detection of the DNA damage marker γ H2AX using immunofluorescence. Additionally, cisplatin-loaded hydrogels have also been tested in order to assess the future potential of PAHT therapy in the locoregional treatment of HNSCC.

2. MATERIALS AND METHODS

2.1. MATERIALS

2.1.1. REAGENTS

All reagents were purchased from Thermo Fisher Scientific and Sigma Aldrich, or as otherwise specified. All cell culture media, penicillin/streptomycin, trypsin, and fetal bovine serum (FBS) were purchased from Gibco or Labtech. Cell culture flasks and cell culture dishes were from Thermo Fisher Scientific, Corning incorporated or Sarstedt.

2.1.2. ANTIBODIES

Table 1. Table of primary and secondary antibodies for Immunofluorescence staining.

Type of antibody	Antibody	Manufacturer/Information	Concentration	Application
Primary	γ -H2AX (pS139) (M)	Abcam, ab26350, monoclonal	1:500	IF
Secondary	Anti-mouse, Alexa Fluor Plus 488	Invitrogen, A32723, polyclonal	1:1000	IF

2.1.3. BUFFERS AND SOLUTIONS

Table 2. Table of compositions for buffers and solutions.

Solution	Recipe
Alamar Blue	5% (w/v) in PBS
Blocking Solution	5% (w/v) skimmed milk powder in TBST or 5% (w/v) BSA in TBST
Bovine serum albumin (BSA)	3% (w/v) in TBST
Vectashield® (Vector Laboratories)	Proprietary formulation (contains antifade agents and DAPI)
Tris-Buffer Saline (10X TBS)	50 mM Tris-Cl, 150 mM NaCl, pH 7.5 in MQW
Tris-Buffer Saline with Tween (1X TBST)	10% (v/v) 10X TBS, 0.1% (v/v) Tween-20
Phosphate-buffered saline (PBS)	1 tablet in 500 mL MiliQ water to produce a solution of 10 mM phosphate, 150 mM sodium chloride, pH 7.3-7.5.

2.1.4. SPHEROID STAINING

Table 3. Table of stains used for live cell staining of spheroids.

Type of stain	Manufacturer Information	Stock Concentration	Working Concentration	Dilution Factor	Application
SYTOX™ Green Nucleic Acid Stain	Invitrogen	5 mM	100 µM	1:50	Live cell staining of spheroids
Hoechst 33342	Invitrogen	10 mg/mL	1 mg/mL	1:1000	Live cell staining of spheroids

2.1.5. TISSUE CULTURE

Head and neck cancer cell lines (A253 and FaDu) were obtained from Dr Jason Parsons' laboratory at the University of Birmingham and were cultured in Dulbecco's modified eagle's medium (DMEM) (Gibco) with 10% (v/v) of fetal bovine serum (FBS) (Sigma-Aldrich), 4 mM L-glutamine, 25 mM D-glucose, 1 mM sodium pyruvate and 1% (v/v) penicillin/streptomycin(PS) (100 units penicillin and 10 µg streptomycin/mL) (Gibco). Cells were grown in an incubator at 37°C and 5% CO₂. Cells were harvested using 0.05% Trypsin (Gibco).

Cells were passaged for no more than thirty passages from the purchased stock. To passage the cells, media were removed from the flask and cells were then washed with PBS and incubated for 2-5 min, depending on cell line, with trypsin at 37°C. Media were added to the trypsinised cells to achieve the desired dilution to seed into new plates or flasks after cell counting using a haemocytometer (Counting chamber, Hawksley, AC1000) and a microscope (AE2000, Motic).

2.1.6. COLD ATMOSPHERIC PLASMA JET

The Cold Atmospheric Plasma (CAP) jet used in this paper comprises a glass tube with a 4 mm inner and a 6 mm outer diameter, and a single, cylindrical copper electrode of 15 mm length and a distance of 40 mm from the nozzle. The electrode was powered by a PVM500 power supply produced by Information Unlimited, USA, and the flow rate of helium gas (BOC) that passed through the glass tube was modulated using a digital mass flow controller produced by APEX, USA, fixed at 0.5 standard litres per minute

(SLPM). The input voltage supplied to the electrode was fixed at 10 kV_{p-p} (peak-to-peak) at a frequency of 30 kHz. This plasma jet has previously been described by Gaur et al., 2020 (Figure 6).

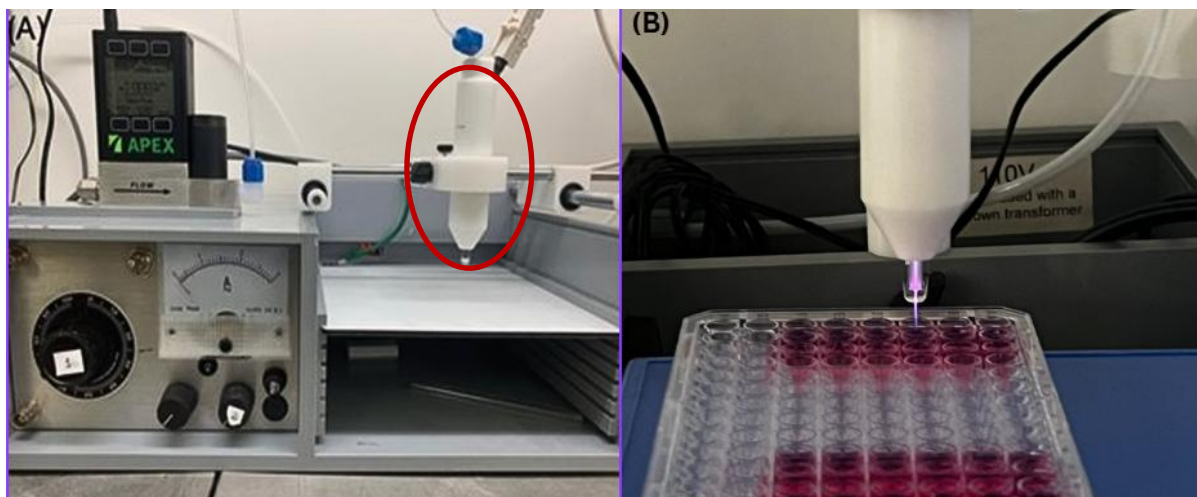


Figure 6: Helium cold atmospheric pressure plasma jet set-up. (A) General CAP jet set-up, displaying the polytetrafluoroethylene (PTFE) housing that covers the glass tube and the electrode (circled in red), the PVM500 power supply, and the digital APEX mass flow controller. **(B)** A photograph taken during the experiments, showing how the plasma jet was used to treat cells in a 96-well plate.

2.1.7. COMPOSITE HYDROGELS

The composite hydrogels used in this paper have been manufactured by Dr Naing Thet in Professor Toby Jenkin's laboratory at the Department of Chemistry of the University of Bath (Gaur et al., 2023).

The composite hydrogels were prepared by dissolving cisplatin (Sigma-Aldrich) in deionized water at a concentration of 0.3 mg/mL. After fully dissolving, PAA (sodium polyacrylate) particles (SAVIVA, BASF), 1% w/v concentration, were added to the cisplatin solution and left at room temperature for 30 minutes, for the PAA particles to

absorb cisplatin. The resulting particles were washed with water and ethanol under vacuum, using a Büchner funnel. After washing, the PAA particles were dried by repeated freeze-thaw cycles using liquid nitrogen and washing with ethanol. After this process, the PAA particles were dried at 60°C under vacuum until a dry powder was achieved. 5 g of PVA (cryo-crosslinked poly(vinyl alcohol)) (Sigma-Aldrich) and 100 mg of dried PAA particles were combined to obtain a homogeneous powder. This powder was dissolved in 100 mL of deionized water and kept in a water bath at 95 °C for 1 h. 20 mL of the cisplatin-PAA-PVA solution were then added to a 9 cm-diameter Petri dish and spread evenly, before being stored at -20 °C until frozen and then defrosted at 25 °C.

2.2. METHODS

2.2.1. CELL PROLIFERATION ASSAY: CISPLATIN AND DDR INHIBITORS

A253 and FaDu were trypsinised and seeded (see Section 2.2) into 96 well plates at 1250 cells per well and incubated at 37°C and 5% CO₂ overnight. Cells were treated with the test compounds at the desired dose, ranging from 0 to 20 µM (Cisplatin, AZD1775, AZD1390, AZD6738) or 0 to 500 µM (Olaparib), and used DMSO as a vehicle control. Compounds were supplemented into 200 µL of media and incubated at 37°C and 5% CO₂ for 72 h. 20 µl of filter-sterilised resazurin solution (100 mg/ml in PBS) was added to each well. Plates were incubated for 3 h at 37°C and 5% CO₂ incubator and the product were measured by absorbance at 570 nm (reference absorbance 595 nm) every

1 h using a Tecan Infinite 200 PRO plate reader. Data analysis was performed using GraphPad Prism 9.2.0.

2.2.2. CELL PROLIFERATION ASSAY: COLD ATMOSPHERIC PLASMA

A253 and FaDu were trypsinised and seeded (see Section 2.2) into 96 well plates at 1250 cells per well and incubated at 37°C and 5% CO₂ overnight. Cells were treated, before or after 30 and 60 seconds of direct CAP (see section 2.1.6) treatment, with the test compounds at the desired dose (1.5 µM Cisplatin, 0.5 nM AZD1390, AZD6738, 1 µM Olaparib, 300 nM AZD1775) and DMSO as vehicle control (0.1% (v/v) DMSO).

Compounds were supplemented into 200 µL of media and incubated at 37°C and 5% CO₂ for 72 h. 20 µL of filter-sterilised resazurin solution (100 mg/ml in PBS) was added to each well. Plates were incubated for 3 h at 37°C and 5% CO₂ incubator and the product was measured by absorbance at 570 nm (reference absorbance 595 nm) using a Tecan Infinite 200 PRO plate reader. Data analysis was performed using GraphPad Prism 9.2.0.

2.2.3. CELL PROLIFERATION ASSAY: COMPOSITE HYDROGELS

A253 and FaDu were trypsinised and seeded (see Section 2.2) into 96 transwell plates at 1250 cells per well and incubated at 37°C and 5% CO₂ overnight. Cisplatin-loaded hydrogel discs (see section 2.1.7) of 0.6 mg/mL concentration and 3-4 mm thickness were prepared using a biopsy punch and then treated with CAP (see section

2.1.6) for 120 seconds (Figure 7). After treatment, the CAP-activated cisplatin-loaded hydrogel discs were placed on top of the target cells and the plate was incubated at 37°C and 5% CO₂ for 72 h. 20 µl of filter-sterilised resazurin solution (100 mg/ml in PBS) was added to each well after incubation. Plates were incubated for 3 h at 37°C and 5% CO₂ incubator and the product was measured by absorbance at 570 nm (reference absorbance 595 nm) using a Tecan Infinite 200 PRO plate reader. Data analysis was performed using GraphPad Prism 9.2.0.



Figure 7: Cisplatin-loaded hydrogel discs. Before being applied to the monolayer culture in 96-transwell plates, the cisplatin-loaded hydrogel discs were activated by CAP as shown in these photographs. The CAP treatment was applied for 30 or 60 seconds from a 1 mm distance.

2.2.4. FOR IMMUNOFLUORESCENCE

Cells were trypsinised and seeded (see Section 2.2) at 1250 cells per well for A253 and FaDu in a 96-well glass bottom plate. For co-treatment with CAP (see section 2.1.6), cells were treated with Cisplatin, AZD1775, AZD1390, AZD6738, Olaparib or

DMSO control (0.1% (v/v) DMSO) at different concentrations (see Section 2.2.2) for 1 hour before direct CAP application. Samples were then directly treated with CAP for 60 seconds, and incubated at 37°C, 5% CO₂ for 24 hours before immunofluorescence.

2.2.5. SPHEROID TREATMENT AND STAINING

A253 and FaDu were seeded into Nunclon Sphera 3D culture 96 well plates at 1250 cells per well and incubated at 37°C and 5% CO₂ for 3 days. Spheroids were then treated with a combination of the test compound at the desired dose, ranging from 0 to 50 µM cisplatin, and direct CAP treatment (see section 2.1.6) for 240 seconds. The spheroid growth was recorded for 5 days using a ZEISS Axio Zoom.V16 microscope, 32x magnification objective (Plan-NEOFLUAR Z 1.0x, NA 0.25). Images were captured using a ZEISS AxioCam 506 mono camera with 200 ms exposure time and analyzed in Fiji (ImageJ). After 5 days of growth, spheroids were labelled with SYTOX Green and Hoechst 33342 to analyse cytotoxicity, using a ZEISS Axio Zoom.V16 microscope, 52x magnification objective (Plan-NEOFLUAR Z 1.0x, NA 0.25).

2.2.6. IMMUNOFLUORESCENCE

See section 2.2.4 for how cells were treated. After treatment, cells were gently washed twice with 3% BSA in PBS before being fixed and permeabilized with 100 µL 4% PFA in PBS per well for 20 min at room temperature. PFA was removed and wells were washed in 3% BSA in PBS twice. 200 µL of 0.5% Triton X-100 in PBS was added per well for 20 min incubation at room temperature. The Triton was removed, and wells

were washed twice with 3% BSA in PBS. 200 μ L of blocking solution (3% BSA in PBS) was added to each well and the plate was incubated in the dark for 1 hour. After incubation, the blocking solution was removed from each well and 50 μ L of primary antibody diluted in 3% BSA in PBS was added per well for 1 hour at room temp protected from light. After the primary incubation, each well was washed thrice with PBS. 50 μ L of secondary antibody diluted in 3% BSA in PBS was added per well for 1 hour at room temperature protected from light. After incubation, wells were washed with PBS 5 times and mounted by adding \sim 25 μ L mounting medium (Vectashield plus DAPI) to each well. The plate was stored at 4 $^{\circ}$ C and protected from light. See Table 2.1 for primary and secondary antibody solutions.

A Zeiss-LSM880-Airyscan confocal microscope and Zen software were used to image the immunofluorescence of stained cells in a 96-well glass bottom plate, using a 20 \times objective dry lens (Plan-Apochromat 20x/0.8 M27) for γ -H2Ax detection. Images were captured with a GaAsP detector and processed using ZEN Black software. Z-stacks were acquired with a 1 μ m step size over a total depth of 20 μ m. Four fields of view were imaged per condition (well) and an average of these was taken to compare repeats. Images were analysed in ImageJ software.

3. CO-TREATMENT OF HNSCC CELLS WITH CISPLATIN AND COLD ATMOSPHERIC PLASMA

3.1. INTRODUCTION

Well-known in the category of chemotherapeutic drugs, **cisplatin** (also known as *cis*-diamminedichloroplatinum (II) or cisplatinum) is a platinum compound that has square planar geometry, only slightly soluble in aqueous solutions. It is usually dissolved in N, N-dimethylformamide and dimethylprimanide when preparing stock solutions for use in cell culture studies or *in vitro* assays. Cisplatin is used as a means of treatment for various human cancers, including testicular, lung, ovarian, bladder and head and neck cancer, affecting carcinomas, sarcomas, lymphomas, and also germ cell tumors (Dasari and Bernard Tchounwou, 2014).

Cisplatin's molecular structure plays a key role in its ability to fight cancer by inhibiting DNA synthesis in a dose-dependent manner. However, despite its effectiveness, its therapeutic use is limited by significant side effects, including renal toxicity, neurotoxicity, and ototoxicity (Tchounwou et al., 2021). These drawbacks, along with the development of drug resistance, make it challenging to maximize cisplatin's efficacy in cancer treatment. Therefore, new strategies are needed to reduce these side effects and overcome resistance. These approaches include searching for less toxic cisplatin analogues, using combination therapies with other cancer drugs, and exploring nanotechnology (Tchounwou et al., 2021).

After being approved by the FDA as the first platinum compound used in cancer treatment (1978) (Kelland, 2007), further studies have been conducted on other metal-containing compounds that could have anticancer properties (Frezza et al., 2010). In addition, multiple studies have focused on the synthesis of cisplatin analogues to enhance its therapeutic index, with 13 of these analogues reaching the clinical trial stage. Carboplatin and oxaliplatin have been the only cisplatin analogues that have received worldwide approval, having similar patient outcomes after treatment, but with a different toxicity profile than cisplatin (Wheate et al., 2010).

One major advantage of carboplatin when compared to cisplatin is the elimination of nephrotoxic effects, which are often-encountered side effects of cisplatin treatment. Carboplatin, however, has strong myelo-suppressive effects, inhibiting the blood cell output from the bone marrow in the body (Dasari and Bernard Tchounwou, 2014). Considering the type of cancer, carboplatin has been proven to be 1/8 to 1/45 as effective, and the standard dosage used clinically is four times higher than the one for cisplatin to achieve the same level of effectiveness (Dasari and Bernard Tchounwou, 2014). Attributable to its more stable properties, once carboplatin enters the body, its stability allows the drug to stay active for longer compared to cisplatin. The drawback of this stability is that it prevents carboplatin from being as reactive as cisplatin – much of the carboplatin remains unaltered and passes through the body without being fully utilized. This is why, in some cases, approximately 60-70% of carboplatin is excreted unchanged in the urine within the first 24 hours after administration, before it has a chance to act on cancer cells (Dasari and Bernard Tchounwou, 2014).

When comparing cisplatin to oxaliplatin, the former typically demonstrates a more favourable tolerability profile, particularly in geriatric patients with advanced

gastric cancer (Montagnani et al., 2011; Chinen et al., 2022), but it is not very effective in treating tumours that have already developed resistance to cisplatin (Bernadett Szikriszt et al., 2020). Additionally, oxaliplatin induces higher amounts of double-strand breaks in DNA through the formation of oxalate-based adducts, surpassing both cisplatin and carboplatin in this regard (Devanabanda and Kasi, 2021). Attributable to the fact that oxaliplatin has an oxalate ligand whereas carboplatin has a carboxylate group bound to platinum, the oxalate ligand makes oxaliplatin more effective against certain types of cancers, such as colorectal cancer, compared to carboplatin. However, oxaliplatin is more likely to cause peripheral neuropathy (Devanabanda and Kasi, 2021), while carboplatin is associated with less severe neuropathy but significant renal toxicity (HAPANI et al., 2022) when compared to oxaliplatin.

The limitations of cisplatin and its analogues are the main reason why new therapeutic approaches need to be studied. Prolonged usage leads to significant toxicity and the development of drug resistance. Efficient treatment options should focus on lowering treatment doses, interfering less with healthy tissue and triggering fewer side effects. Developing new drug delivery systems and new combinational therapies could be the next step towards better quality of life and survival for cancer patients.

3.2. MECHANISM OF ACTION

Cisplatin's cytotoxicity, or its ability to kill cancer cells, is primarily due to its binding to DNA. Once inside the cytoplasm, cisplatin becomes activated by replacing its chloride atoms with water molecules, forming an electrophile that is highly reactive

towards proteins and nucleic acids (Cepeda et al., 2007; Ishida et al., 2002). This allows cisplatin to selectively bind to purine bases in DNA, particularly forming cross-links between two adjacent guanine bases, which further blocks cell division and triggers apoptosis, or programmed cell death (Brown, Kumar and Tchounwou, 2019). In many cases, the cisplatin-DNA interaction occurs at the N7 positions of guanine (imidazole ring), creating strong covalent bonds, a process known as adduct formation. Both interstrand and intrastrand cross-links, as well as nonfunctional DNA adducts, are the factors that lead to the high toxicity of cisplatin (Tchounwou et al., 2021).

Cancer cells have a high metabolic rate, requiring elevated levels of reactive oxygen species (ROS) to support their rapid growth. ROS play a crucial role in activating signaling proteins that promote cell proliferation and regulate various biological pathways essential for tumour development, such as activating ERK1/2 and receptor tyrosine kinases (RTKs) independent of ligands (Sosa et al., 2013). They also help cancer cells evade apoptosis (programmed cell death) and anoikis (detachment-induced cell death) by activating proteins like Src, NF- κ B, and PI3K. In addition, ROS contribute to the secretion of metalloproteinases, enabling tissue invasion, metastasis, and the formation of new blood vessels (angiogenesis) through the release of vascular endothelial growth factors (Sosa et al., 2013).

It has been proven that cisplatin generates ROS either directly or indirectly through mitochondrial processes (Ueda, Kaushal and Shah, 2000). Its cytotoxicity has been linked to lipid peroxidation, a process in which ROS cause damage to cell membranes. This triggers the production of malondialdehyde (MDA), a by-product of lipid peroxidation, which causes oxidative damage to proteins and cell membranes, eventually leading to cell death (Tchounwou et al., 2021). Research has shown that

cisplatin induces DNA damage through significant oxidative stress, leading to lipid peroxidation, reduced glutathione (GSH) activity, and increased MDA levels in different types of cancer cells. These oxidative mechanisms play a major role in cisplatin's ability to kill cancer cells (Tchounwou et al., 2021).

Apoptosis, or programmed cell death, is triggered in cancer cells via two main pathways: intrinsic (mitochondrial) and extrinsic (receptor-mediated). Both pathways involve the activation of caspases, enzymes that break down proteins to initiate cell death (Carneiro and El-Deiry, 2020). The intrinsic pathway is driven by mitochondrial outer membrane permeabilization, leading to the release of pro-apoptotic proteins like cytochrome c, which activates the apoptosome and initiates caspase cascades. The extrinsic pathway is activated by extracellular signals, such as Fas or TNF, which engage death receptors and form the death-inducing signal complex (DISC), activating caspases directly (Fernald and Kurokawa, 2013).

Cisplatin induces apoptosis primarily through the intrinsic pathway, although the specific mechanism varies by cell type. It activates tumour protein p53, which leads to cell cycle arrest by upregulating p21 and downregulating cyclins and cyclin-dependent kinases (Kumar and Tchounwou, 2015). Cisplatin also triggers apoptosis by altering mitochondrial membrane potential, releasing cytochrome c, and increasing caspase 3 activity. The drug can additionally activate stress pathways, such as p38 MAPK and JNK, further promoting apoptosis (Jeong et al., 2002; Perfettini et al., 2005).

Interestingly, cisplatin-induced cell death is not limited to apoptosis. It may also involve necrosis (uncontrolled cell death) or autophagy (self-degradation of cell components), making its effect on cancer cells multifaceted. This highlights the

complexity of cisplatin's action and suggests that its effectiveness can extend beyond a single-cell death mechanism (Gonzalez et al., 2001; Milad Ashrafizadeh et al., 2019).

This study aims to elucidate the synergistic effects of cisplatin in the treatment of HNSCC when administered in conjunction with cold atmospheric plasma (CAP).

3.3. RESULTS AND DISCUSSION

3.3.1. CISPLATIN: CELL PROLIFERATION ASSAY

Knowing the half-maximal inhibitory concentration (IC_{50}) of a drug is essential in evaluating its potency, and it represents the concentration at which the drug inhibits biological processes by 50% (Aykul and Martinez-Hackert, 2016). It plays a key role in drug development, aiding in dosage decisions and evaluation of therapeutic potential. Therefore, a cell proliferation assay was conducted on FaDu (derived from a squamous cell carcinoma of the hypopharynx, p53 mutant) and A253 (derived from a submandibular gland squamous cell carcinoma, p53 negative) cell lines to assess the proliferation of cancer cells, as measured by metabolic activity assay, when treated with different concentrations of cisplatin. This first step was important for the optimization of the cisplatin dose to be used in subsequent experiments.

The two cell lines were, therefore, treated with cisplatin at different concentrations, ranging from 20 μ M to 19.5 nM. After adding the treatment, cells were incubated for 72 hours. The relative proliferation of cells at each cisplatin concentration

was measured using resazurin, after 3 hours of further incubation, at 570nm wavelength (reference 595 nm) (Figure 8). This experiment was conducted in both technical and biological triplicates for both cell lines to assess the reproducibility and reliability of the results. All further calculations were done using the mean of the biological triplicates.

Using the untreated cells as control for 100% proliferation, the top concentration of 20 μM cisplatin inhibited proliferation by 77.2% for FaDu cells and 85.4% for A253 cells. The treatment with 2.5 μM cisplatin inhibited proliferation by 55.4% for FaDu and 45.5% for A253. Therefore, for future experiments, we have considered an IC_{50} value of 2 μM to be the optimal dose of cisplatin for both cell lines.

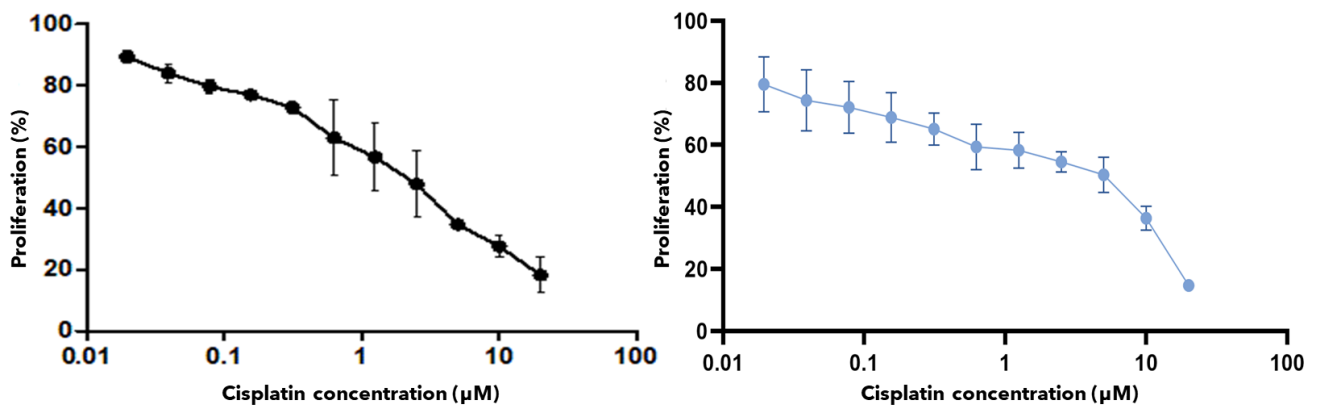


Figure 8: Cell proliferation inhibition rate and IC_{50} for FaDu (A) and A253 (B) cell lines. FaDu and A253 cells were treated with different concentrations of cisplatin (20 μM to 19.5 nM) for 72 h. The IC_{50} value was estimated to be around 2 μM for both cell lines, using the AlamarBlue Assay. This estimated IC_{50} value was used in further experiments. Error bars are \pm SD of biological replicates. A standard curve is fit through the data (SD – standard deviation).

3.3.2. CISPLATIN: DIRECT PLASMA TREATMENT

To assess how potent the plasma treatment is in comparison to cisplatin treatment only, A253 cells were treated with a combination of 1.5 μ M cisplatin an hour before treatment with cold atmospheric plasma (CAP), for 30 and 60 seconds. Plasma operational parameters were 0.5 SLPM (standard litres per minute) helium flow rate, voltage 10kV, frequency 30kHz, and treatment distance 0.5 cm. After CAP treatment, cells were incubated for 72 hours, and metabolic activity was measured using resazurin (Figure 9).

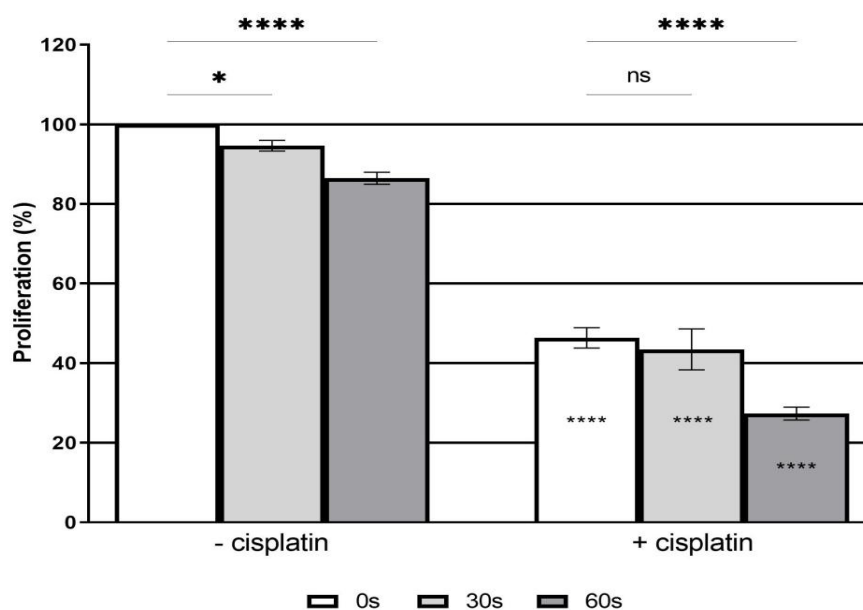


Figure 9: Post-treatment of cisplatin-treated A253 cells with CAP enhances anti-proliferative effects. Cells were treated with 1.5 μ M cisplatin for 1 hour before treatment with plasma for the indicated times, followed by 72h incubation. Error bars are \pm SD RM one-way ANOVA * $p < 0.05$, ** $p < 0.01$, *** $p < 0.001$, **** $p < 0.0001$. Asterisks on the +cisplatin bars are used to compare the relevant condition without cisplatin. Experiments were performed in triplicate and repeated three times with similar results.

The results indicate a significant difference when comparing the 60s CAP-treated condition with the equivalent cisplatin-only condition. Attributable to the fact that there is no significant difference in cell proliferation between the cisplatin-only treated cells and the 30s CAP treatment combination, for further experiments, the 30s treatment was omitted. The data suggests a possible synergistic effect between CAP and cisplatin. This means that the combination of cisplatin and CAP works in a way that enhances each other's actions, allowing for a more powerful response at lower doses than if cisplatin or CAP were used separately. Synergism is especially valuable in therapeutic applications, as it can reduce side effects, improve efficacy, and help in overcoming drug resistance (Castañeda et al., 2022).

The Response Additivity approach is a model that proves there are synergistic effects when the drug combination triggers a greater response when compared to the sum of the impact of the individual drugs (Duarte and Vale, 2022). Based on the results presented in Figure 2, proliferation is inhibited by 53.65% in the cisplatin treatment only, with the CAP treatment only inhibiting proliferation by 5.38% for the 30s treatment and by 13.57% for the 60s treatment. The co-treatment of cisplatin and CAP inhibits proliferation by 56.56% for the 30s treatment and by 72.67% for the 60s treatment.

Taking the Response Additivity approach into account, there is a possible synergistic effect in the co-treatment of cisplatin with CAP for the 60s treatment. The observed proliferation inhibition of the two treatments combined in co-treatment is greater than the sum of the individual effects (67.22%), suggesting a possible synergistic interaction between CAP and cisplatin in the co-treatment. This result indicates that, when applied together, CAP and cisplatin enhance each other's effects,

potentially through complementary mechanisms of action or by targeting different pathways involved in cell proliferation. This probable synergy can result in more effective inhibition of cell proliferation as the treatments work together to overcome cellular resistance or activate different types of cell death (Castorina, Martorana and Forte, 2022).

On the other hand, an additive effect was observed for the 30s co-treatment. The proliferation inhibition of the two treatments combined in co-treatment is lower than the sum of the individual effects (59.03%).

Following the same conditions previously mentioned, the same experiment was conducted with 1.5 μ M cisplatin treatment being added 1 hour after the 30s and 60s CAP treatment. Cells were incubated for 72 hours, and the metabolic activity was measured using resazurin (Figure 10).

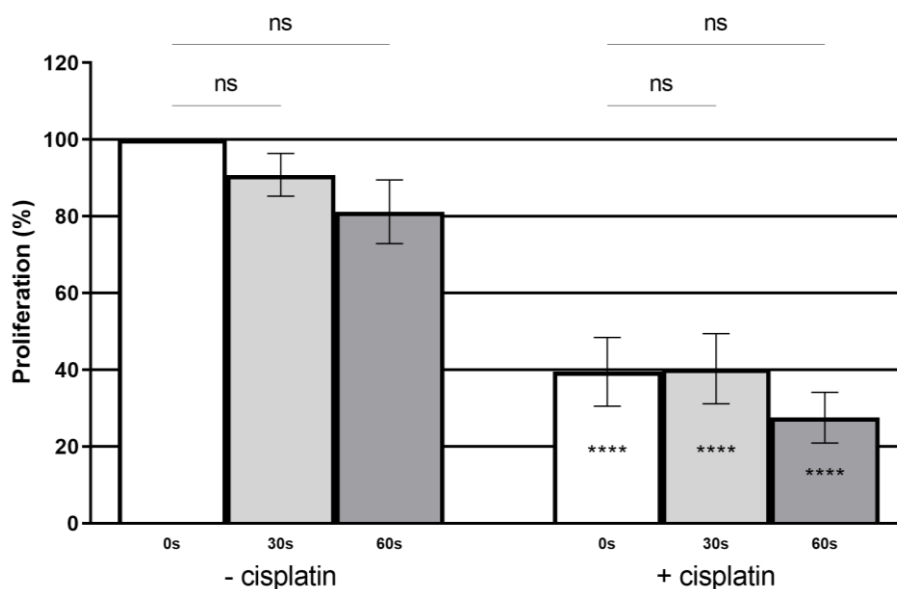


Figure 10: Pre-treatment of cisplatin-treated A253 cells with CAP does not cause statistically significant enhancement of anti-proliferative effects. Cells were treated with CAP for the indicated times, 1 hour before 1.5 μ M cisplatin treatment was administered, followed by 72h incubation. Error bars are \pm SD RM one-way ANOVA * $p < 0.05$, ** $p < 0.01$, *** $p < 0.001$, **** $p < 0.0001$. Asterisks on the +cisplatin bars are used to compare the relevant

condition without cisplatin. Experiments were performed in triplicate and repeated three times with similar results.

The data suggests no significant difference when comparing the CAP treatment only with the untreated cells. However, there is a significant difference ($p < 0.0001$) between the combination of CAP and cisplatin and the relevant condition without cisplatin. We believe that post-treatment of cells with CAP may cause statistically significant greater enhancement of anti-proliferative effects due to cell membrane permeabilisation.

Past studies have shown that plasma can trigger the generation of pores on cell membranes, caused mainly by the electric field and the reactive radicals generated by CAP (Sreedevi and Suresh, 2023). When the hydroxyl (OH) radicals released from the plasma jet into the medium reach the cell membrane, they react with the lipid bilayer, specifically with the polar phosphate head groups of the fatty acids, leading to bond cleavage and peroxidation of fatty acid tails. This generates alterations in the structure of the cell membrane, affecting its permeability (Tero et al., 2014; Yusupov et al., 2017; Yusupov et al., 2017b).

Taking all of these into account, treating the cells with cisplatin 1 hour before applying the CAP treatment could be facilitated by electroporation, allowing cisplatin to enter cells through the channels that open in the cell membrane. The pre-treatment of cells with CAP might not be as effective due to the pores being only temporarily open. Incubating the cells one hour in between treatments allows the cell to seal the pores in the cell membrane, therefore affecting the efficiency of the co-treatment.

In order to assess if the same effect can be observed in a different HNSCC cell line, FaDu cells were treated with a combination of 1.5 μ M cisplatin an hour before 60s CAP treatment, following the same conditions previously mentioned (Figure 11).

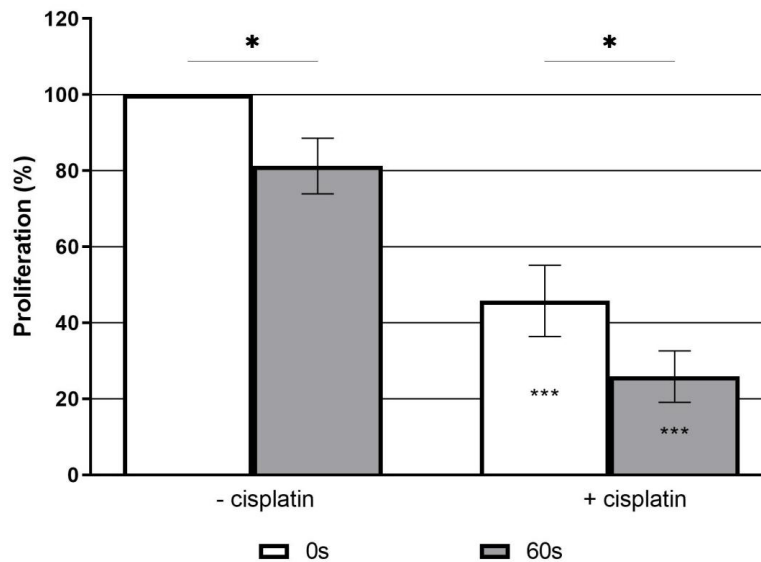


Figure 11: Post-treatment of cisplatin-treated FaDu cells with CAP enhances anti-proliferative effects. Post-treatment of cells (FaDu cell line) with cisplatin before plasma treatment. Cells were treated with 1.5 μ M cisplatin for 1 hour before treatment with plasma for the indicated times, followed by 72h incubation. Error bars are \pm SD RM one-way ANOVA * $p < 0.05$, ** $p < 0.01$, *** $p < 0.001$, **** $p < 0.0001$. Asterisks on the +cisplatin bars are used to compare the relevant condition without cisplatin. Experiments were performed in triplicate and repeated three times with similar results.

The results presented in Figure 11 indicate a significant difference ($p < 0.05$) when comparing the 60s CAP-cisplatin combination with the equivalent cisplatin-only condition. In addition to this, the same likely synergistic effect can be seen in the FaDu cell lines, following the Response Additivity approach. The inhibition rate for the co-treatment of cisplatin and 60s CAP is 76.41%, while the inhibition rate of cisplatin-only treatment is 51.75% and the 60s CAP treatment only has an inhibition rate of 20.5% (their sum is 72.25%, lower than the inhibition rate of co-treatment of cisplatin and 60s CAP).

Therefore, the data corroborates and strengthens the findings of the initial experiment, displaying the enhancement of the anti-proliferative effects of cisplatin when combined with CAP.

3.3.3. CISPLATIN: IMMUNOFLUORESCENCE

Immunofluorescence (IF) is a versatile and sensitive technique used to detect and localize specific antigens within tissues or cell preparations. By leveraging fluorescently labelled antibodies, IF allows the visualization of the distribution and abundance of target proteins with high sensitivity (Im et al., 2019). Compared to immunohistochemistry, IF provides enhanced signal amplification and is compatible with a range of microscopy techniques, including confocal and fluorescence microscopy. IF can be performed using two main approaches: direct immunofluorescence (Primary IF) or indirect immunofluorescence (Secondary IF) (Im et al., 2019).

Primary IF uses a single, fluorescently labelled antibody that binds directly to the target antigen. It is simpler and faster, as it requires only one antibody step, but may have limited signal amplification. In secondary IF, however, an unlabeled primary antibody binds to the target antigen, and a fluorescently labelled secondary antibody, which recognizes the primary antibody, is added. This approach offers greater signal amplification because multiple secondary antibodies can bind to a single primary antibody, making it more suitable for detecting low-abundance targets or achieving stronger signals (Zaqout, Becker and Kaindl, 2020).

To assess the DNA damage triggered in A253 and FaDu cell lines by CAP, secondary IF has been conducted after the treatment of monolayer culture with 1.5 μ M

cisplatin and 60s CAP combination. The primary antibody used in this technique is a γ H2AX antibody, with γ H2AX being a crucial early step in the DDR, as it facilitates the recruitment and localization of DNA repair proteins to the site of damage (Kuo and Yang, 2008). When DNA damage occurs, leading to the formation of DSBs, it triggers the phosphorylation of H2AX, a variant of the H2A histone family that is part of the nucleosome structure. This phosphorylation is carried out by kinases such as ATM and ATR, which are activated in response to DNA damage via the PI3K signaling pathway (Kuo and Yang, 2008).

γ H2AX forms visible foci at the sites of DSBs, representing the damage in a 1:1 correlation, making it a reliable biomarker for assessing DNA damage (Kuo and Yang, 2008). These foci can be visualized using an antibody raised against γ H2AX in techniques such as immunofluorescence, where secondary antibodies amplify the signal for microscopic observation. The secondary antibody used in our experiments is AlexaFluor 488 labelled anti-mouse secondary antibody, which will allow the visualization of γ H2AX in the monolayer culture.

The results of this experiment are presented in Figure 12 and Figure 13 and were focused on qualitative analysis rather than quantitative analysis due to only one repeat having been carried out as a consequence of time limitations. This approach was chosen to observe and evaluate the presence, localization, and overall distribution patterns of γ H2AX within the cells after CAP treatment compared to cisplatin-only treatment. The primary goal was to assess the quality of the signal and confirm the expected expression patterns, rather than to measure fluorescence intensity or quantify the target protein levels.

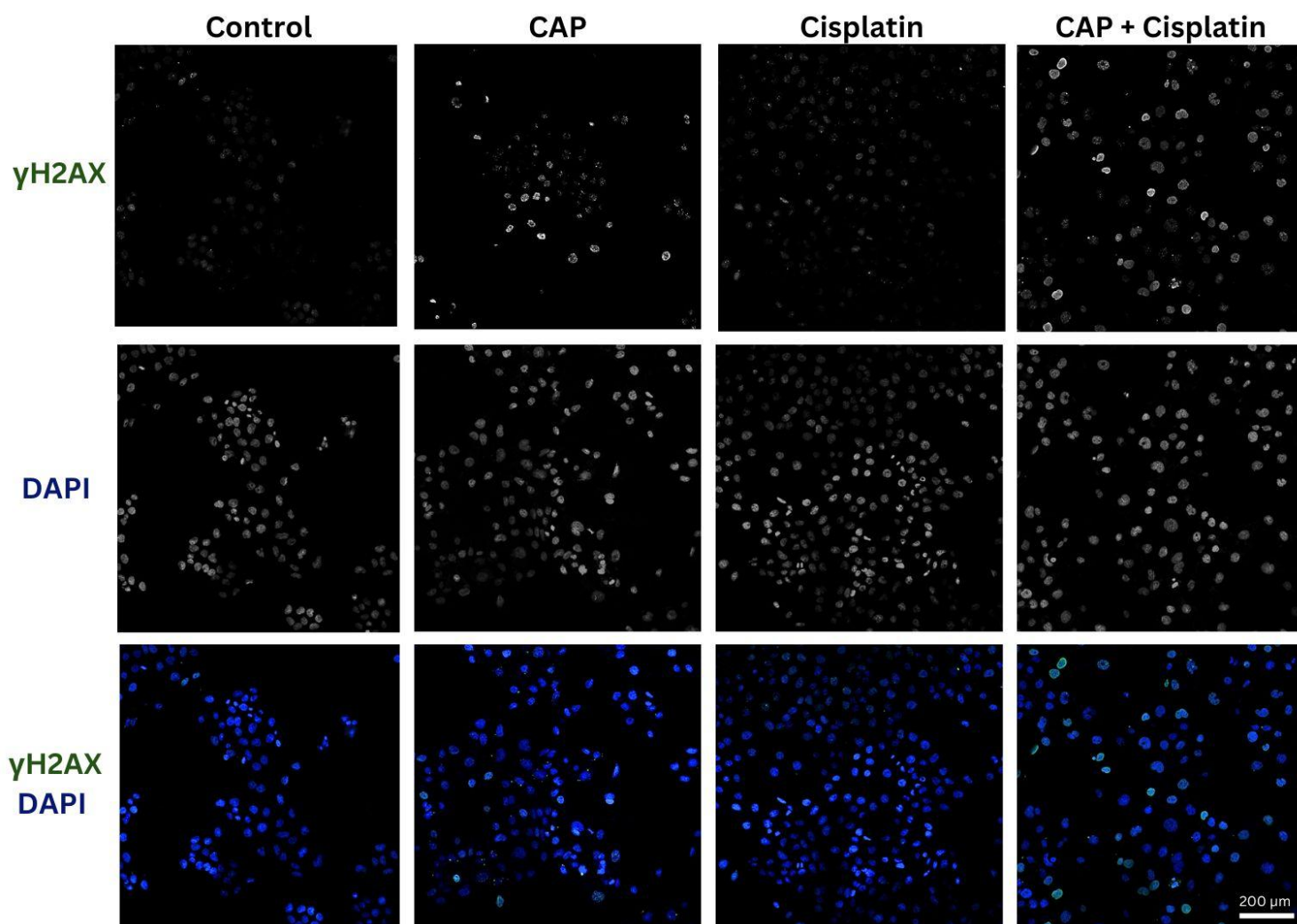


Figure 12: DNA damage after treatment with CAP in the presence or absence of cisplatin in the A253 cell line. A253 cells were incubated with 1.5 μ M cisplatin for 1 hour before treatment with CAP for 60s. After 24 hours of incubation, the cells were fixed and stained with DAPI and anti- γ H2AX antibody, before imaging on a Zeiss LSM880 confocal microscope equipped with a Plan-Apochromat 20x/0.8 M27 objective (n=1). Images were captured with a GaAsP detector and processed using ZEN Black software. DAPI (excitation: 358 nm, emission: 461 nm) and Alexa Fluor 488 (excitation: 488 nm, emission: 525 nm) were used to stain nuclei and cytoplasm, respectively. Z-stacks were acquired with a 1 μ m step size over a total depth of 20 μ m. Image analysis was performed using Fiji (ImageJ) software. Scale bar: 200 μ m.

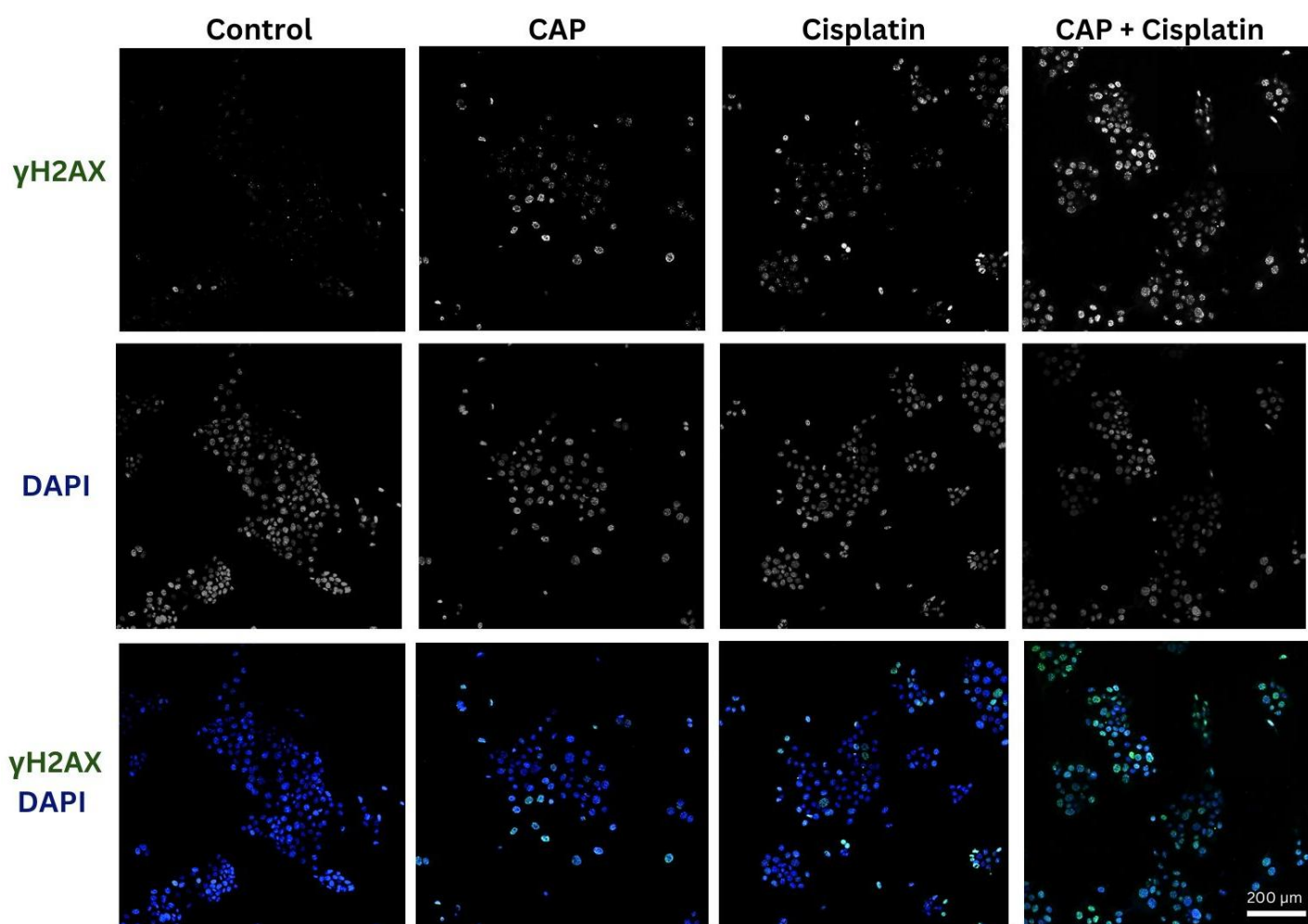


Figure 13: DNA damage after treatment with CAP in the presence or absence of cisplatin in the FaDu cell line. FaDu cells were incubated with 1.5 μ M cisplatin for 1 hour before treatment with CAP for 60s. After 24 hours of incubation, the cells were fixed and stained with DAPI and anti- γ H2AX antibody, before imaging on a Zeiss LSM880 confocal microscope equipped with a Plan-Apochromat 20x/0.8 M27 objective ($n=1$). Images were captured with a GaAsP detector and processed using ZEN Black software. DAPI (excitation: 358 nm, emission: 461 nm) and Alexa Fluor 488 (excitation: 488 nm, emission: 525 nm) were used to stain nuclei and cytoplasm, respectively. Z-stacks were acquired with a 1 μ m step size over a total depth of 20 μ m. Image analysis was performed using Fiji (ImageJ) software. Scale bar: 200 μ m.

The intensity of γ H2AX staining and the proportion of γ H2AX-positive cells is higher in the combination of cisplatin and 60s CAP compared to cisplatin-only treatment or CAP-only treatment for both A253 cells (Figure 12) and FaDu cells (Figure 13) after 24 hours of treatment. The difference in γ H2AX intensity between co-treatment and the application of cisplatin only reflects their distinct effects on DNA

damage and repair processes. Being a marker of DNA damage, higher levels of γ H2AX foci indicate enhanced activity of the DNA damage response. Pairing cisplatin with CAP potentially enhances the cytotoxicity of the oxidative stress triggered by the higher levels of RONS, which is seen in both cell lines. One main catalyst in the high amount of DDR seen in the co-treatment with cisplatin and CAP could be the process of electroporation previously discussed. Because cancer cells have lower cholesterol levels compared to other cell membranes, they are more likely to undergo peroxidation after CAP treatment (Nitsch et al., 2022). The infusion of cisplatin treatment, together with RONS, into the cancer cells could be facilitated by the increased porosity of the cell membrane (Paal et al., 2015), leading to an enhanced presence of γ H2AX in the co-treated cells compared to cisplatin-only treated cells.

These results are consistent with other studies in the literature. A study by Brunner et al. (2022) examined the cytostatic effects of CAP on HNSCC cell lines, both individually and in combination with low-dose cisplatin. The study utilized IF to evaluate DNA damage and apoptosis, finding that CAP exposure significantly reduced cell viability and increased DNA damage. The combination treatment showed additive effects, suggesting that CAP may enhance the therapeutic efficacy of low-dose cisplatin.

Another study by Afrasiabi et al. (2022) compared the effects of CAP and cisplatin on oral squamous cell carcinoma cells, utilizing IF to evaluate mitochondrial damage and apoptosis markers. The study found that both treatments induced mitochondrial damage and apoptosis. However, the combination therapy exhibited enhanced efficacy, suggesting a synergistic effect similar to the results of our study.

These results corroborate the findings of the proliferation assays and further demonstrate that combining direct plasma with an anti-cancer drug is significantly

more effective in inducing DNA damage in both HNSCC cell lines than standalone plasma or drug-only treatment.

3.3.4. SPHEROID TESTING

Our preliminary findings so far demonstrate that the combination of CAP with cisplatin treatment results in significantly enhanced cell death in both cell lines as compared to plasma or drug alone, which could be a significant breakthrough in the multimodal treatment of HNSCC. After testing the 2D monolayer cultures with co-treatment of cisplatin and CAP, future experiments focused on 3D tumour spheroid models, which represent tumour biology and drug responses more accurately, thus enhancing translational relevance. Tumour spheroids mimic the structural and biological features of real tumours more closely than traditional 2D cell cultures. The fact that they are avascular means they replicate the early stages of tumour growth before they develop their blood supply, which is a critical step in cancer progression. This makes spheroids an excellent model for studying early-stage cancer biology and drug responses (Browning et al., 2021). The growth inhibition of spheroids in response to a drug can serve as a measure of its efficacy. If a drug can prevent the spheroid from growing or trigger a size reduction, it suggests that the drug is effective against the tumour cells.

For reliable and meaningful results, spheroids must be uniform in size at the start and end of an experiment. If spheroids are of different sizes, it can introduce variability in the results, making it harder to draw accurate conclusions about the drug's

effects. For example, larger spheroids may naturally be more resistant to treatment simply because they have more cells, while smaller ones may be more sensitive. Consistent spheroid sizes reduce this variability, ensuring that differences in growth or drug response are due to the treatment and not due to the differences in spheroid size (Browning et al., 2021).

To optimize the number of cells that need to be seeded for the spheroid to have an optimal size, A253 and FaDu were seeded into Nunclon Sphera 3D culture 96 well plates from 20,000 cells to 312 cells per well. The 7-day evolution of A253 and FaDu spheroids displays the dependence of the spheroid size on the number of plated cells. As presented in Figure 14 and Figure 15, the spheroids lose their natural shape around day 4 in the wells with the greatest number of cells plated, which is most visible for the A253 cell line. Past studies have shown that large spheroids have poor uptake of drugs when using spheroids for drug toxicity assays, leading to errors when quantifying viability or cell death (Suraj Kumar Singh et al., 2020).

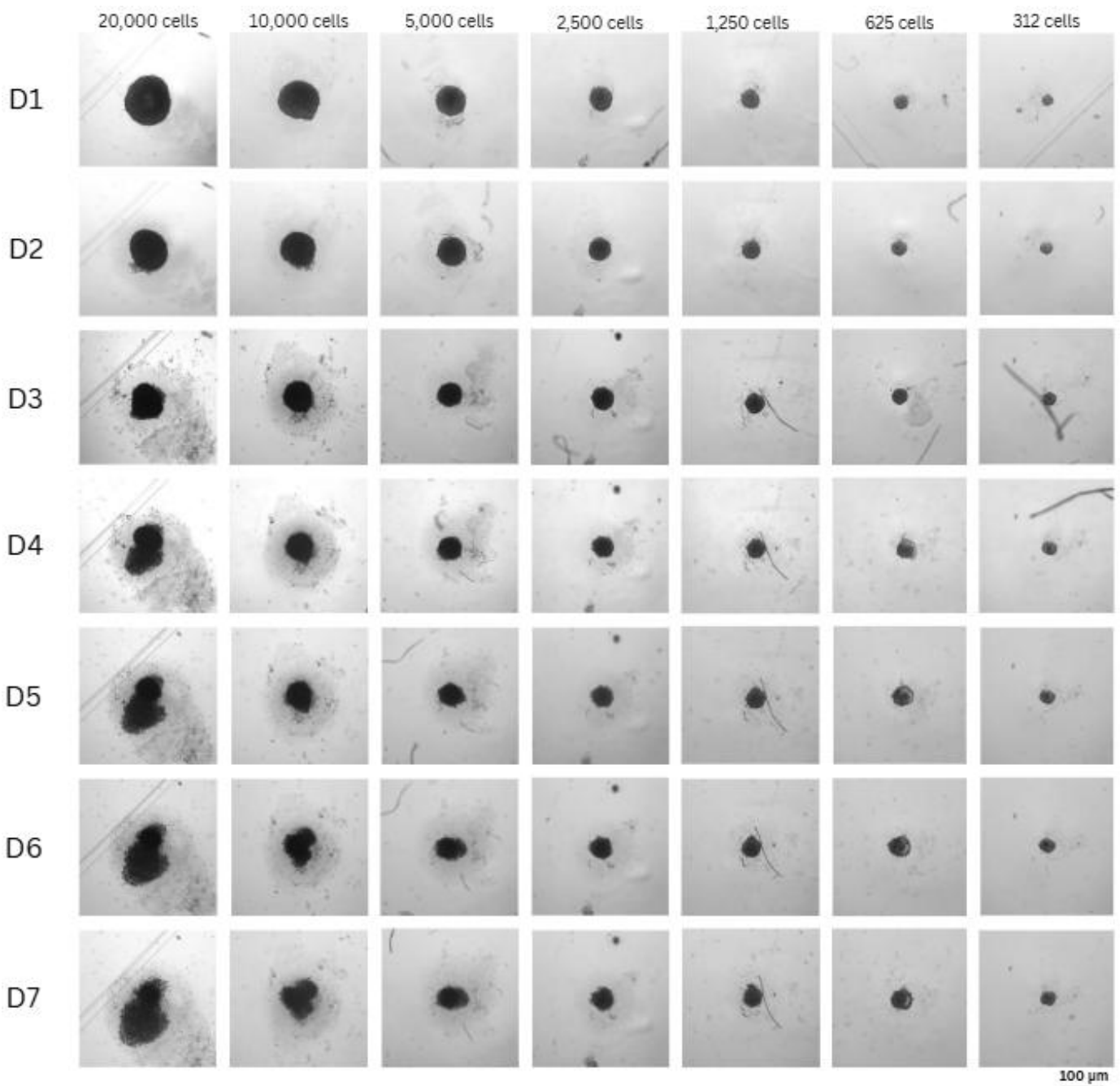


Figure 14: The 7-day evolution of A253 spheroids displays the dependence of the spheroid size on the number of plated cells. Various quantities of A253 cells were seeded into Nunclon Sphera 3D culture 96 well plates and incubated at 37°C and 5% CO₂ for 3 days. The spheroid growth was recorded for 7 days using a ZEISS Axio Zoom.V16 microscope, 32x magnification (Plan-NEOFLUAR Z 1.0x, NA 0.25). Images were captured using a ZEISS AxioCam 506 mono camera with 200 ms exposure time and analyzed in Fiji (ImageJ). Scale bar: 100 µm.

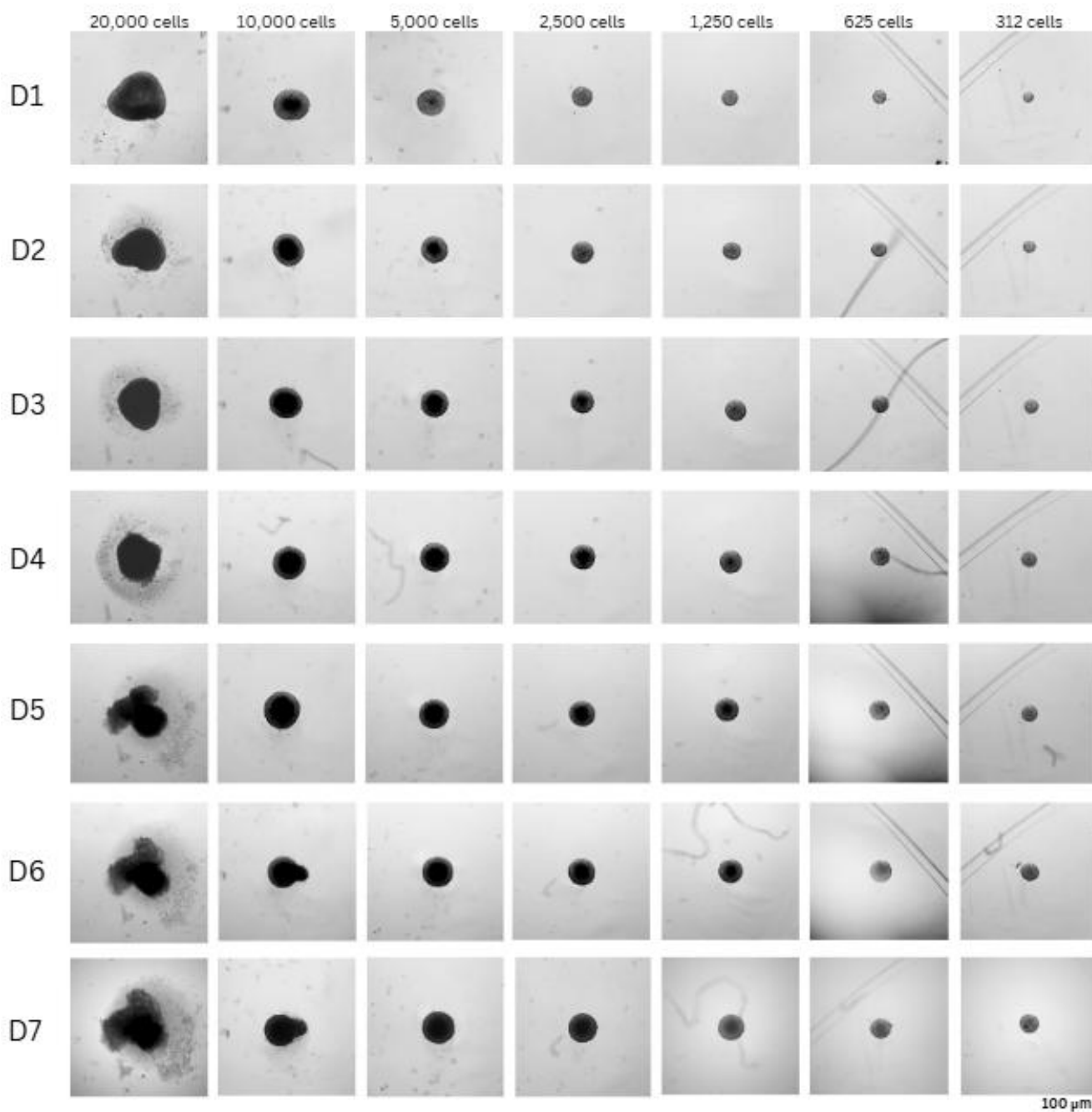


Figure 15: The 7-day evolution of FaDu spheroids, displaying the dependence of the spheroid size on the number of plated cells. Various quantities of FaDu cells were seeded into Nunclon Sphera 3D culture 96 well plates and incubated at 37°C and 5% CO₂ for 3 days. The spheroid growth was recorded for 7 days using a ZEISS Axio Zoom.V16 microscope, 32x magnification (Plan-NEOFLUAR Z 1.0x, NA 0.25). Images were captured using a ZEISS AxioCam 506 mono camera with 200 ms exposure time and analyzed in Fiji (ImageJ). Scale bar: 100 µm.

Additionally, Figure 16 displays the changes in volume for both A253 and FaDu spheroids at different cell seeding densities tracked over 7 days. The standard curve correlates initial cell seeding densities with spheroid size or cell number over time. It provides a reference framework to monitor growth kinetics and evaluate how initial seeding densities influence spheroid formation and proliferation.

Taking this into account and to avoid the generation of necrotic cores in spheroids due to over-population and lack of nutrients, because the medium in wells can not be changed without disrupting the spheroid, it was decided to use 1,250 cells/well when testing the co-treatment of cisplatin with CAP. At 1250 cells per well, the cell density is sufficient to promote consistent aggregation and form compact spheroids within the desired timeframe. This density prevents the formation of both too-small (which would affect the growth dynamics) and too-large spheroids (which may cause crowding and affect nutrient and oxygen availability). It also provides reproducible spheroid sizes, making it ideal for subsequent drug treatment and imaging analysis.

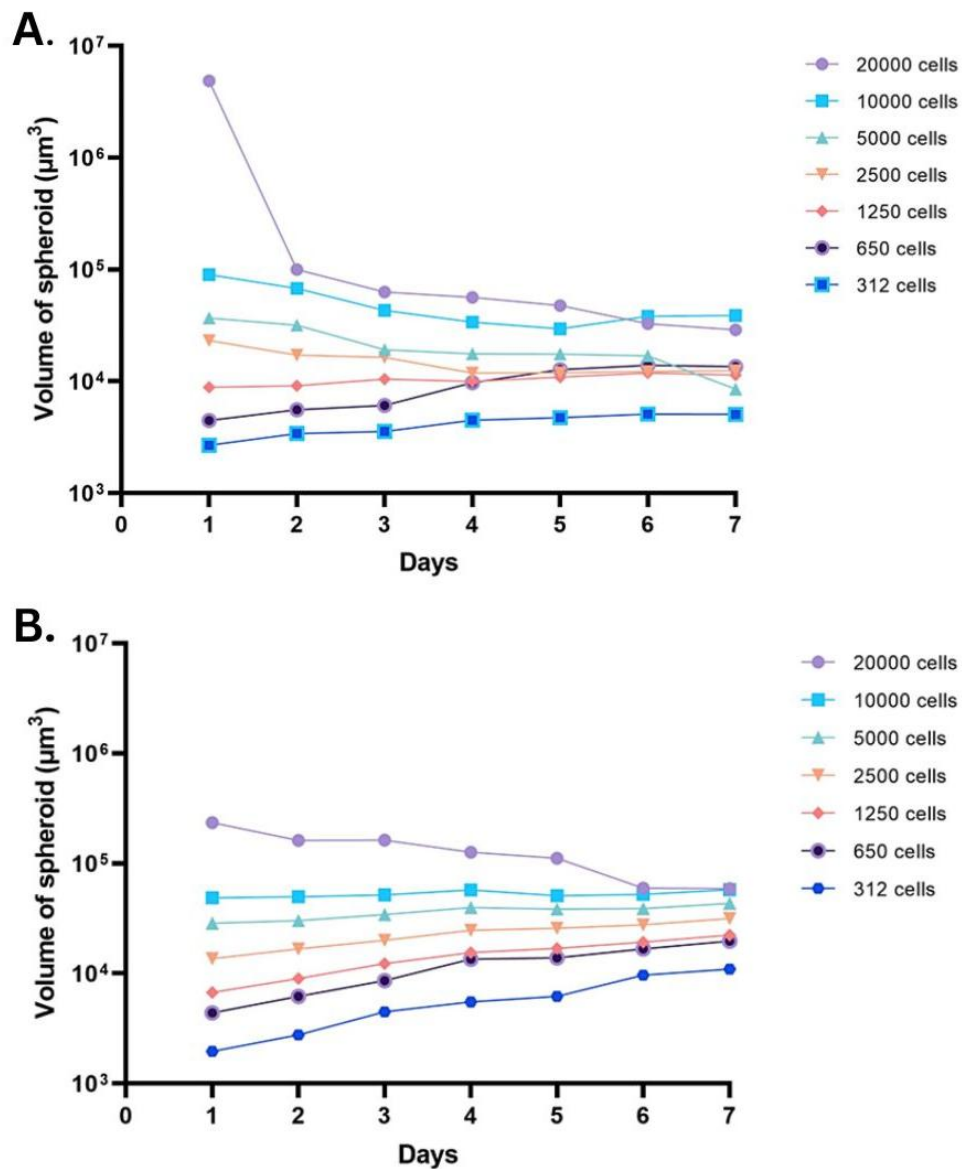


Figure 16: Growth kinetics of A253 (A) and FaDu (B) spheroids formed from different numbers of plated cells (20,000 cells to 312 cells/well). The graph displays spheroid size (volume of spheroids in μm^3) over 7 days, plotted against a standard curve generated for cell number using GraphPad Prism 10.4.1. Growth rates were analyzed using ImageJ (Fiji), and data were normalized to initial seeding densities ($n=1$).

To assess how co-treatment of cisplatin and CAP affects 3D models, A253 and FaDu cells were seeded into Nunclon Sphera 3D culture 96 well plates at 1250 cells per well. Spheroids were treated with a combination of cisplatin ranging from 0 to 50 μM and direct CAP treatment for 240 seconds after 3 days of growth. The spheroid growth after applying treatment was recorded for 5 days by brightfield microscopy. After 5

days of growth, spheroids were labelled with SYTOX Green and Hoechst 33342 to analyse cytotoxicity by fluorescence microscopy. The results are presented in Figure 17 and Figure 18.

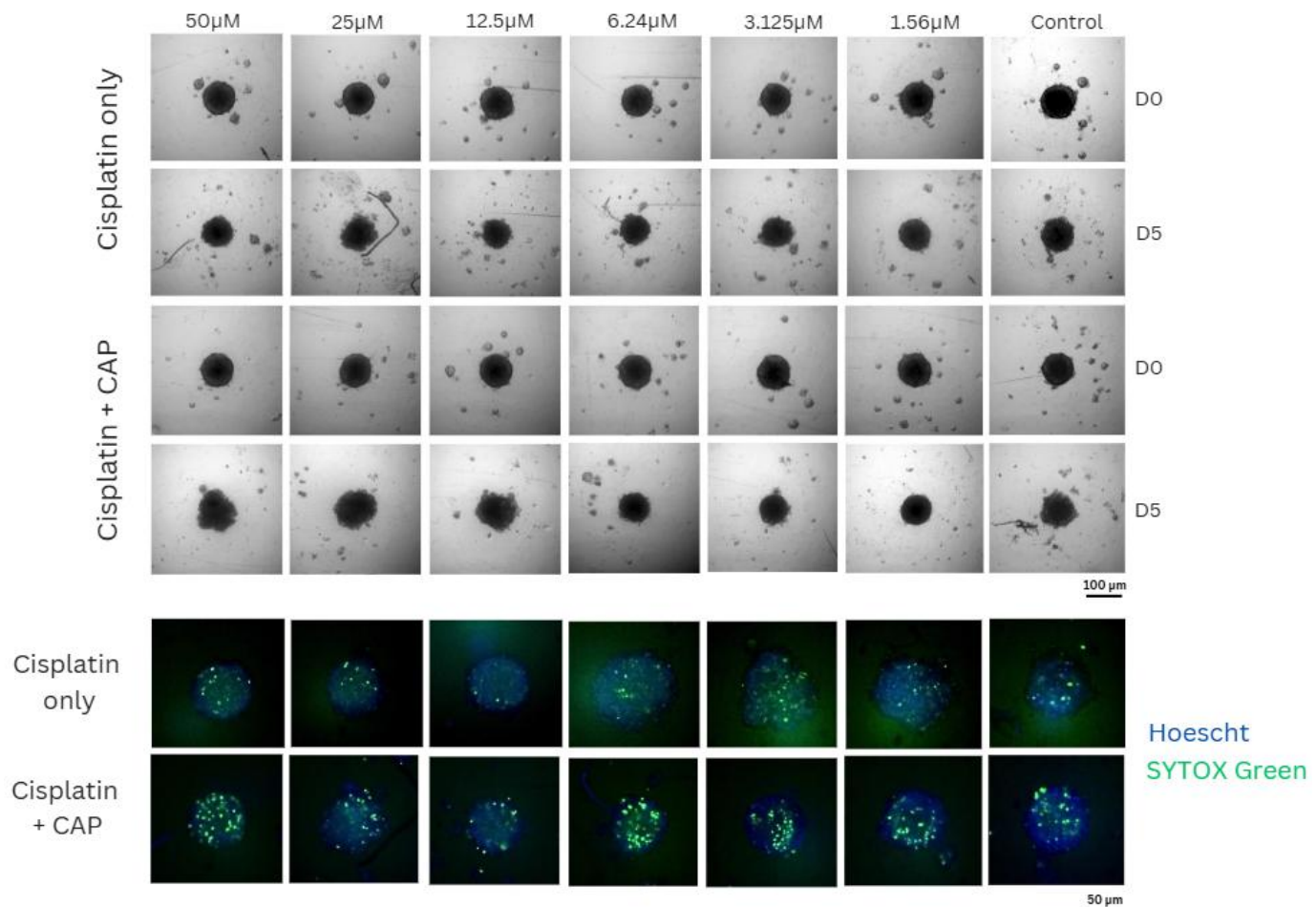


Figure 17: Treatment of A253 spheroids with cisplatin alone or cisplatin and CAP combination. A253 spheroids were treated with a combination of direct CAP treatment (240s) and cisplatin at the indicated concentrations. On day 5, A253 spheroids were then labelled with SYTOX Green and Hoechst to analyse the cytotoxicity of the combination of CAP and cisplatin compared to cisplatin treatment only. Representative fluorescence image of A253 cell spheroids acquired using a ZEISS Axio Zoom.V16 microscope with a 52× magnification objective (Plan-NEOFLUAR Z 1.0x, NA 0.25). Images were acquired using a ZEISS Axiocam 506 mono camera with 200 ms exposure time and analyzed in Fiji (ImageJ). Z-stacks were captured at 1 µm intervals over a 30 µm depth. Scale bar: 50 µm. Experiments were performed in triplicate and repeated three times with similar results.

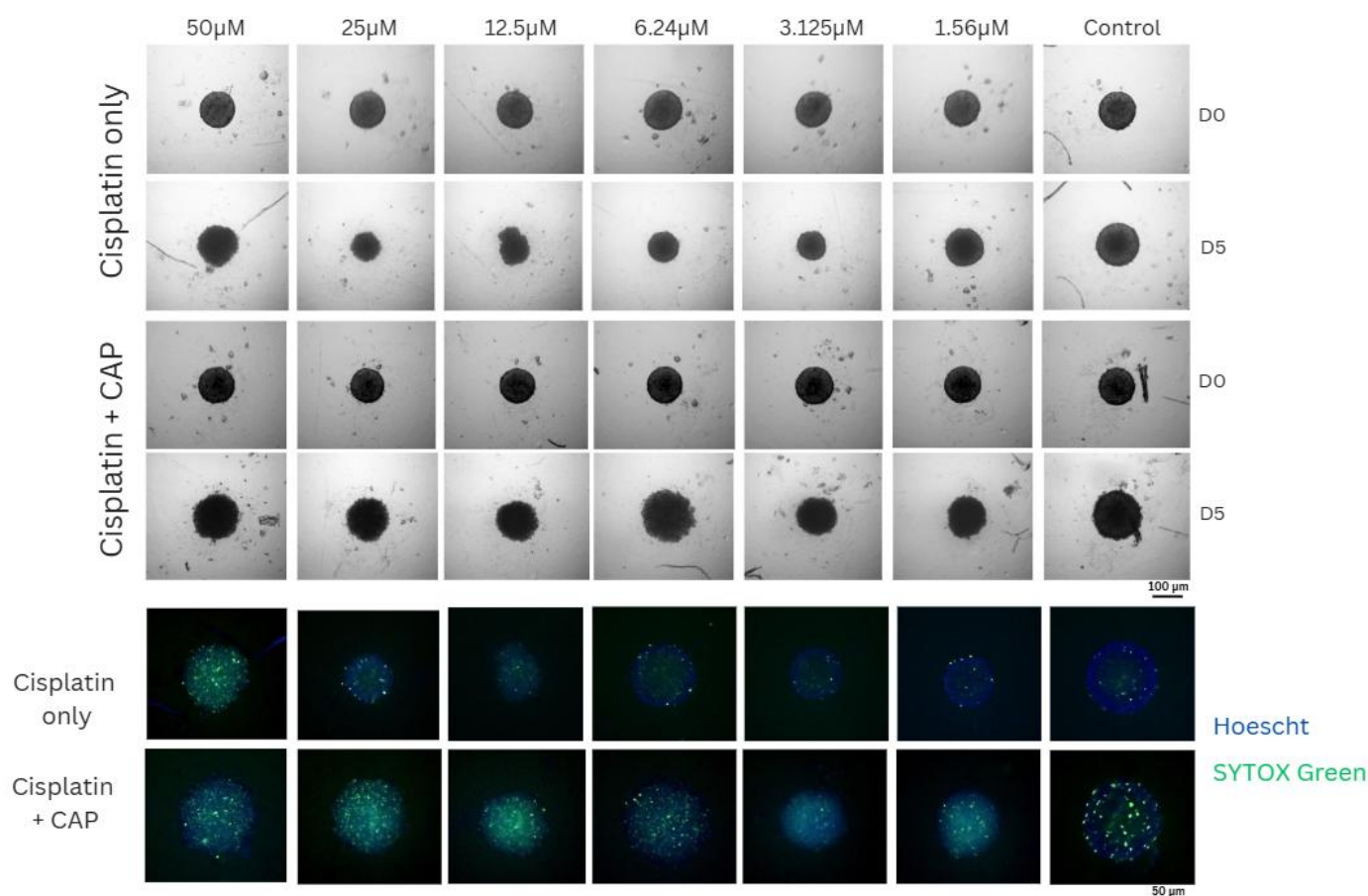


Figure 18: Treatment of FaDu spheroids with cisplatin alone or cisplatin and CAP combination. FaDu spheroids were treated with a combination of direct CAP treatment (240s) and cisplatin at the indicated concentrations. On day 5, FaDu spheroids were then labelled with SYTOX green and Hoechst to analyse the cytotoxicity of the combination of CAP and cisplatin compared to cisplatin treatment only. Representative fluorescence image of FaDu cell spheroids acquired using a ZEISS Axio Zoom.V16 microscope with a 52× magnification objective (Plan-NEOFLUAR Z 1.0x, NA 0.25). Images were acquired using a ZEISS AxioCam 506 mono camera with 200 ms exposure time and analyzed in Fiji (ImageJ). Z-stacks were captured at 1 µm intervals over a 30 µm depth. Scale bar: 50 µm. Experiments were performed in triplicate and repeated three times with similar results.

Hoechst 33342 is a membrane-permeable fluorescent dye that easily penetrates the plasma membrane of nucleated cells (Kessel et al., 2016). Once inside, it binds specifically to the DNA in the cell nucleus, resulting in a bright blue fluorescence. This property makes it a useful tool for staining and visualizing nuclei in live or fixed cells, allowing the identification and analysis of nucleated cells under fluorescence

microscopy (Kessel et al., 2016). SYTOX Green is a dye that remains nonfluorescent outside of viable cells due to its inability to cross intact plasma membranes. When cells undergo death and their plasma membranes become permeabilized, the dye can enter the cells and bind to their DNA (Demuynck et al., 2020). Upon binding, SYTOX Green becomes highly fluorescent. This fluorescence serves as an indicator of cell death, as it only occurs when the membrane integrity is lost, marking the final stages of the cell death process (Demuynck et al., 2020).

The results of this experiment showed that the treatment with cisplatin inhibited spheroid growth either in the presence or absence of CAP, but the combination of the drug with 240s CAP showed greater amounts of cell death in both cell lines. The enhanced cell death in the spheroids is highlighted by the intense green staining. Although there is green staining in the cisplatin-only treatment as well, there is more damage visible in spheroids when treated with the co-treatment of CAP and cisplatin. This effect is particularly notable at lower doses of cisplatin, where almost no SYTOX Green staining is visible in the absence of CAP, but in combination with CAP, punctate and diffuse green fluorescence staining is seen.

3.3.5. INDIRECT PLASMA TREATMENT: COMPOSITE HYDROGELS

After the promising results displayed by the co-treatment of HNSSC cell lines with a combination of cisplatin and direct CAP treatment, the next step in our research focuses on composite hydrogels. Attributable to the fact that CAP application is limited to surface area treatments and the depth of tissue penetration of CAP is less than 100

μm (Partecke et al., 2012), a novel drug delivery system (DDS) that could allow CAP components to be delivered to the targetted cells/tissue is being investigated.

Hydrogels have been used in a wide range of medical applications, including wound healing or in nicotine and fentanyl patches (Pastore et al., 2015). However, when used as a drug delivery system, hydrogels need to react to a specific stimulus to release the drug that needs to be administered to different regions of the body (Gaur et al., 2023). Previously presented by Gaur et al., 2023, these drug-loaded composite hydrogels can facilitate the delivery of various drugs through CAP activation, an emerging DDS.

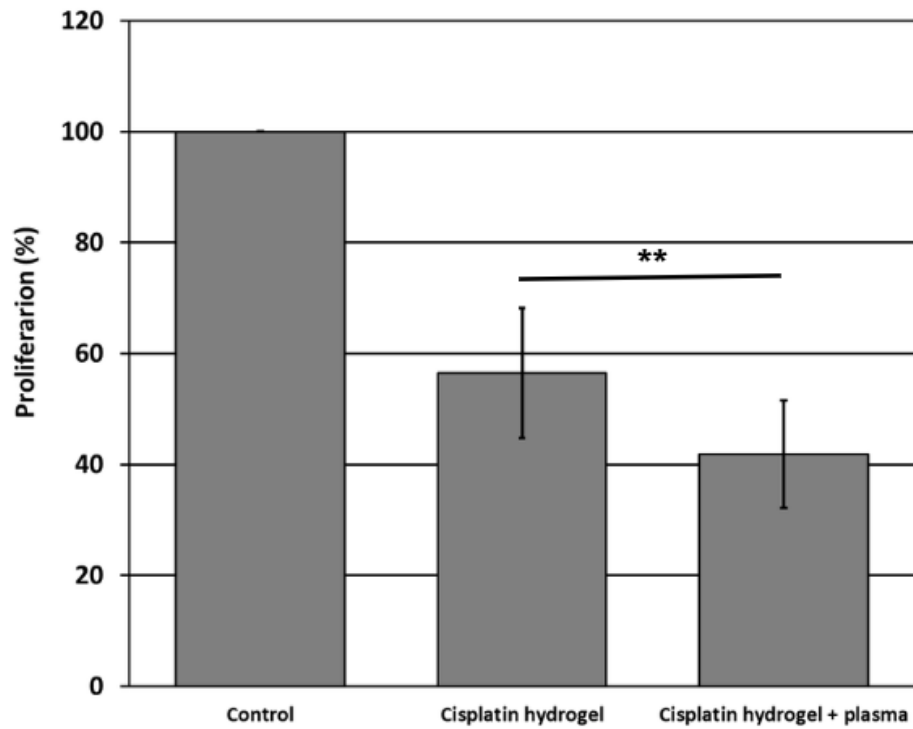
The composite hydrogels are manufactured from affordable polymers and their synthesis does not require elaborate chemical steps. The base of the hydrogel is the sodium polyacrylate (PAA) particles that are further dispersed within a poly(vinyl alcohol) (PVA) hydrogel matrix. PVA is highly effective for controlled drug release, and it has been extensively studied in pharmacology, being recognized as a safe material due to its nontoxic, odourless, and nonirritating nature, as well as its low likelihood of causing allergic reactions (Lei et al., 2022).

Smart hydrogels respond to environmental factors like light, magnetic fields, pH, temperature or ionic strength (Lei et al., 2022). When these stimuli exceed a certain threshold, smart hydrogels undergo significant changes, such as volume transitions (swelling or shrinking), allowing the release of different agents, such as antimicrobials or chemotherapeutics. This responsiveness makes them adaptable and dynamic, with applications in various fields, particularly in medicine (Lei et al., 2022).

However, the main drawback of this drug-loaded composite hydrogel is its limitation to only cationic drugs. The passive release of the drug decreases as the number of cationic groups increases, due to their interaction with the carboxylate groups in the PAA particles (Gaur et al., 2023). This limitation could be addressed by using a positively charged drug-loaded carrier vehicle. This carrier, with a positive charge, can facilitate the delivery and release of the drug, even if the drug itself is not inherently cationic. This approach expands the range of drugs that can be used with the composite hydrogel, providing more flexibility in drug delivery applications (Gaur et al., 2023).

For our experiments, cisplatin was encapsulated in the hydrogel at a concentration of 0.6 mg/mL. Cisplatin-loaded hydrogel discs of 3-4 mm thickness were prepared using a biopsy punch. Cell culture medium was used to hydrate the hydrogel discs 30 minutes before CAP treatment. The cisplatin-loaded hydrogel discs were then treated with CAP for 120 seconds, from a 1 mm distance (the glass tube of the CAP jet should not be in direct contact with the hydrogel surface). The discs were inserted in the 96 transwell plate and submerged in the cell medium, followed by 72 h incubation. In addition to the CAP-treated cisplatin-loaded hydrogel and the untreated cisplatin-loaded hydrogel, untreated cells and cisplatin-only treated cells were used as controls. The experiment has been conducted in both technical and biological replicates and the data presented in Figure 18 is the average of the three biological replicates.

A.



B.

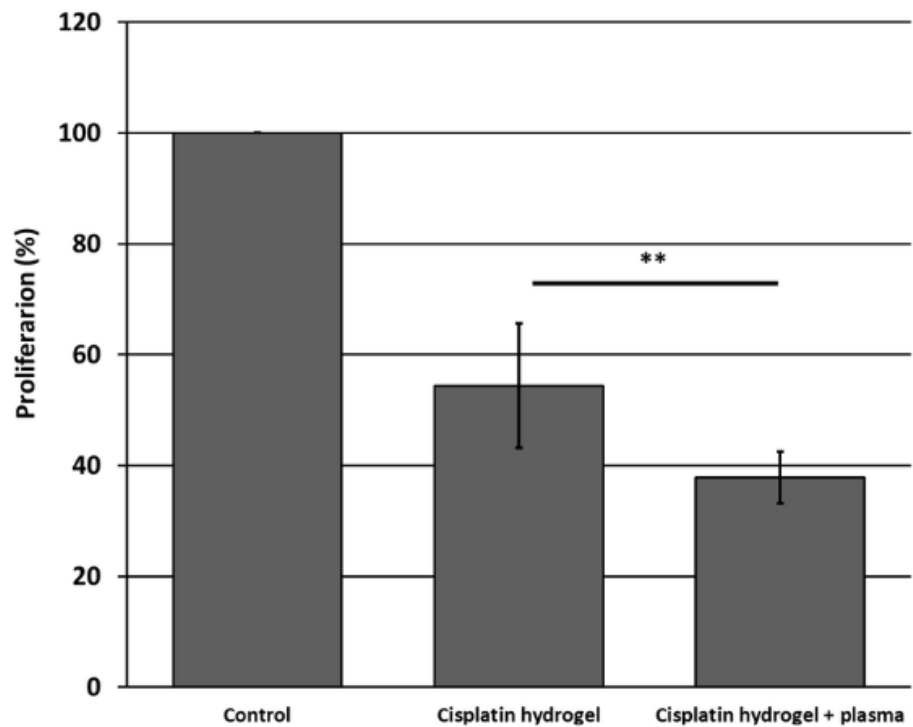


Figure 18: Anti-proliferative effects on HNSCC of cisplatin-loaded hydrogels activated by CAP treatment. Treatment of A253 (A) and FaDu (B) cell lines with hydrogels loaded with 0.6 mg/ml cisplatin at 3-4 mm thickness, before 120s CAP treatment, followed by 72h incubation. Error bars are \pm SD unpaired t-tests * $p < 0.05$, ** $p < 0.01$. Experiments were performed in triplicate and repeated three times with similar results.

The results suggest that plasma-activated hydrogel therapy (PAHT) has high anti-proliferative effects on both FaDu and A253 cell lines when compared to unactivated cisplatin hydrogels ($p < 0.01$). The untreated cisplatin-loaded hydrogel inhibits proliferation by $43.5\% \pm 11.7\%$ for A253 and by $45.62\% \pm 11.22\%$ for FaDu while the CAP-treated hydrogels inhibit proliferation by $58.19\% \pm 9.69\%$ for A253 and by $62.19\% \pm 4.7$ for FaDu.

The highest standard dose of cisplatin actively used in the treatment of HNSCC is 100 mg/m^2 , delivered every three weeks for 3 cycles in combination with radiotherapy (Gupta et al., 2022), while the lowest standard dose is a weekly regimen of 40 mg/m^2 cisplatin for seven weeks (Anouk W. M. A. Schaeffers et al., 2023). The locoregional delivery of cisplatin, however, will result in a much lower dose. This result is of high relevance, as a lower dosage of cisplatin could minimize systemic toxicity while delivering the drug directly to the target site, making it suitable for controlled, localized treatments. By achieving therapeutic benefits at reduced concentrations, we could open the door to potentially safer and more manageable treatment protocols for HNSCC patients.

However, one limitation this experiment has is the passive release of cisplatin in the unactivated cisplatin-loaded hydrogel as observed through the decrease in proliferation seen with hydrogel that had not been activated with CAP. We noticed that the passive release of the drug inside the PAA particles of the hydrogel is influenced by the time that passed since the hydrogel was manufactured. We believe that, as time progresses, factors such as changes in the hydrogel's hydration, possible swelling, or the stability of the drug within the matrix can affect how the drug is released. Therefore, the

time that passes since the hydrogel's production can significantly impact the drug's release pattern and has implications for how this technology might be applied clinically.

4. CO-TREATMENT OF HNSCC CELLS WITH DNA DAMAGE INHIBITORS AND COLD ATMOSPHERIC PLASMA

4.1. INTRODUCTION

The cell cycle is a greatly controlled process, with various mechanisms being involved in regulating DNA damage before the cell can undergo mitosis (Geenen and Schellens, 2017). The cell cycle consists of a sequence of events that enable a cell to grow, replicate its DNA, and divide into two daughter cells. It is divided into four main phases: G1, S, G2, and M phases (Song et al., 2024). During the G1 phase, the cell prepares for DNA synthesis by producing large amounts of RNA and proteins needed for subsequent phases. In the S phase, the primary activity is DNA replication to ensure that each daughter cell inherits an identical copy of the genome. The G2 phase involves further preparation for division, with the synthesis of small amounts of RNA and proteins. Finally, the M phase encompasses karyokinesis (nuclear division) and cytokinesis (cytoplasmic division), leading to the formation of two new cells (Song et al., 2024).

Throughout the cell cycle, various factors, including environmental influences and intrinsic cellular conditions, can compromise the integrity of the cell's genetic material (Li et al., 2022). To address these challenges, cells have evolved sophisticated regulatory mechanisms collectively known as the cell cycle regulatory system. This system ensures that the cell cycle progresses smoothly, allowing accurate replication and distribution of genetic material to maintain genomic stability and support proper cellular function (Song et al., 2024).

A key pathway in cell cycle regulation when DNA damage is triggered in the cell is the DNA damage response pathway (DDR). Following the same steps involved in any other transduction pathway, the lesions that might appear in the DNA due to different types of DNA damage activate the DDR signaling pathway. A protein kinase cascade is then initiated and mediators aid in phosphorylation. The effectors, which are also kinase substrates, will further coordinate vital processes such as DNA repair and replication, aiding in maintaining genomic stability through a controlled cell cycle (Marechal and Zou, 2013).

DNA damage checkpoints are vital mechanisms that precede the DNA repair processes and are part of the DDR pathway. Acting as tumour-suppressors, DNA damage checkpoints postpone the cell cycle progression of the affected cells and allow said cells to undergo DNA repair. Moreover, apoptosis and senescence can also be triggered by DNA damage checkpoints when the damaged cells need to be eliminated (Ermolaeva and Schumacher, 2014). The activation of these DNA damage checkpoints is best outlined when correcting DNA double-strand breaks (DSBs) through MRE11–RAD50–NBS1 (MRN) protein complex activation.

MRE11/RAD50/NBS1 proteins from the MRN are recruited at the DSB sites, activating the checkpoint ataxia–telangiectasia mutated (ATM), which is a protein member of the PIKK (phosphoinositide-3-kinase-related kinase) family (Hakem, 2008). Other important kinases involved in this process are ATR (ATM and Rad3-related) and DNA-dependent protein kinase (DNA-PK), which phosphorylate multiple proteins necessary for DDR. Within the DDR pathway, ATM is the main kinase activated by DSBs, while ATR is triggered as a response to multiple types of DNA damage, including damage that affects the replication processes (Marechal and Zou, 2013). In comparison to ATM and ATR, DNA-PK is known to regulate fewer proteins, and it is mainly involved in nonhomologous end joining (NHEJ) (Beli et al., 2012).

Histone H2AX, for instance, becomes γ H2AX after being phosphorylated by ATM, ATR and DNA-PK at the DSB site and allows chromatin remodelling through the recruitment of other proteins (Hakem, 2008). BRCA1, 53BP1, and MDC1, which are also ATM substrates, are other proteins responsible for DNA repair at DSB sites. γ H2AX is detected by MDC1, which amplifies the activation of γ H2AX and ATM across large chromatin areas. A ubiquitination process is then triggered at the site of the DSB, in which the E3 ligases RNF168 and RNF8 ubiquitinate histones H2AX and H2A (Berger et al., 2017).

When ubiquitin chains are extended due to HERC2, a complex is formed with BRCA1, the main protein involved in homologous recombination (HR) (Marechal and Zou, 2013). The further coating of single-stranded DNA which is left after DSBs is done by replication protein A (RPA), coordinated by the MRN complex. This mechanism regulates the activation of ATR and ATR Interacting Protein (ATRIP), triggering ATR-dependent phosphorylation of various proteins such as Rad17 and claspin (Hakem,

2008). Both ATM and ATR are vital for the cell's genomic integrity, being the main moderators of the G1/S, intra-S-phase, and G2/M checkpoints. When DNA damage is induced in healthy cells, the DDR pathway arrests the cell in the G1 phase of the cell cycle to trigger the DNA repair processes (Figure 19). In tumour cells, however, G1 checkpoint aberrations are often encountered, mostly in p53-deregulated cells, which allows the G2 checkpoint to aid in DNA repair (Esposito et al., 2021).

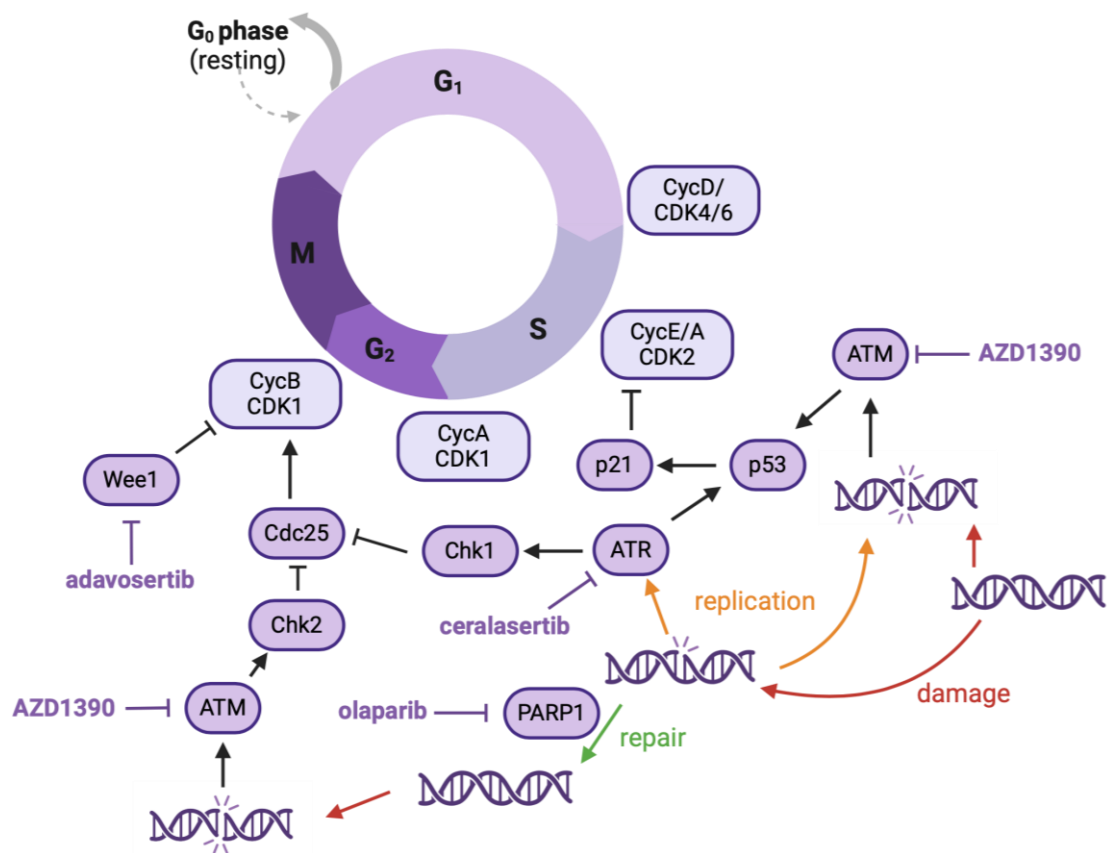


Figure 19: DNA Damage Response (DDR) Pathways and Cell Cycle Regulation with Targeted Inhibitors. The figure illustrates the regulation of the cell cycle and the DNA damage response (DDR) pathways, highlighting key proteins and their interactions. The cell cycle phases (G₁, S, G₂, M) are shown, with checkpoints regulated by cyclins (Cyc) and cyclin-dependent kinases (CDKs) to ensure proper progression. DNA damage activates ATM and ATR kinases, which phosphorylate downstream effectors (Chk1, Chk2, p53) to pause the cell cycle and facilitate DNA repair. Figure prepared by Professor Sarah Allinson using Biorender.

Another important gatekeeper for both the G₂/M checkpoint and S-phase is Wee1. Wee1 is part of a family of protein kinases that includes two Wee1 kinases (Wee1 and Wee1B) and PKMYT1 (membrane-associated tyrosine- and threonine-specific cdc2-inhibitory kinase) (Esposito et al., 2021). These kinases share sequence similarity in their catalytic (kinase) domains but differ in their localization, expression timing, and regulatory mechanisms. Such differences allow them to carry out distinct functions while contributing to the overall coordination of cell cycle progression and genome stability (Esposito et al., 2021).

Wee1 is primarily localized in the nucleus, where it plays a crucial role in coordinating DNA replication and ensuring that mitosis does not occur prematurely (Esposito et al., 2021). By regulating the timing of the G₂/M transition, Wee1 helps maintain the integrity of the cell cycle, allowing sufficient time for DNA replication to complete before the cell enters mitosis. It has recently been identified that Wee1 plays a critical role in the S-phase of the cell cycle as well. DNA synthesis during the S-phase and mitosis are tightly coordinated processes (Esposito et al., 2021). If replication errors occur during the S-phase, Wee1 can help activate regulatory mechanisms that slow down or temporarily halt progression. This pause provides an opportunity for DNA repair, preventing the inheritance of chromosomal abnormalities or genetic mutations in daughter cells (Esposito et al., 2021).

Wee1 exerts its effects by negatively regulating the Cdk1-cyclin B complex (also known as the mitosis-promoting factor, or MPF), which is essential for the initiation of mitosis. Wee1 phosphorylates Cdk1 at the Y15 residue within its ATP-binding site, preventing its activation during interphase (Esposito et al., 2021). In contrast, the kinase PKMYT1 also phosphorylates Cdk1, but at both the Y15 and T14 residues, further

inhibiting its activity. This phosphorylation by Wee1 and PKMYT1 keeps Cdk1 inactive until the appropriate time (Esposito et al., 2021). The activity of Cdk1 is counterbalanced by Cdc25 phosphatases, which remove the phosphates from Y15 and T14, allowing Cdk1 to become active when cyclin B levels rise. This balance between Wee1, PKMYT1, and Cdc25 is crucial for the precise control of the cell cycle, ensuring that mitosis occurs only after DNA replication is properly completed (Esposito et al., 2021).

The downregulation of Wee1 promotes the entry of the cell into mitosis by reducing the levels of this kinase. This reduction is typically achieved through a combination of decreased synthesis and targeted proteolytic degradation of Wee1. The key event leading to Wee1 degradation is its phosphorylation by specific kinases (Esposito et al., 2021). When Wee1 is phosphorylated by Plk1 (polo-like kinase 1) at the S53 residue and by Cdk1 (cyclin-dependent kinase 1) at the S123 residue, it becomes recognized as a target for degradation by specific E3 ubiquitin ligases. These include the SCF β -TrCP and SCFTome-1 complexes, both of which are F-box protein-containing ubiquitin ligases (Esposito et al., 2021). Upon phosphorylation, Wee1 is tagged for ubiquitination, marking it for proteasomal degradation. While phosphorylation itself does not directly inactivate Wee1, it triggers the proteasome-dependent degradation process that ultimately lowers Wee1 levels, facilitating the transition into mitosis. This ensures that the cell cycle progresses at the correct time, preventing premature mitosis before DNA replication is complete (Esposito et al., 2021).

The PARP (poly ADP-ribose polymerase) family, also known as diphtheria-toxin-like ADP-ribosyltransferases (ARTDs), consists of 17 enzymes. Among these, PARP1 and PARP2 are the most extensively studied and are closely related in structure and

function (Zong et al., 2022). Both play essential roles in the DNA damage response, with PARP1 being more abundant and providing the majority of the poly(ADP-ribosyl)ation (PARylation) activity. This modification of chromatin structure and DNA repair factors facilitates the repair of DNA damage.

When DNA damage occurs, PARP1 is the first responder, catalyzing PARylation to recruit and modulate DNA repair proteins, thereby maintaining genomic integrity. It interacts with various repair pathways to address single-strand breaks (SSBs) and other lesions (Zong et al., 2022). As a nuclear chromatin-related enzyme, PARP1 is involved in several essential processes, including genomic integrity maintenance, programmed cell death, transcription regulation, chromatin remodelling, and telomere maintenance. Its central role in DNA damage repair makes it a significant therapeutic target, particularly in cancer treatment (Zong et al., 2022).

DNA damage repair involves five key pathways: mismatch repair (MMR), base excision repair (BER), homologous recombination (HR), nucleotide excision repair (NER), and nonhomologous end joining (NHEJ). BER, MMR, and NER primarily address single-strand breaks (SSBs), while HR and NHEJ repair double-strand breaks (DSBs) (Zong et al., 2022). PARP1 is active in multiple repair pathways, including BER, NER, HR, and both classical and alternative NHEJ. Its most critical function lies in BER, where it is essential for stabilizing the replication fork and coordinating repair steps. The complex nature of DNA repair, involving overlapping and distinct steps, highlights the multifaceted role of PARP1 in safeguarding genomic stability and ensuring proper cell function (Zong et al., 2022).

In response to DNA damage caused by intrinsic factors or external genotoxic agents like alkylating agents or ionizing radiation, the DNA-binding domain (DBD) of

PARP1 detects and binds to DNA nicks at the damaged site (Zong et al., 2022). This interaction triggers the recruitment of additional PARP1 domains to the site of damage, leading to a conformational change in the helical domain (HD) that relieves its self-inhibitory function. This allosteric activation increases PARP1's catalytic activity by up to 500-fold (Rudolph, Roberts and Luger, 2021).

The activated catalytic domain (ART) facilitates the PARylation of substrate proteins, including histones H1 and H2B, using NAD⁺ as a donor molecule to generate negatively charged PAR chains (Hananya et al., 2021). These PAR chains cause chromatin fibers to loosen and undergo rapid decondensation. This structural change dissociates histones from the DNA, providing access for DNA repair factors to the damaged site. Through this mechanism, PARP1 identifies and binds to DNA damage and creates the proper environment for efficient repair by recruiting and enabling other DNA repair processes (Zong et al., 2022).

PARP1 plays a dual role in DNA repair by not only modifying chromatin structure through PARylation but also recruiting key repair factors to damaged DNA sites. Among these, PARP1 facilitates the recruitment of X-ray repair cross-complementing protein 1 (XRCC1), a critical scaffold protein in the BER pathway (Zong et al., 2022). XRCC1 enhances the activity of various repair enzymes and supports the processing of Okazaki fragments during DNA replication (Azarm and Smith, 2020). Additionally, PARP1 interacts with other repair proteins such as DNA topoisomerases I and II and DNA polymerase β , further driving the BER process to efficiently address SSBs (Zong et al., 2022). For DSB repair, instead of directly repairing DSBs, PARP1 may contribute through alternative mechanisms, such as chromatin remodelling or signaling, to facilitate the recruitment or activity of repair processes (Audebert, Salles and Calsou,

2004). This versatility highlights PARP1's importance in maintaining genomic integrity across various types of DNA damage and repair pathways.

4.2. INHIBITORS OF THE DNA DAMAGE RESPONSE

Pharmacological targeting of the DNA damage response (DDR) is a promising strategy for cancer treatment due to its therapeutic advantages. Many cancer therapies, such as chemotherapy and radiation, work by inducing DNA damage to hinder the proliferation of cancer cells (Drew, Zenke and Curtin, 2024). By co-administering a DDR inhibitor (DDRi), these therapies can be enhanced, as the inhibition of repair pathways prevents cancer cells from repairing the induced DNA damage, making them more susceptible to treatment. This is particularly effective in fast-dividing cancer cells, which rely heavily on efficient DNA repair mechanisms (Qian et al., 2024).

Genome instability, a hallmark of cancer, often arises from the loss or dysfunction of key pathways involved in genome maintenance. This creates a reliance on the remaining functional DDR pathways for survival. Targeting these residual pathways with DDR inhibitors exploits the concept of synthetic lethality, where the simultaneous loss of two compensatory pathways leads to cell death (O'Neil, Bailey and Hieter, 2017). In cancer cells, this disruption can selectively kill tumour cells while sparing normal cells, as they typically have intact repair mechanisms (Drew, Zenke and Curtin, 2024). This dual approach makes DDR inhibition a compelling strategy in precision cancer therapy.

Poly(ADP-ribose) polymerase inhibitors (PARPis) are a class of small molecule drugs designed to induce cell death by inhibiting PARP activity during DNA damage repair. Tumour cells with BRCA1 or BRCA2 mutations (germline or somatic) are particularly sensitive to PARPis due to the principle of synthetic lethality (Farmer et al., 2005; Bryant et al., 2005). PARP inhibition prevents the repair of single-strand breaks (SSBs), which persist and are converted into double-strand breaks (DSBs) during DNA replication fork progression (Zheng et al., 2020).

In normal cells, these DSBs are repaired through the error-free HR pathway, which depends on functional BRCA1/2 proteins (Helleday, 2011). However, in tumour cells with defective *BRCA1/2* or similar defects in genes involved in HR, HR repair is compromised. The failure to restart stalled replication forks leads to their collapse, resulting in irreparable DSBs (Lomonosov, 2003). This causes chromosomal instability, cell cycle arrest, and ultimately apoptosis in the tumour cells. By selectively exploiting these repair deficiencies in cancer cells, PARPis provide a targeted therapeutic approach that spares normal cells with intact DNA repair mechanisms (Farmer et al., 2005).

PARPis induce synthetic lethality in cancer cells through multiple mechanisms that disrupt DNA repair processes, leading to cytotoxicity. These mechanisms include the cytotoxicity of unrepaired SSBs, DNA trapping, and the toxic effects of the NHEJ pathway (Zong et al., 2022). First, PARPis block the NAD⁺ binding site of PARP1 and PARP2, preventing PARylation and causing the accumulation of unrepaired SSBs. This results in the buildup of single-strand break repair (SSBR) and BER intermediates (Zong et al., 2022). When replication forks encounter these unrepaired SSBs, the breaks are converted into DSBs, which require homologous recombination for repair. Tumour cells

with HR deficiencies (HRD) cannot repair these DSBs effectively, leading to the accumulation of markers like RAD51 and γ H2AX in the nucleus, severe genomic instability, and cytotoxicity (Noël et al., 2006; Saleh-Gohari et al., 2005).

Second, some PARPis have the ability to block PARP1 and PARP2 at the site of SSBs, forming stable and toxic PARP-DNA complexes (Zandarashvili et al., 2020). These complexes are more damaging than unrepaired SSBs because they obstruct the progression of replication forks and exacerbate DNA damage. Overactivation of NHEJ, a non-conservative DNA repair pathway, occurs in HRD cells treated with PARPis. NHEJ often introduces errors, such as deletions, insertions, and translocations (Patel, Sarkaria and Kaufmann, 2011). In HRD cells lacking accurate repair mechanisms, this overactivation leads to further genomic instability and cell death. These combined effects make PARPis particularly effective in targeting cancer cells with HRD or similar repair defects (Patel, Sarkaria and Kaufmann, 2011).

Olaparib, the first PARPi approved for clinical use, leverages the principle of synthetic lethality to target cancers with defects in DNA damage repair pathways, particularly BRCA1/2 mutations. Initially developed for treating ovarian and breast cancers, where BRCA1/2 mutations occur in approximately 20% of cases, olaparib has since expanded its therapeutic scope (Koboldt et al., 2012).

Currently, olaparib is prescribed for a range of cancers characterized by BRCA1/2 mutations or related DDR deficiencies. These include recurrent, platinum-sensitive high-grade serous or poorly differentiated ovarian carcinoma (Pujade-Lauraine et al., 2017), triple-negative breast cancer (TNBC) (Gelmon et al., 2011), and refractory prostate cancer with DDR defects (Mateo et al., 2015). It is also used to treat

metastatic pancreatic cancer associated with BRCA mutations (Golan et al., 2019). Its ability to selectively target cancer cells with impaired HR repair has made olaparib a critical treatment option in precision oncology, particularly for tumours reliant on alternative, error-prone DNA repair pathways (Zong et al., 2022).

WEE1 inhibitors (WEE1i) have gained significant attention in recent years as promising cancer therapies targeting the cell cycle checkpoints, specifically the S-G2 checkpoint (Zhang et al., 2024). WEE1 plays a key role in preventing premature entry into mitosis by inhibiting cyclin-dependent kinases (CDK1/2), thereby ensuring that cells have properly completed DNA replication and are ready for mitosis. Inhibition of WEE1 disrupts this checkpoint, leading to uncontrolled activation of CDK1/2 and initiating two intertwined effects: induction of replication stress and premature entry into mitosis (Zhang et al., 2024). Given this mechanism, WEE1 inhibition has shown promise as an anti-tumour strategy, particularly in ovarian cancers, and has been validated clinically for its potential to enhance the effectiveness of cancer therapies.

However, the first-in-human WEE1 inhibitor, adavosertib (AZD1775), has faced challenges in clinical trials due to dose-limiting adverse events. These side effects have prompted efforts to identify predictive biomarkers and optimize combination therapy schedules to minimize toxicity while maintaining efficacy (Zhang et al., 2024). Recent studies suggest that the best use of WEE1 inhibitors might involve dose-reducing combinations with traditional anticancer drugs, tailored to specific patient populations based on biomarkers (Zhang et al., 2024). By refining treatment strategies, researchers aim to enhance the therapeutic benefits of WEE1 inhibitors while reducing harmful side effects, thereby improving their overall clinical application.

Clinical trials with adavosertib have revealed significant cytotoxicity to healthy cells, particularly in terms of myelosuppression, a condition where bone marrow activity is reduced, leading to low blood cell counts. While some of the reported toxicity might be due to off-target effects on PLK1 (polo-like kinase 1), studies suggest that the inhibition of WEE1 kinase itself is also responsible for these adverse effects (Wright et al., 2017). In a recent preclinical study, researchers developed an inhibitor similar to adavosertib that was designed to avoid PLK1 inhibition, yet still observed a positive correlation between anti-tumour efficacy and thrombocytopenia (a reduction in platelet count) *in vitro* (Guler et al., 2023). This finding indicates that thrombocytopenia, along with other aspects of myelosuppression, is likely an on-target effect of WEE1 inhibition rather than a result of off-target effects. These findings underscore the inherent toxicity of WEE1 inhibition, especially in terms of its impact on blood cell production (Zhang et al., 2024).

Another inhibitor still in preclinical testing, AZD1390 is a highly potent inhibitor of ATM kinase, which is a critical regulator of the DDR. Its brain-penetrant nature allows it to effectively target ATM-dependent signaling pathways and block the repair of DNA DSBs (Dong et al., 2022). By inhibiting ATM, AZD1390 disrupts key mechanisms cells use to maintain genomic stability following DSB-inducing treatments such as irradiation or chemotherapy. As a result, this compound enhances the cytotoxic effects of these agents, making it a powerful candidate for combination therapies (Dong et al., 2022).

Additionally, ATM inhibition with AZD1390 has the potential to exploit synthetic lethality in tumour cells with defects in other DDR pathways, such as HR. Tumour cells with compromised DDR rely heavily on ATM signaling to survive DNA damage. By inhibiting ATM, AZD1390 may selectively target these cells, further reducing their

capacity for DNA repair and driving them toward apoptosis (Dong et al., 2022). This dual role, augmenting the efficacy of DNA-damaging agents and targeting DDR-defective tumours, positions AZD1390 as a promising therapeutic strategy in cancer treatment.

AZD6738, also known as ceralasertib, is a potent and selective oral inhibitor of ATR kinase, a key regulator of the DDR activated during replication stress. ATR plays a crucial role in stabilizing stalled DNA replication forks, facilitating their restart, and promoting the G2-M checkpoint to prevent premature mitosis (Wilson et al., 2022). AZD6738 disrupts these processes, modulating DDR signaling pathways, including phosphorylation of CHK1 (pCHK1), activation of ATM-dependent signaling (pRAD50), and the induction of the DNA damage marker γ H2AX. By impairing break-induced replication and homologous recombination repair, AZD6738 enhances DNA damage and genomic instability in cancer cells (Wilson et al., 2022).

Preclinical studies revealed that AZD6738 is particularly effective in tumour cells with ATM pathway defects or elevated replication stress, such as those with *CCNE1* amplification. The drug demonstrated significant *in vivo* antitumor activity, with continuous dosing required to maintain its effects, as indicated by persistent induction of DDR markers (pCHK1, pRAD50, γ H2AX) (Wilson et al., 2022).

AZD6738 also showed strong synergistic efficacy in combination with agents that induce replication fork stalling and collapse, such as carboplatin, irinotecan, and olaparib. Optimized dosing schedules were critical for maximizing efficacy while minimizing toxicity, with combination treatments achieving superior antitumor activity at lower doses compared to monotherapy (Wilson et al., 2022).

Combining DDR inhibitors with plasma-based therapies could improve cancer treatment outcomes by exploiting complementary mechanisms. Attributable to the fact that CAP generates RONS that induce DNA damage, including strand breaks and oxidative lesions, when combined with DDR inhibitors, such as Wee1, PARP, ATR, or ATM inhibitors, the cancer cell's ability to repair this damage is further compromised, leading to enhanced genomic instability and apoptosis. The following experiments aim to assess the potency of CAP co-treatment with various DDRi, such as adavosertib, olaparib, ceralasertib and AZD1390.

4.3. RESULTS AND DISCUSSION

4.3.1. SINGLE AGENT DDRi: CELL PROLIFERATION ASSAY

A cell proliferation assay was conducted on FaDu and A253 cell lines in order to assess the metabolic activity of cancer cells after being treated with various DDR inhibitors at different concentrations. After adding the treatment, cells were incubated for 72 hours. The proliferation inhibition was detected using resazurin, after 3 hours of further incubation, at 570nm wavelength (reference 595 nm). The IC₅₀ value was determined to find the appropriate drug concentration used in the next experiments (Figure 20). This experiment was conducted in both technical and biological triplicates for both cell lines to assess the reproducibility and reliability of the results. All further calculations were done using the average of the biological triplicates.

Using the untreated cells as a control for 100% survival, the top concentration of 20 μM Wee1i inhibited proliferation by 66.8% for A253 cells and 82.53% for FaDu cells. The treatment with 300 nM concentration of Wee1i inhibited proliferation by 40.38% for A253 and 53.13% for FaDu. Therefore, for future experiments, we have considered an IC_{50} value of 300 nM to be the optimal dose of Wee1i for both cell lines.

For ATMi and ATRi, the top concentration of 100 nM ATMi and ATRi inhibited proliferation by 68.82% and 62.1%, respectively, for the A253 cell line and by 79.59% and 72.59%, respectively, for the FaDu cell line. The treatment with 5 nM concentration of ATMi and ATRi inhibited proliferation by 49.66% and 48.32%, respectively, for the A253 cell line and by 56.24% and 50.25%, respectively, for the FaDu cell line. An IC_{50} value of 5 nM ATMi and ATRi was therefore considered the optimal dose of DDRi for future experiments.

The top concentration of 500 μM PARPi inhibited proliferation by 58.2% for A253 cells and by 63.15% for FaDu cells. The treatment with 250 μM olaparib inhibited proliferation by 48.79% for A253 cells and by 55.13% for FaDu cells. However, this value showed significant variation from the IC_{50} values reported in well-established studies (Norris et al., 2013), which showed an approximate IC_{50} value of 3.6 μM (range: 1–33.8 μM). Discrepancies in IC_{50} values can arise due to differences in experimental conditions, such as cell lines used, assay design, drug preparation, or incubation times. Since the experimental conditions in this setup might differ from those in other studies, the observed IC_{50} may not fully align with the broader body of evidence in the literature.

To ensure the reproducibility and relevance of future results, the standard IC_{50} value of olaparib was used in future work, as reported in widely accepted scientific literature. This decision provides consistency with prior studies and facilitates

meaningful comparisons of findings with existing data, minimizing the influence of variability due to experimental conditions. Therefore, a concentration of 1 μM PARPi has been used in further CAP testing.

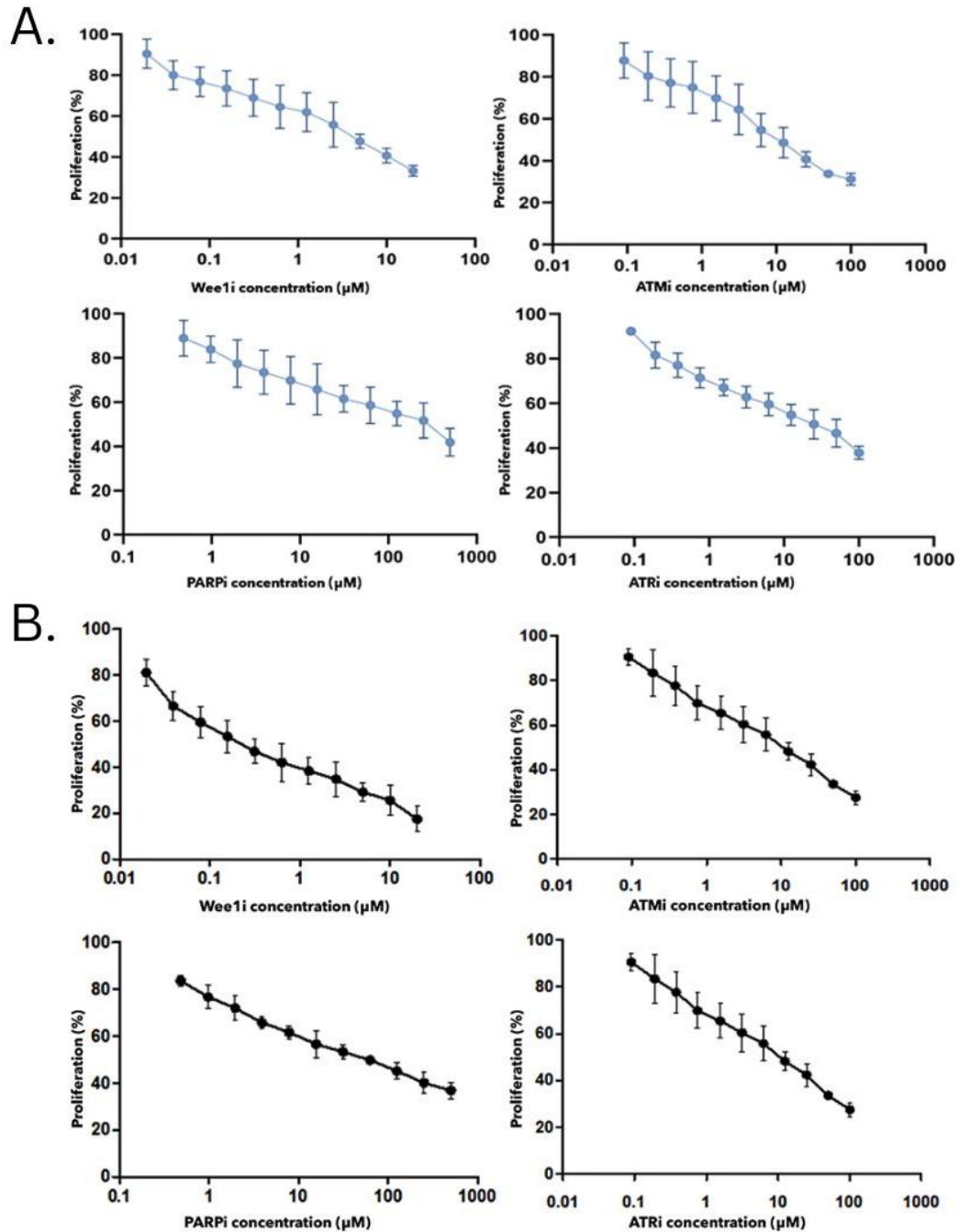


Figure 20: Cell proliferation inhibition rate and IC_{50} for A253 (A) and FaDu (B) cell lines. A253 cells were treated with different concentrations of Wee1i (20 μM to 0 μM), PARPi (500 μM to 0 μM), ATMi, and ATRi (100nM to 0nM) for 72 h. Cell proliferation inhibition rate was detected by resazurin assay, and the IC_{50} value was calculated for further experiments.

4.3.2. DDRIS IN COMBINATION WITH DIRECT PLASMA TREATMENT

To further investigate the effect of combining CAP treatment with anti-cancer drugs, A253 and FaDu cell lines were treated with a combination of DDR inhibitors at different concentrations (300nM for Wee1i, 1 μ M for PARPi, 5nM for ATMi and ATRi, respectively) and CAP treatment for 60 seconds, following the same protocol previously presented (see 3.3.2.). The results displayed in Figure 21 suggest a possible synergistic effect between CAP and some of the DDRi tested.

For the A253 cell line, the analysis of the results indicates a significant difference when comparing the 60s CAP-treated condition with the equivalent DDRi-only condition for all DDRi besides ATMi. There is also a significant difference when comparing the survivability rate of the DDRi-only treatment and the DDRi and CAP combination in all DDRi tested but ATMi. Following the Response Additivity approach, a synergistic effect can be seen in the co-treatment of CAP with Wee1i, PARPi and ATRi. The CAP-only treatment inhibited proliferation by 13.73%, while the Wee1i, PARPi and ATRi-only treatments inhibited proliferation by 38.85%, 15.83% and 22.04% respectively. The co-treatment for each DDRi in combination with CAP inhibited proliferation as follows: by 64.97% for Wee1i, by 32.39% for PARPi and by 48.74% for ATRi. For ATMi, the co-treatment inhibited proliferation by 24.65%, while ATMi treatment on its own inhibited proliferation by 27.73%.

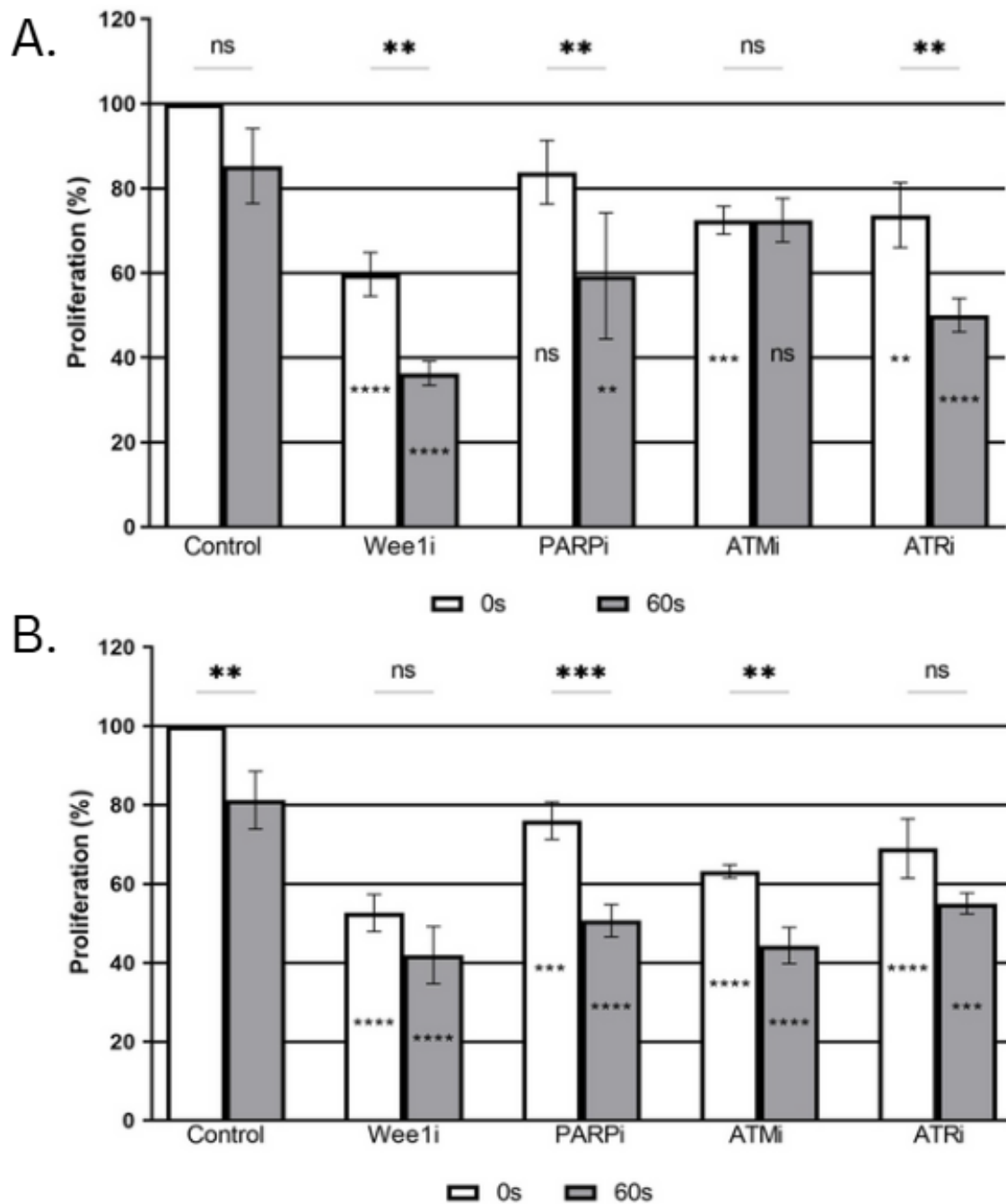


Figure 21: Post-treatment of A253 (A) and FaDu (B) cell lines with CAP after DDR inhibitors treatment. Cells were treated with different concentrations of the DDR inhibitors for 1 hour before treatment with CAP for the indicated times, followed by 72h incubation. Error bars are SD RM one-way ANOVA * $p < 0.05$, ** $p < 0.01$, *** $p < 0.001$, **** $p < 0.0001$. Asterisks on the inhibitor's bars are for comparisons with the relevant condition without an inhibitor. Experiments were performed in triplicate and repeated three times with similar results.

In comparison, for the FaDu cell line, the analysis of the results indicates a significant difference when comparing the 60s CAP-treated condition with the

equivalent DDRi-only condition for all DDRi besides Wee1i and ATRi. There is also a significant difference when comparing viability following DDRi-only treatment with the DDRi and CAP combination for both PARPi and ATMi, but not for Wee1i and ATRi. The possible synergistic effect can be seen only in the co-treatment of CAP with PARPi. The CAP-only treatment inhibited proliferation by 22.47%, while the PARPi-only treatment inhibited proliferation by 21.29%. Their co-treatment inhibits proliferation by 46.97%. For Wee1i, ATMi and ATRi, the DDRi-only treatments inhibited proliferation by 50.09%, 35.95% and 35.14% respectively, while the co-treatments with CAP inhibited proliferation by 61.7%, 57.68% and 43.5% respectively.

The difference in response between the two cell lines might have been triggered by the different p53 profiles of the cell lines used in the experiments. Although they are both p53-negative cell lines, they provide different p53 characteristics. A study by Cuneo et al. (2016) highlighted that Wee1i sensitizes cells to radiation in both p53-mutant and p53 wild-type cells but through different mechanisms. In *TP53*-null and *TP53*-mutant cell lines, inhibition of Wee1 increased histone H3 phosphorylation, which is indicative of G2 checkpoint blockage (Cuneo et al., 2016). This disruption forced cells into early mitosis, leading to cell death. However, in p53 wild-type cells treated with AZD1775, histone H3 phosphorylation was minimally affected, likely due to the ability of these cells to arrest at the G1 checkpoint, allowing DNA damage repair before mitotic entry (Cuneo et al., 2016). The study also emphasizes that the functionality of the entire p53 pathway in these contexts remains uncertain.

Other studies have shown that Wee1 inhibition is effective in p53 wild-type tumours, suggesting that mechanisms beyond p53 mutations might contribute to this sensitivity (Kato et al., 2015). One such alternative mechanism is related to aberrations

in the CDKN2A locus, which are common in many tumour types. These aberrations disrupt the G1/M checkpoint, leading to reliance on the S/G2 checkpoint regulated by Wee1. This dependence makes tumour cells with CDKN2A loss or dysregulation vulnerable to synthetic lethality when Wee1 is inhibited, providing a possible explanation for the sensitivity of p53 wild-type tumours to Wee1 inhibitors (Kato et al., 2015).

In our case, A253, which is a p53-negative cell line, are cells typically more reliant on alternative DNA repair and checkpoint mechanisms (e.g., Wee1 or ATR pathways) because they lack p53-mediated stress responses (Arutyunyan et al., 2023). They might show different sensitivity to DNA-damaging agents and targeted therapies like Wee1 or ATR inhibitors. FaDu, however, is a p53-mutant cell line, which are cells with partial functionality or gain-of-function phenotypes, making their response to therapies variable. The exact mutation in FaDu p53 affects how these cells handle stress or repair DNA damage (Arutyunyan et al., 2023). Moreover, studies have shown that, despite PARP inhibitors being effective regardless of p53 status, in p53-negative and p53 mutant cells, reliance on alternative repair mechanisms makes them particularly sensitive to the synthetic lethality induced by PARPi and DNA-damaging agents (Jiang et al., 2009a).

Taking all of these into account, the co-treatment of DDRi and CAP has higher enhanced anti-proliferative effects in A253 when using Wee1i, ATRi and PARPi attributable to the p53-profile of the cell line. For FaDu cells, all DDRi combinations have an additive effect when paired with CAP, besides PARPi, which provides the same possibly synergistic effect due to FaDu being a p53-mutant cell line, which might be more sensitive to synthetic lethality (Ye et al., 2016). Attributable to the fact that the

loaded composite hydrogels previously used in our experiments are limited to cationic drugs, using adavosertib and olaparib-loaded hydrogels could be the next step in assessing the anti-proliferative effects of CAP therapy, due to both adavosertib and olaparib being cationic drugs.

The results of ATMi testing in A253 and FaDu cell lines did not align with the expected trend. However, CAP is producing different types of DNA damage, such as oxidative base damage and single strand breaks, and ATM kinase is activated by double strand breaks. Other pathways might be involved to repair the DNA damage triggered by CAP. The effectiveness of these pathways may be attributed to the complex and variable characteristics of p53-deficient cells. Additionally, genetic aberrations within p53-negative/mutant cell lines, including variations in mutations or loss of other key repair genes, such as *CDKN2A*, *KDMC5* or *SMAD4*, could significantly impact their response to ATM inhibition (Arutyunyan et al., 2023), (Lavery et al., 2024). Further testing is required to account for these variables and clarify the mechanisms underlying the observed responses. This will involve optimizing experimental conditions, testing a range of concentrations of the ATMi and a range of different doses of CAP.

4.3.3. PHOSPHORYLATION OF H2AX AFTER COMBINATION TREATMENT WITH CAP AND DDRiS

The mechanism of the enhanced cytotoxicity after the co-treatment of direct CAP treatment and DDRi is discussed in the context of activation of the DDR, measured through the detection of γ H2AX. This approach could be particularly effective in cancer cells with pre-existing DDR defects (for example, *BRCA* mutations), as they rely heavily

on the remaining repair pathways. The combination can selectively target tumour cells by using CAP to amplify DNA damage and DDR inhibitors to block repair, minimizing harm to normal cells and improving therapeutic efficacy.

This phenomenon can be seen in IF staining of A253 and FaDu cell lines after co-treatment of DDRi and 60s CAP. Cells were fixed and stained after 24h incubation. Following a qualitative analysis of the results, higher levels of DNA damage are triggered in the presence of CAP. Increased levels of γ H2AX were expected in cells treated with Wee1i, PARPi, ATRi and ATMi, because these inhibitors impair critical DNA damage response pathways, leading to an accumulation of DNA damage. ATMi and ATRi block the repair of DSBs and stalled replication forks, respectively. However, when these inhibitors are combined with direct CAP treatment, which generates ROS and RNS, we hypothesise that the resulting DNA damage could be amplified. CAP-induced ROS can cause additional DNA damage, including strand breaks and oxidative modifications. This synergistic effect results in even higher levels of γ H2AX compared to treatment with the inhibitors alone, as the combined treatment causes a greater burden of DNA damage that the cells are unable to repair efficiently.

The IF results for each inhibitor will be analysed and discussed individually in order to provide a detailed evaluation of their effects based on cell lines and in comparison with the proliferation assay data.

4.3.3.1. DIRECT CAP TREATMENT AND ADAVOSERTIB (WEE1I)

As previously mentioned, the cell lines used in these experiments have different p53 status. A253 is p53-deficient (null) with no p53 expression at all, while FaDu has a missense mutation in the *TP53* gene, which leads to a mutant, non-functional or partially functional p53 (Cai et al., 2022). Adavosertib (AZD1775) shows promise in the targeted therapy of p53-deficient HNSCC, inducing replication stress and disruptions in the G2/M checkpoint of cancer cells while also having selective cytotoxicity in p53-mutant cells (Kao et al., 2017). Both p53-mutated and wild-type cells are affected by Wee1 inhibition. Adavosertib, which is a Wee1 inhibitor, prevents the proper activation of the G2/M checkpoint (Ku et al., 2017). This leads to mitotic catastrophe and apoptosis, justifying the greater effect it has in p53-deficient (null) lines, where the G1 checkpoint is already defective due to the non-functional p53 (Ku et al., 2017).

Based on the qualitative analysis of γ H2AX as presented in Figure 22 and Figure 23, an increase in the DNA damage response can be seen in the co-treatment of CAP and Wee1i for A253. In comparison, the γ H2AX signal in the co-treatment of Wee1i and CAP compared to the Wee1i-only treatment in the FaDu cell line is similar. The p53 profile of the cells might play a role in the different results, attributable to the fact that FaDu cells may handle replication stress and CAP-induced DNA damage better, showing minimal changes in the γ H2AX signal (Diab et al., 2019). In p53-deficient A253 cells, this oxidative stress cannot be efficiently countered due to impaired DNA repair pathways, leading to cumulative DNA damage and higher γ H2AX staining. In contrast, p53-mutant

FaDu cells may activate alternative DNA repair pathways, resulting in reduced γ H2AX intensity under the same treatment conditions (Diab et al., 2019).

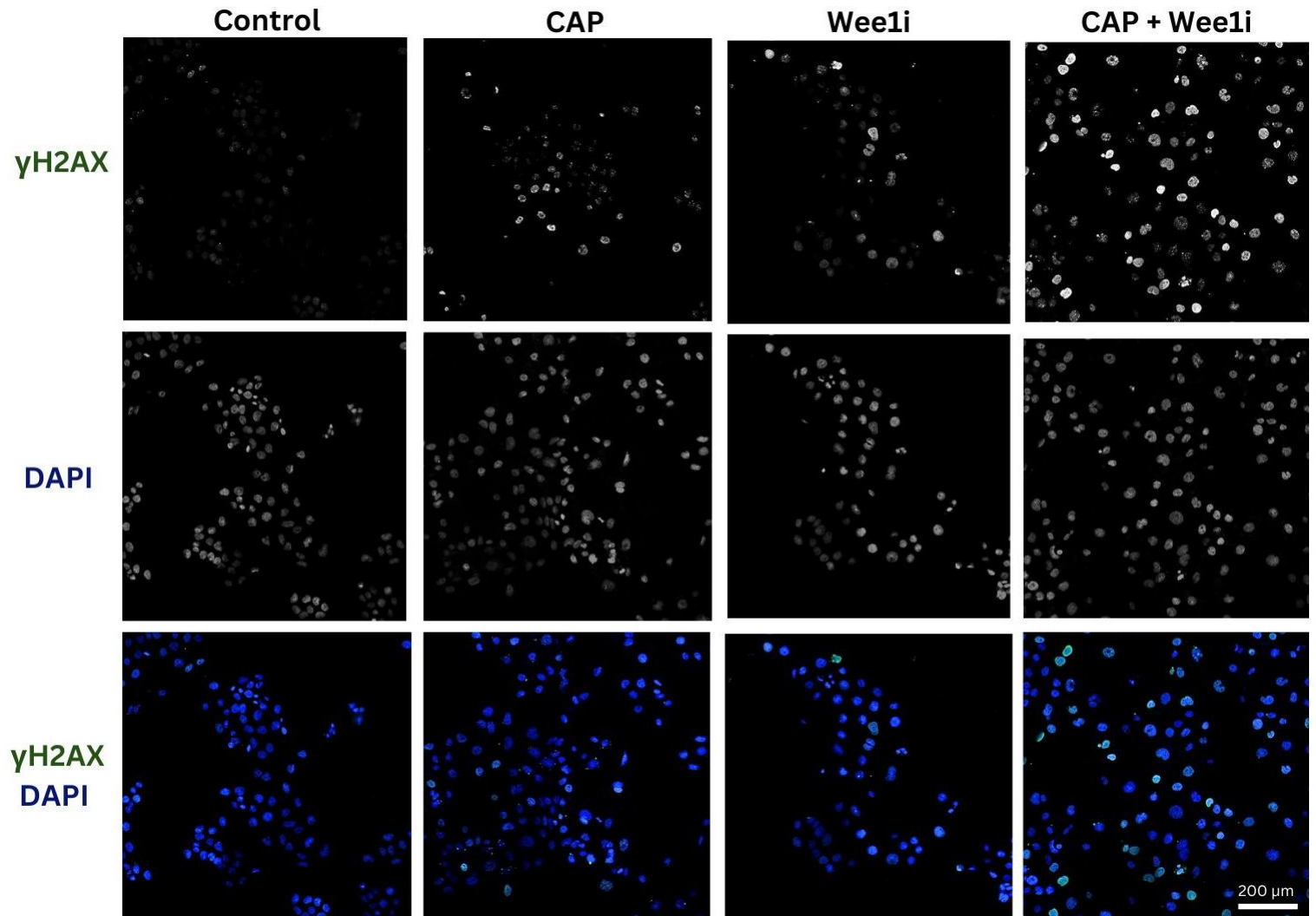


Figure 22: DNA damage after treatment with CAP in the presence or absence of Wee1i in the A253 cell line. A253 cells were incubated with 300 nM Wee1i (adavosertib) for 1 hour before treatment with CAP for 60s. After 24 hours of incubation, the cells were fixed and stained with DAPI and anti- γ H2AX antibody, before imaging on a Zeiss LSM880 confocal microscope equipped with a Plan-Apochromat 20x/0.8 M27 objective (n=1). Images were captured with a GaAsP detector and processed using ZEN Black software. DAPI (excitation: 358 nm, emission: 461 nm) and Alexa Fluor 488 (excitation: 488 nm, emission: 525 nm) were used to stain nuclei and cytoplasm, respectively. Z-stacks were acquired with a 1 μ m step size over a total depth of 20 μ m. Image analysis was performed using Fiji (ImageJ) software. Scale bar: 200 μ m.

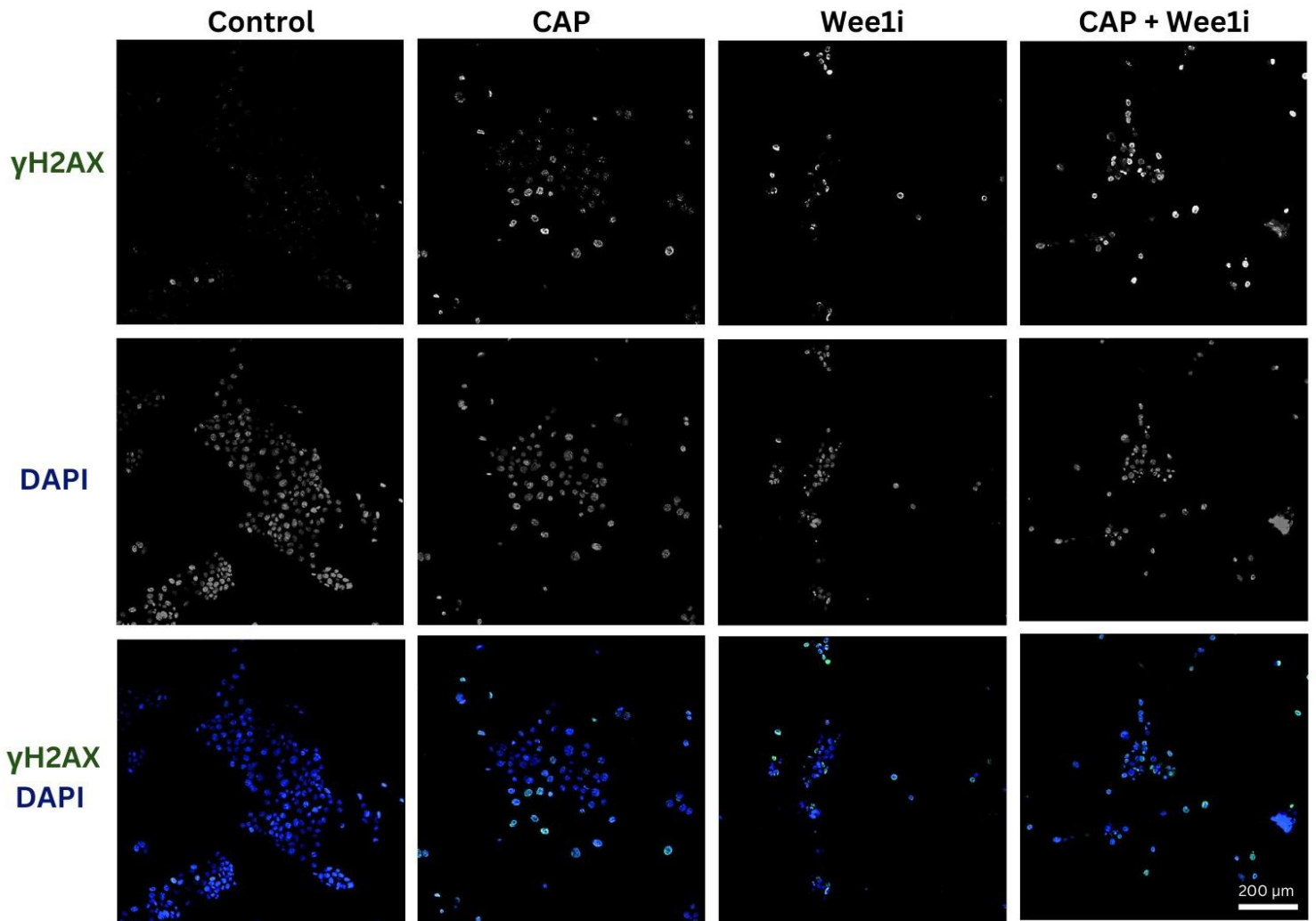


Figure 23: DNA damage after treatment with CAP in the presence or absence of Wee1i in the FaDu cell line. FaDu cells were incubated with 300 nM Wee1i (adavosertib) for 1 hour before treatment with CAP for 60s. After 24 hours of incubation, the cells were fixed and stained with DAPI and anti- γ H2AX antibody, before imaging on a Zeiss LSM880 confocal microscope equipped with a Plan-Apochromat 20x/0.8 M27 objective (n=1). Images were captured with a GaAsP detector and processed using ZEN Black software. DAPI (excitation: 358 nm, emission: 461 nm) and Alexa Fluor 488 (excitation: 488 nm, emission: 525 nm) were used to stain nuclei and cytoplasm, respectively. Z-stacks were acquired with a 1 μ m step size over a total depth of 20 μ m. Image analysis was performed using Fiji (ImageJ) software. Scale bar: 200 μ m.

The combination of CAP and Wee1 inhibitor generates greater γ H2AX intensity in A253 cells due to their p53 deficiency, which makes them highly dependent on the G2/M checkpoint and more susceptible to DNA damage accumulation when this checkpoint is disrupted. Meanwhile, FaDu cells may retain enough residual repair capacity through their mutant p53, showing no significant increase in γ H2AX signal (Diab et al., 2019).

The similar IF results for γ H2AX staining in both A253 and FaDu cells, despite their different responses to DDR inhibitors and CAP when assessing proliferation, likely indicate that both cell lines accumulate similar levels of DNA damage following treatment. However, the p53 profile influences how each cell line responds to damage (i.e., repair, cell cycle progression, or cell death), which results in differences in proliferation, even if the DNA damage (reflected by γ H2AX foci) is similar. The IF assay primarily reports on the extent of DNA damage, while proliferation assays or cell cycle analysis better capture the cellular consequences of that damage. Moreover, γ H2AX foci in IF assays may reflect a threshold of detectable DNA damage, beyond which the cells may still show similar results in terms of staining intensity treatment (Stenvall et al., 2020; Sykora et al., 2018; Nikitaki et al., 2020). While A253 cells may proliferate more despite DNA damage, and FaDu may show a more regulated response with additive effects from the treatments, both could still exhibit similar levels of γ H2AX because the damage threshold (i.e., amount of DNA breaks) needed for γ H2AX detection may be reached in both cell lines after treatment (Stenvall et al., 2020; Sykora et al., 2018; Nikitaki et al., 2020).

Other markers of DNA damage response were observed in the A253 cell line. Mitosis is a fundamental process in eukaryotic cell division, where a parent cell divides

to form two genetically identical daughter cells. This process ensures that the genetic material is accurately replicated and distributed to the daughter cells, facilitated by the spindle microtubules that organize and separate the chromosomes, and cytokinesis, which divides the cell's cytoplasm (Chandra, 2002). Errors during mitosis, such as improper chromosome segregation or failure to complete cell division, can lead to aneuploidy (an abnormal number of chromosomes) or mitotic arrest (a halt in cell division), both of which can disrupt normal cellular function and contribute to disease (Kops, Weaver and Cleveland, 2005).

CAP-generated ROS can cause mitotic arrest by disrupting the normal progression of cell division, damaging various cellular components, including DNA and proteins, and leading to delays or halts in mitosis (Wang et al., 2017). Specifically, ROS interfere with the formation and function of the mitotic spindle, a structure that is crucial for accurate chromosome segregation. The dysfunction of the spindle caused by ROS can result in improper chromosome alignment and separation, which may contribute to errors in cell division and genetic instability (Wang et al., 2017).

One key protein affected by oxidative stress during mitosis is Aurora A, a kinase that regulates spindle formation and centrosome function (Wang et al., 2017). Under oxidative stress, Aurora A becomes hyperphosphorylated, meaning it accumulates excessive phosphate groups, which can alter its activity. Despite this hyperphosphorylation, Aurora A maintains its normal localization at the centrosomes, where it is involved in organizing the mitotic spindle (Wang et al., 2017). While the phosphorylation status of Aurora A is affected by ROS, its centrosomal positioning does not change, suggesting that oxidative stress primarily impacts its function rather than its cellular location (Wang et al., 2017).

This disruption of Aurora A activity can further contribute to the mitotic delays and abnormalities observed under oxidative stress, such as abnormalities in chromosome alignment and spindle formation (Wang et al., 2017). When a cell has more than two spindle poles instead of the usual two, the proper alignment and separation of chromosomes are disrupted, leading to misalignment and unequal distribution of genetic material. These abnormalities were also noticed in the IF stainings of the co-treatment of CAP and Wee1i in the A253 cell line (Figure 24). This result supports our hypothesis that co-treatment with CAP enhances the anti-proliferative effects of Wee1i.

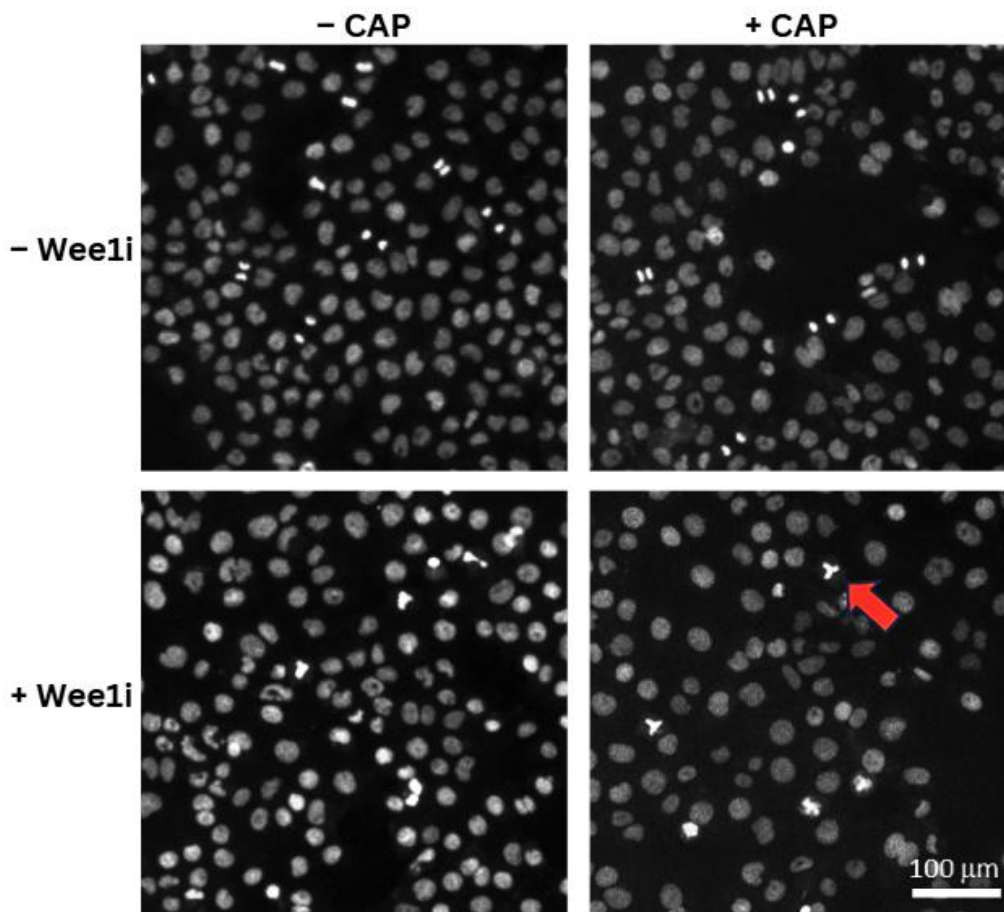


Figure 24: Abnormalities in chromosome alignment and spindle formation in the co-treatment of CAP and Wee1i in the A253 cell line. Expanded images of the DAPI channel. Multipolar spindle indicated by the red arrow.

4.3.3.2. DIRECT CAP TREATMENT AND OLAPARIB (PARPi)

Olaparib inhibits PARP (Poly(ADP-ribose) polymerase), which is crucial for repairing single-strand DNA breaks through the base excision repair (BER) pathway. When PARP is inhibited, single-strand breaks are triggered. Unrepaired SSBs could be converted into double-strand breaks during DNA replication, overwhelming the cell's repair capacity, particularly in p53-deficient or mutant p53 cells (Lafontaine et al., 2020).

Differential γ H2AX staining was observed after co-treatment of PARPi and CAP in A253 and FaDu cells, reflecting their distinct p53 profiles, similar to the Wee1i data. When using the co-treatment of PARPi and CAP on A253 cells, which lack p53, higher γ H2AX intensity was exhibited, indicating the accumulation of impaired DNA repair in response to PARP inhibition, as displayed in Figure 25 and Figure 26. The same combination in FaDu cells has similar γ H2AX intensity as the PARPi-only treatment.

The observed higher γ H2AX intensity in A253 cells supports the idea that p53-deficient tumors may be more sensitive to PARP inhibition, as the lack of functional p53 elevates the levels of DNA damage induced by PARPi. FaDu cells, despite being p53-mutant, may still have some DNA repair capacity, suggesting that PARPi's effectiveness could be reduced in mutant p53 cancers, but may still provide therapeutic benefit depending on the degree of DNA repair deficiency. This difference highlights the role of p53 status in modulating the efficacy of olaparib and its potential in targeting p53-deficient cancers with PARP inhibitors to exploit their compromised DNA repair mechanisms. Caspase-3/7 or cleaved PARP staining could be used to correlate the

γ H2AX signal with cell death, providing a broader picture of how DNA damage translates into cytotoxicity in these cell lines (Bajrami et al., 2012).

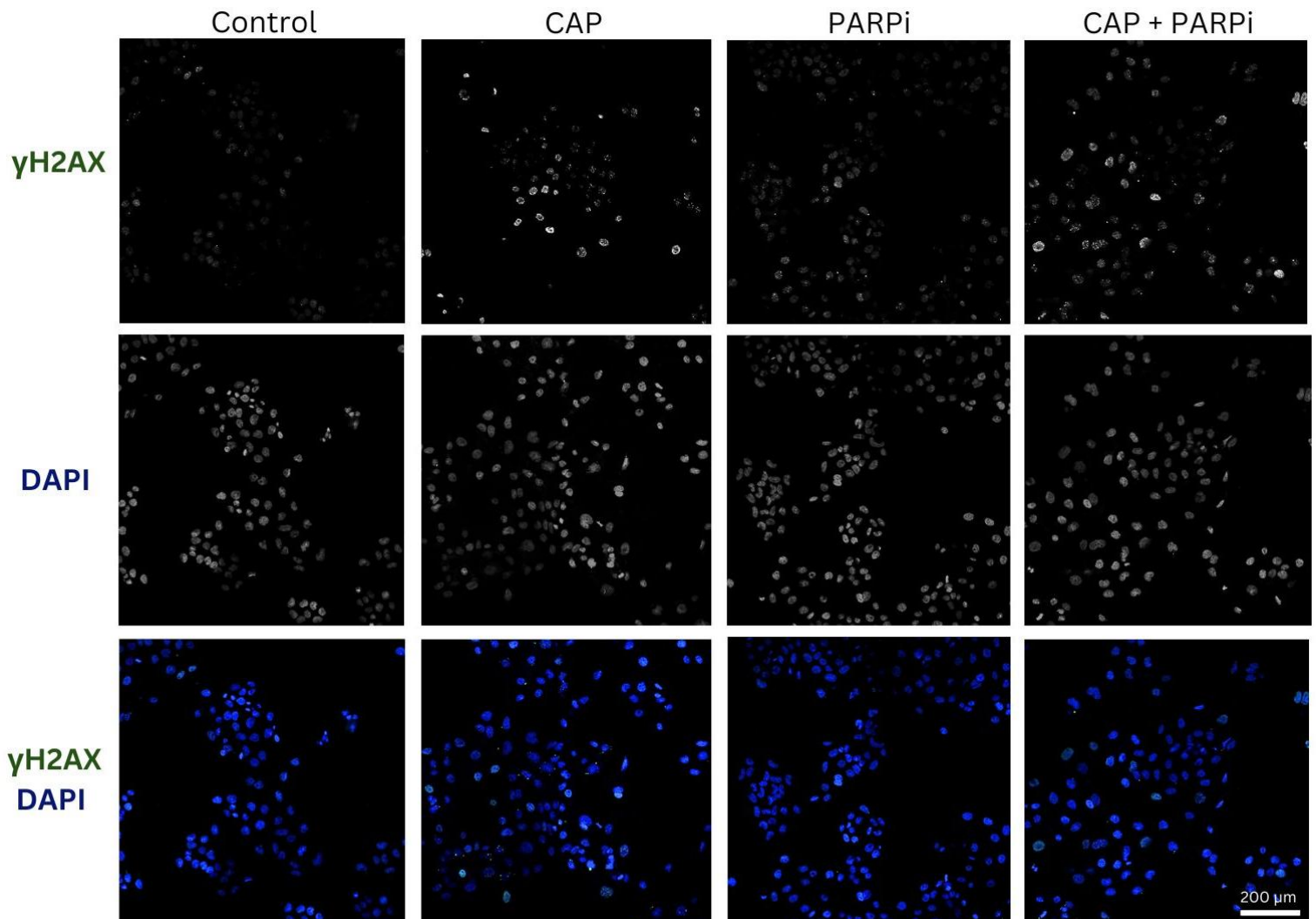


Figure 25: DNA damage after treatment with CAP in the presence or absence of PARPi in the A253 cell line. A253 cells were incubated with 1 μ M PARPi (olaparib) for 1 hour before treatment with CAP for 60s. After 24 hours of incubation, the cells were fixed and stained with DAPI and anti- γ H2AX antibody, before imaging on a Zeiss LSM880 confocal microscope equipped with a Plan-Apochromat 20x/0.8 M27 objective (n=1). Images were captured with a GaAsP detector and processed using ZEN Black software. DAPI (excitation: 358 nm, emission: 461 nm) and Alexa Fluor 488 (excitation: 488 nm, emission: 525 nm) were used to stain nuclei and cytoplasm, respectively. Z-stacks were acquired with a 1 μ m step size over a total depth of 20 μ m. Image analysis was performed using Fiji (ImageJ) software. Scale bar: 200 μ m.

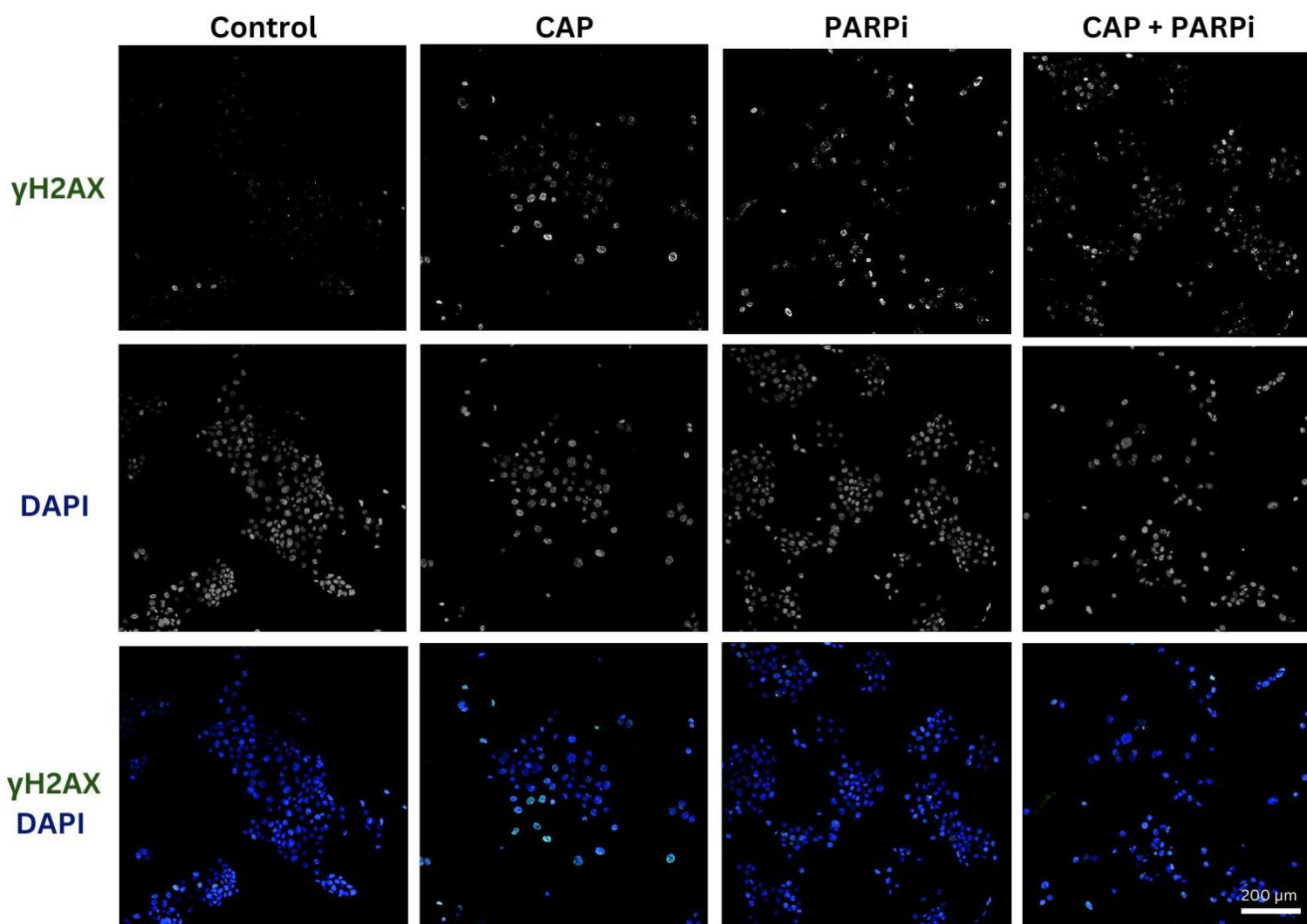


Figure 26: DNA damage after treatment with CAP in the presence or absence of PARPi in the FaDu cell line. FaDu cells were incubated with 1 μ M PARPi (olaparib) for 1 hour before treatment with CAP for 60s. After 24 hours of incubation, the cells were fixed and stained with DAPI and anti- γ H2AX antibody, before imaging on a Zeiss LSM880 confocal microscope equipped with a Plan-Apochromat 20x/0.8 M27 objective ($n=1$). Images were captured with a GaAsP detector and processed using ZEN Black software. DAPI (excitation: 358 nm, emission: 461 nm) and Alexa Fluor 488 (excitation: 488 nm, emission: 525 nm) were used to stain nuclei and cytoplasm, respectively. Z-stacks were acquired with a 1 μ m step size over a total depth of 20 μ m. Image analysis was performed using Fiji (ImageJ) software. Scale bar: 200 μ m.

The combination of PARPi and CAP may also be facilitated by the induced oxidative stress, which leads to DNA breaks. CAP generates ROS and RNS when applied to biological cells, mimicking oxidative stress. These reactive molecules can cause DNA

damage, which in turn activates PARP-1. When combining CAP with a PARP-1 inhibitor like olaparib, the PARP-1 activity is blocked, preventing the repair of DNA damage, especially in cells with defective DNA repair mechanisms (Csaba Hegedűs and László Virág, 2014).

Additionally, p53 presents antioxidant activity able to inhibit oxidative DNA damage triggered by ROS generation (Liu et al., 2020). A study by Sablina et al. (2005) suggests that the lack of p53 in mice leads to higher levels of reactive oxygen species (ROS) inside cells. These ROS can cause damage to the cells' DNA, which increases the likelihood of cancer developing. This may justify the higher amount of DDR in the co-treatment of A253 cells with the PARPi and CAP, due to A253 cell line being p53 defective (null). Therefore, these data highlight the potential CAP has in combination with PARP when using it against cells with defective DNA repair mechanisms, such as p53-null HNSCC.

4.3.3.3. DIRECT CAP TREATMENT AND CERALASERTIB (ATRi)

Ceralasertib, also known as AZD6738, is a potent and selective ATR kinase inhibitor. ATR, which responds to stalled DNA replication forks, is involved in cell-cycle checkpoints and fork restart. A study by Wilson et al. (2022) suggests that combining ATR inhibition with other therapies enhances antitumor efficacy, especially in tumors with DNA damage or replication stress. Additionally, ATR is a kinase responsible for phosphorylating γ H2AX.

When treating A253 and FaDu cell lines with co-treatment of ATRi and CAP, low levels of γ H2AX signal would have been expected. However, because the cells were incubated for 24 hours with the DDRi treatment, the γ H2AX signal displayed in Figure 27 and Figure 28 might be impaired DNA repair of endogenous damage in the DDRi only treatment and impaired DNA repair of CAP damage in the treatment combination. Therefore, γ H2AX is being phosphorylated by the PIKK kinases that are not being inhibited.

A study by Mordes and Cortez (2008) suggests that PIKK kinases (including ATM and DNA-PKcs) can compensate for ATR inhibition by still phosphorylating γ H2AX in response to DNA damage. This supports the idea that when ATR is inhibited, other kinases, such as those in the PIKK family, can still trigger γ H2AX activation, ensuring a continued DNA damage response despite the absence of ATR's usual role in initiating it.

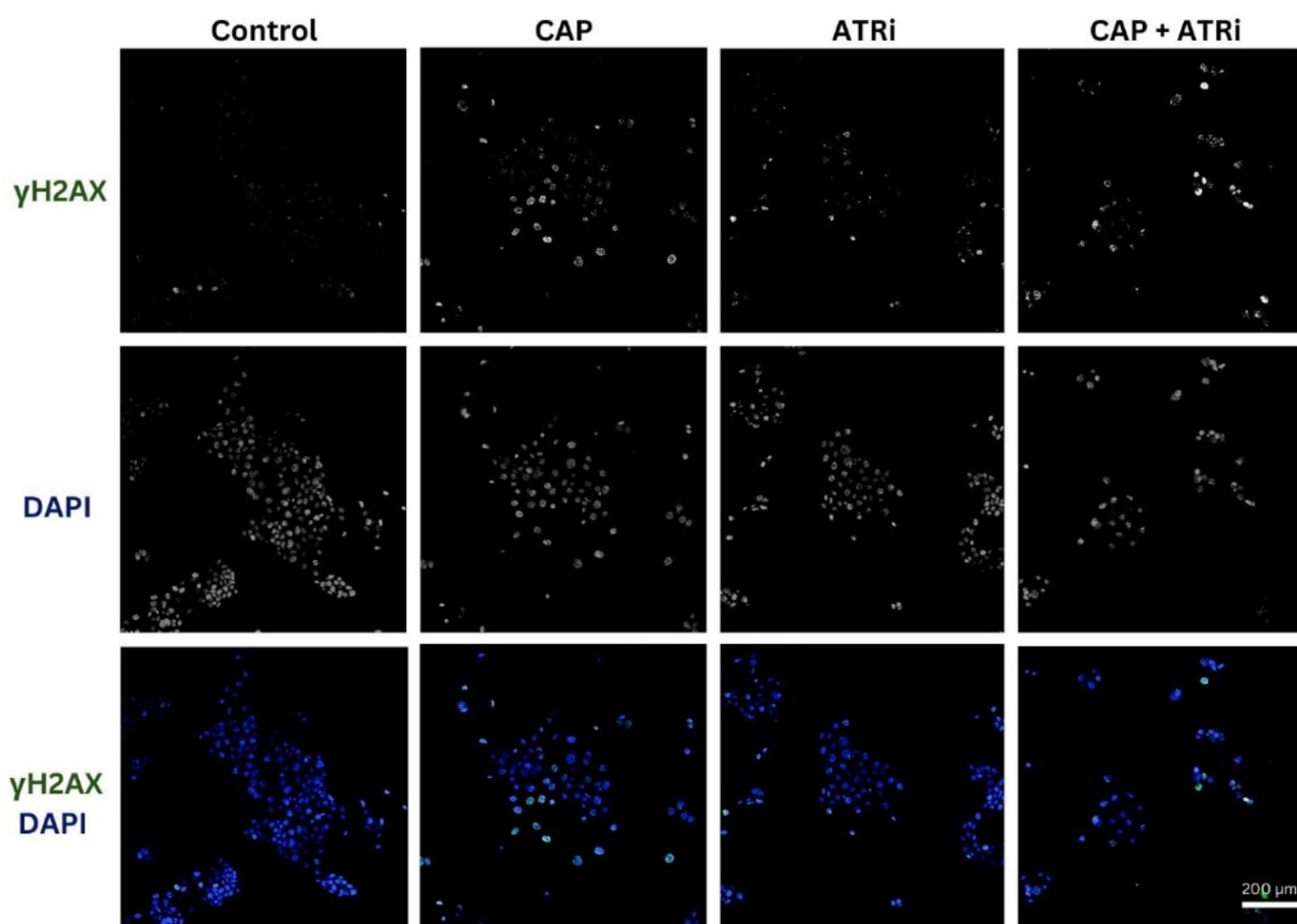


Figure 27: DNA damage after treatment with CAP in the presence or absence of ATRi in the A253 cell line. A253 cells were incubated with 5 nM ATRi (ceralasertib, AZD6738) for 1 hour before treatment with CAP for 60s. After 24 hours of incubation, the cells were fixed and stained with DAPI and anti- γ H2AX antibody, before imaging on a Zeiss LSM880 confocal microscope equipped with a Plan-Apochromat 20x/0.8 M27 objective (n=1). Images were captured with a GaAsP detector and processed using ZEN Black software. DAPI (excitation: 358 nm, emission: 461 nm) and Alexa Fluor 488 (excitation: 488 nm, emission: 525 nm) were used to stain nuclei and cytoplasm, respectively. Z-stacks were acquired with a 1 μ m step size over a total depth of 20 μ m. Image analysis was performed using Fiji (ImageJ) software. Scale bar: 200 μ m.

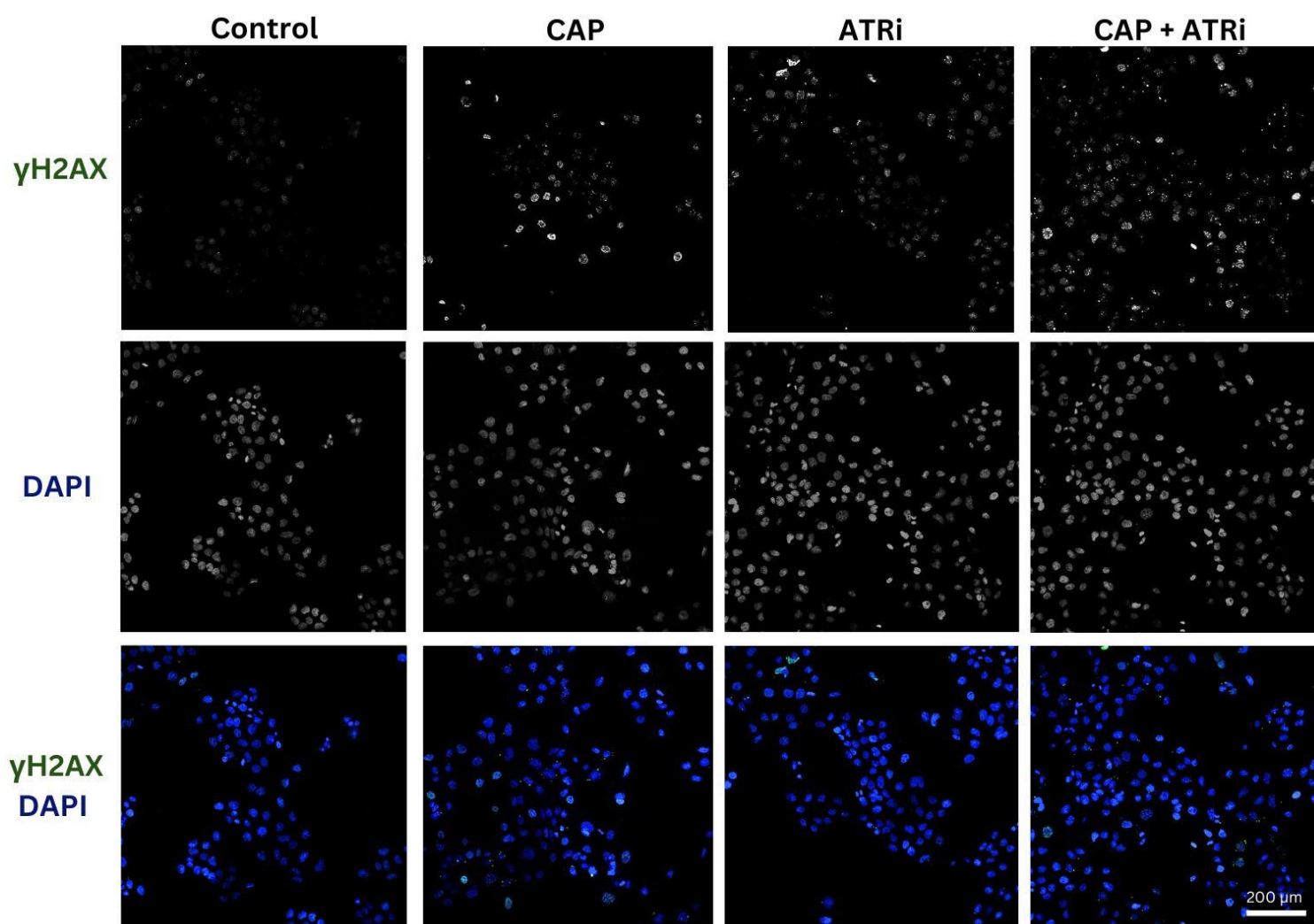


Figure 28: DNA damage after treatment with CAP in the presence or absence of ATRi in the FaDu cell line. FaDu cells were incubated with 5 nM ATRi (ceralasertib, AZD6738) for 1 hour before treatment with CAP for 60s. After 24 hours of incubation, the cells were fixed and stained with DAPI and anti- γ H2AX antibody, before imaging on a Zeiss LSM880 confocal microscope equipped with a Plan-Apochromat 20x/0.8 M27 objective (n=1). Images were captured with a GaAsP detector and processed using ZEN Black software. DAPI (excitation: 358 nm, emission: 461 nm) and Alexa Fluor 488 (excitation: 488 nm, emission: 525 nm) were used to stain nuclei and cytoplasm, respectively. Z-stacks were acquired with a 1 μ m step size over a total depth of 20 μ m. Image analysis was performed using Fiji (ImageJ) software. Scale bar: 200 μ m.

Additionally, there is a link between p53 and ATR inhibition. A study by Middleton, Pollard and Curtin (2018) discusses how ATR inhibitors, such as VE-821, may be more effective in p53-deficient or mutant cells, enhancing their radiosensitivity

and chemosensitivity, particularly at higher doses. While p53-deficient cells have increased replication stress and rely on ATR signaling, ATR inhibition targets this dependency, especially in tumors with p53 defects. The findings of this Middleton, Pollard and Curtin (2018) study suggests that ATR inhibitors could offer tumor-specific treatments, but their effectiveness depends on the p53 status of the cells. These results may highlight the increased amount of γ H2AX signal in the co-treatment of A253 and FaDu cell lines with ATRi and CAP, justifying how prone these cells are to DNA damage when ATR protein kinase is inhibited.

4.3.3.4. DIRECT CAP TREATMENT AND AZD1390 (ATMi)

AZD1390 is a brain-penetrant ATM inhibitor that has the potential to improve clinical outcomes by targeting another key kinase involved in the DNA damage response, which is ATM kinase. While ceralasertib inhibits ATR and AZD1390 targets ATM, both kinases play central roles in maintaining genome stability and responding to DNA damage. Both drugs are being tested for their potential to sensitize tumors to DNA-damaging therapies, such as chemotherapy and radiotherapy (Durant et al., 2018).

Following a similar trend previously displayed by the co-treatment of A253 and FaDu cells with ATRi, the ATMi and CAP co-treatments exhibited higher amounts of γ H2AX signal than expected, as presented in Figure 29 and Figure 30. Even though ATM phosphorylates H2AX to form γ H2AX, inhibiting ATM can lead to increased γ H2AX levels due to the compensatory activation of other kinases like DNA-PKcs, very similar to the mechanism of ATRi and CAP co-treatment. This compensatory mechanism results

in the accumulation of DNA damage markers, including γ H2AX, despite the inhibition of ATM (Chiu et al., 2023). Additionally, ATR and DNA-PKcs can phosphorylate H2AX in response to DNA damage, contributing to γ H2AX formation when ATM is inhibited (Watanya Trakarnphornsombat and Kimura, 2023).

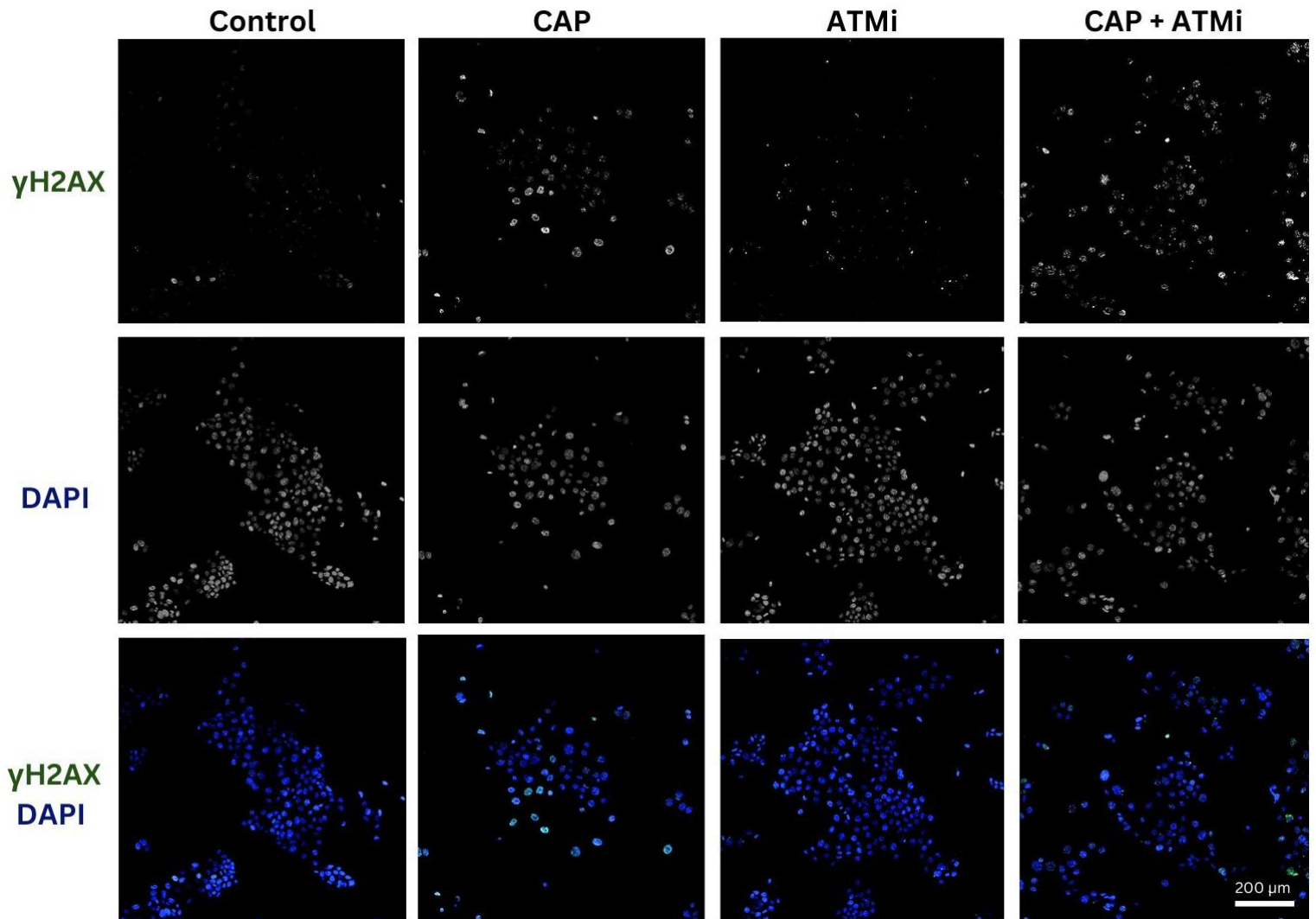


Figure 29: DNA damage after treatment with CAP in the presence or absence of ATMi in the A253 cell line. A253 cells were incubated with 5 nM ATMi (AZD1390) for 1 hour before treatment with CAP for 60s. After 24 hours of incubation, the cells were fixed and stained with DAPI and anti- γ H2AX antibody, before imaging on a Zeiss LSM880 confocal microscope equipped with a Plan-Apochromat 20x/0.8 M27 objective (n=1). Images were captured with a GaAsP detector and processed using ZEN Black software. DAPI (excitation: 358 nm, emission: 461 nm) and Alexa Fluor 488 (excitation: 488 nm, emission: 525 nm) were used to stain nuclei and cytoplasm, respectively. Z-stacks were acquired with a 1 μ m step size over a total depth of 20 μ m. Image analysis was performed using Fiji (ImageJ) software. Scale bar: 200 μ m.

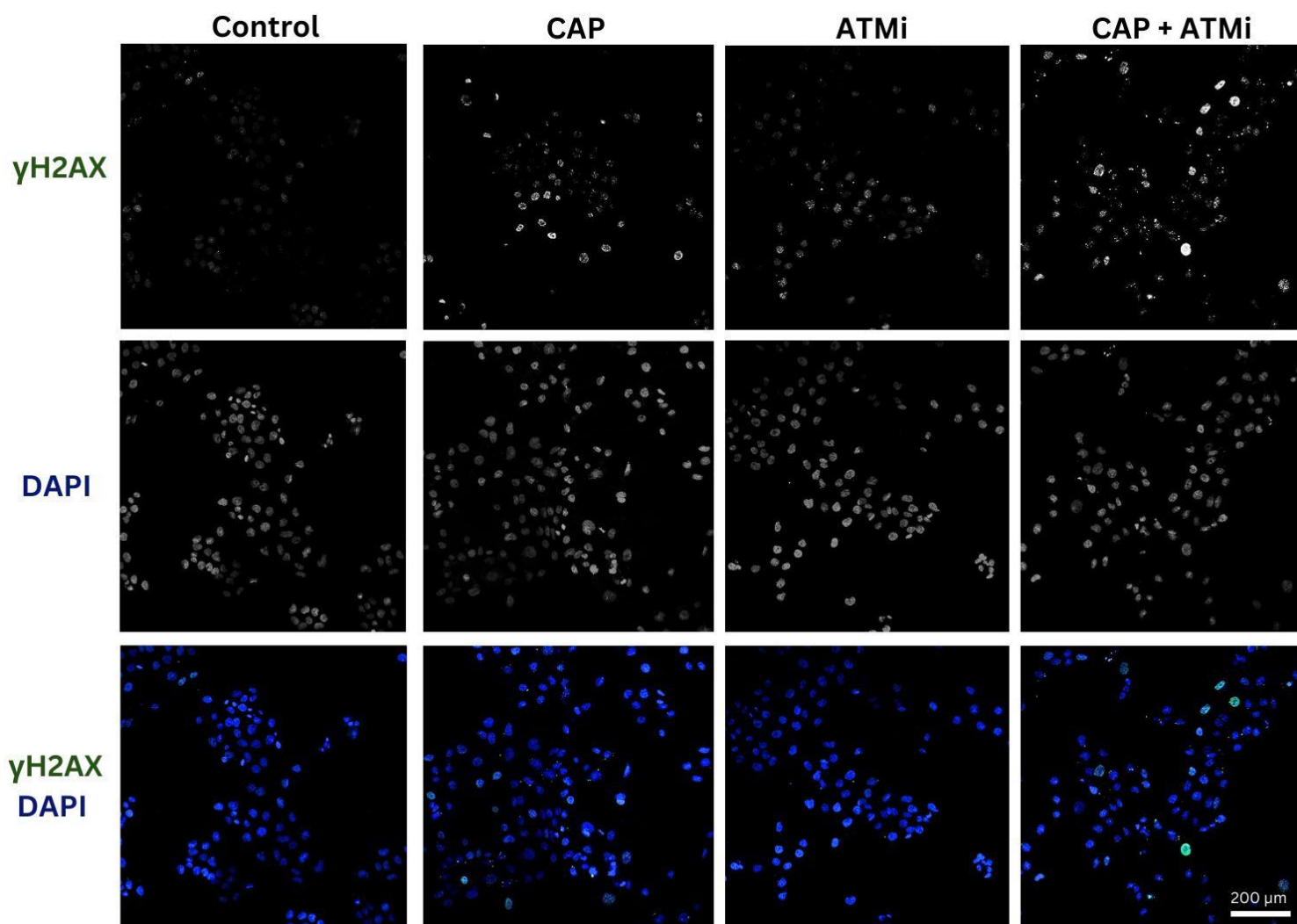


Figure 30: DNA damage after treatment with CAP in the presence or absence of ATMi in the FaDu cell line. FaDu cells were incubated with 5 nM ATMi (AZD1390) for 1 hour before treatment with CAP for 60s. After 24 hours of incubation, the cells were fixed and stained with DAPI and anti- γ H2AX antibody, before imaging on a Zeiss LSM880 confocal microscope equipped with a Plan-Apochromat 20x/0.8 M27 objective (n=1). Images were captured with a GaAsP detector and processed using ZEN Black software. DAPI (excitation: 358 nm, emission: 461 nm) and Alexa Fluor 488 (excitation: 488 nm, emission: 525 nm) were used to stain nuclei and cytoplasm, respectively. Z-stacks were acquired with a 1 μ m step size over a total depth of 20 μ m. Image analysis was performed using Fiji (ImageJ) software. Scale bar: 200 μ m.

Similar to the other DDRi tested, there is a significant link between p53 and ATM inhibition. Attributable to the fact that ATM is a key regulator of the DNA damage response, it also plays a crucial role in activating p53 following DNA damage. When

normal conditions are met, ATM phosphorylates p53 in response to DNA damage, leading to p53 stabilization and activation. This process will result in cell cycle arrest, allowing the start of DNA repair or triggering apoptosis if the damage is irreparable (Abuetabh et al., 2022). ATM also interacts with the mRNA of the p53 protein, influencing the protein's levels post-transcriptionally. This interaction highlights the multifaceted role of ATM in regulating p53 activity beyond direct phosphorylation (Konstantinos Karakostis et al., 2024).

A study by Biddlestone-Thorpe et al. (2013) shows that ATM inhibition can sensitize p53-mutant glioma cells to radiation therapy. In p53-mutant cells, the absence of functional p53 makes rely on ATM more when DNA damage repair is needed. Therefore, inhibiting ATM in these cells can lead to increased DNA damage and reduced survival, enhancing the effectiveness of treatments like radiation. Taking this into account, in A253 cells, the lack of p53 may lead to persistent γ H2AX signals without repair progression, showing higher DNA damage accumulation. In FaDu cells, however, because partial p53 activity could enable slower repair, could show a more dynamic γ H2AX response initially but still end up indicating elevated damage compared to untreated cells. Additionally, the oxidative stress induced by CAP enhances the DNA damage, previously seen in all DDRi tested besides Wee1i in FaDu cell line when comparing the co-treatment of DDRi and CAP to the CAP-only or DDRi-only condition.

5. CONCLUSIONS AND FUTURE RESEARCH

Plasma medicine is an emerging field that holds promise for addressing a wide range of conditions because it can target harmful bacteria, viruses, and damaged cells while promoting healing in healthy tissue. This emerging field could provide new treatment options for diseases that are currently difficult to manage, offering a safer, more effective alternative to traditional therapies. Co-treatment of CAP and chemotherapeutics or DNA damage response inhibitors could be the next step in treating head and neck squamous cell carcinoma and other types of cancer. Moreover, using CAP-activated hydrogels to deliver this combined therapy to target tissue allows for gradual and localized delivery of drugs, minimizing the need for high doses and reducing systemic side effects. By releasing the drug directly to the target area over time, hydrogels enhance drug efficacy while lowering the risk of adverse effects commonly associated with conventional methods.

Multiple studies on 2D cultures prove the potential CAP has in adjunctive therapy in cancer treatment, particularly when combined with traditional chemotherapeutics. A study by Gjika et al. (2020) investigated the effects of CAP combined with temozolomide (TMZ) in treating glioblastoma cells (U87MG). Their results prove that CAP induces cell death in glioblastoma cells and enhances the cytotoxicity of TMZ when used in combination. CAP treatment increases DNA damage, oxidative stress, and apoptosis in the cells, suggesting a synergistic effect with TMZ.

Similar results were displayed in a study by Brunner et al., 2022, in which CAP treatment was combined with low-dose cisplatin to treat HNSCC cells. This study's

results demonstrates that CAP enhances the cytotoxic effects of cisplatin, suggesting a potentially synergistic therapeutic approach. Although the optimization between the two studies is slightly different (120s CAP treatment compared to 60s CAP treatment and 1 μM cisplatin compared to 1.5 μM cisplatin), this data corroborates the results of our study, even more so when comparing the anti-proliferative effects their co-treatment had when treating FaDu cells. In the Brunner et al., 2022 study, the combination of 120s CAP treatment and 1 μM cisplatin inhibited FaDu cell proliferation by approximately 40-50%, very similar to how much proliferation was inhibited in our study (76.41%). However, in the Brunner et al., 2022 study, CAP treatment was applied before cisplatin. The cells were first exposed to CAP for 120 seconds, followed by the addition of 1 μM cisplatin shortly after.

The enhanced proliferation effect displayed in our experiment could be the cause of CAP treatment being applied after cisplatin treatment, linked to the possible electroporation process triggered by CAP in the cell membrane, which facilitates the entrance of cisplatin inside the cell. In order to assess this theory and have more conclusive results, testing the possible electroporation triggered by CAP using a fluorescent dye uptake assay such as propidium iodide or calcein-AM could aid in assessing whether or not there are any membrane permeability changes through flow cytometry to quantify dye uptake, confirming electroporation effects (Crowley et al., 2016). Other methods that could be used in future work to have a better understanding of this subject is measuring the electrical impedance to detect changes in membrane resistance after CAP treatment (Moghtaderi et al., 2024).

Additional to preclinical *in vitro* studies, clinical trials undergo CAP testing in cancer therapy. According to Canady et al. (2023), this Phase I clinical trial examined the use of

CAP as a treatment for advanced solid tumors, focusing on its safety and efficacy. CAP was applied intraoperatively, targeting tumor cells with minimal damage to surrounding healthy tissue. The study showed that CAP treatment was well-tolerated by patients and did not cause significant adverse effects, providing a basis for its potential as an adjunctive therapy in cancer treatment. Moreover, the trial demonstrated that CAP could assist in controlling residual cancer after surgery, suggesting a promising new therapeutic strategy for advanced cancers.

Additionally to 2D culture studies, 3D culture studies corroborate our study findings. A study by Shaw et al. (2021) explores how CAP enhances the sensitivity of glioblastoma spheroids to temozolomide (TMZ) by inhibiting the glutathione (GSH)/glutathione peroxidase 4 (GPX4) antioxidant pathway, leading to increased DNA damage and cell death. Another very similar study was conducted by Murillo et al. (2023), investigating how CAP can be used to overcome drug resistance in glioblastoma, including its combination with chemotherapeutic agents like TMZ in spheroid models. Although the experiment presented in our study used a longer CAP exposure of 240 seconds and different cell lines compared to the studies referenced, the overall findings are consistent, particularly regarding the use of spheroids.

All studies demonstrate that CAP treatment enhances the efficacy of chemotherapeutic agents in spheroid models. Despite variations in CAP exposure time and cell lines, the core mechanism remains the same: CAP induces oxidative stress, DNA damage, and apoptosis, which in turn sensitizes spheroid cells to chemotherapy. The longer CAP exposure in our experiment may result in more extensive oxidative damage, potentially explaining the stronger cytotoxic effect observed in the spheroids, aligning with the synergistic effects noted in the literature. Additionally, even though our study

used different cell lines in spheroid models, the underlying biology, such as increased ROS production and impaired cellular repair mechanisms, appears to be consistent with what has been observed in glioblastoma spheroids, where CAP enhances drug sensitivity.

Along with the studies conducted on direct CAP treatment in cancer therapy, further literature investigates how CAP can trigger the release of chemotherapeutic agents from hydrogels, enhancing their therapeutic efficacy through PAHT. Studies by Gaur et al. (2023) and Li et al. (2023) present the synergistic potential of CAP and drug-loaded hydrogels in cancer therapy. One of the key findings of Gaur et al. (2023) is that CAP exposure significantly enhanced the release rate of the encapsulated drug, doxorubicin, from the hydrogel matrix. This suggests that CAP can act as an external stimulus to enhance the release of drugs, making the hydrogel drug delivery system more responsive and effective in cancer treatment. Additionally, the study demonstrated the cytotoxicity of the released doxorubicin in HeLa and MCF-7 cancer cell lines, confirming that the combination of CAP and drug-loaded hydrogels can lead to increased cell death and reduced proliferation.

In the Li et al. (2023) study, the combination of CAP with hydrogels leads to a dual approach to cancer treatment: the hydrogel ensures targeted and sustained drug release, while CAP enhances the efficacy of this release by acting as a trigger. This study suggests that this combination could be highly effective in solid tumors, where controlled drug release is critical for penetration and longer therapeutic action within tumor tissues.

The drug's passive release displayed by the cisplatin-loaded hydrogels in our experiments have been mentioned in other literature as well. In both studies previously

discussed, passive release is mentioned as being part of the natural drug release process in hydrogel systems. The introduction of CAP as an external trigger is shown to improve the release rate and drug bioavailability, aiding in overcoming the limitations of passive drug release, such as slow-release rates and low efficiency. The release kinetics and targeting of the therapeutic agents are more effective toward cancer cells when the hydrogel is activated by CAP.

Although the co-treatment of CAP and DDRi is not extensively studied, our results show that DDR inhibitors enhance the effectiveness of CAP, similar to the effects observed with cisplatin in combination with direct and indirect CAP treatment. This may suggest that these findings could serve as a pioneering step towards developing combination therapies involving CAP and DDR inhibitors, offering insights into how CAP can be integrated into cancer treatment regimens, paving the way for future research to explore this synergistic approach further and contribute to improved therapeutic outcomes for cancer patients.

Future research should focus on expanding upon the intricate DDR pathways affected by CAP and how these pathways can be further targeted with DDR inhibitors (DDRi). While this research has demonstrated that DDRi can sensitize cancer cells to CAP-induced DNA damage, the underlying molecular mechanisms are still not fully understood. Future experiments could focus on specific DDR pathways such as base excision repair (BER) or homologous recombination (HR) to try and determine how CAP interacts with these repair processes and how DDR inhibitors can be optimized to disrupt these pathways. This could involve using gene knockdown or CRISPR-Cas9 technologies to selectively inhibit key DDR proteins and observe their effect on CAP-induced DNA damage and cellular responses (Feng et al., 2024). Future studies could

also assess the combination of CAP and DDRi with other therapeutic modalities, such as immunotherapies or chemotherapies, to explore multimodal treatment strategies that may further improve treatment efficacy (Zhang and Zhang, 2016).

Overall, the research presented in this study aligns with the existing literature by demonstrating how CAP treatment, in direct combination with a chemotherapeutic like cisplatin or DDRi and indirectly applied through cisplatin-loaded hydrogels, can enhance chemotherapeutic efficacy in both 2D and 3D models. These results may contribute to the growing body of evidence supporting the synergistic potential of combining physical therapies like CAP with drug treatments in cancer therapy, emphasizing the need for multi-modal approaches to overcome drug resistance and improve patient outcomes.

REFERENCE LIST

- Abuetabh, Y., Wu, H.H., Chai, C., Al Yousef, H., Persad, S., Sergi, C.M. and Leng, R. (2022). DNA damage response revisited: the p53 family and its regulators provide endless cancer therapy opportunities. *Experimental & Molecular Medicine*.
- Adhikari, B.R. and Khanal, R. (2013). Introduction to the Plasma State of Matter. *Himalayan Physics*, 4, pp.60–64.
- Afrasiabi, M., Ghazaleh Tahmasebi, Eslami, E., Enayatollah Seyedi and Jalal Pourahmad (2022). Cold Atmospheric Plasma Versus Cisplatin Against Oral Squamous Cell Carcinoma: A Mitochondrial Targeting Study. *Deleted Journal*, 21(1).
- Aggarwal, V., Tuli, H.S., Varol, A., Thakral, F., Yerer, M.B., Sak, K., Varol, M., Jain, A., Khan, Md.A. and Sethi, G. (2019). Role of Reactive Oxygen Species in Cancer Progression: Molecular Mechanisms and Recent Advancements. *Biomolecules*, 9(11), p.735.
- Agrawal, N., Frederick, M.J., Pickering, C.R., Bettegowda, C., Chang, K., Li, R.J., Fakhry, C., Xie, T.-X., Zhang, J., Wang, J., Zhang, N., El-Naggar, A.K., Jasser, S.A., Weinstein, J.N., Treviño, L., Drummond, J.A., Muzny, D.M., Wu, Y., Wood, L.D. and Hruban, R.H. (2011). Exome Sequencing of Head and Neck Squamous Cell Carcinoma Reveals Inactivating Mutations in NOTCH1. *Science*, 333(6046), pp.1154–1157.
- Al-Bedeary, S., Getta, H. and Al-Sharafi, D. (2020). The hallmarks of cancer and their therapeutic targeting in current use and clinical trials. *Iraqi Journal of Hematology*, 9(1), p.1.
- Anderson, G., Ebadi, M., Vo, K., Novak, J., Govindarajan, A. and Amini, A. (2021). An Updated Review on Head and Neck Cancer Treatment with Radiation Therapy. *Cancers*, 13(19), p.4912.
- Anouk W. M. A. Schaeffers, Devriese, L.A., Carla, Dankbaar, J.W., Jens Voortman, Paul, J., Slingerland, M., Hendriks, M.P., Smid, E.J., Geert W. J. Frederix and Bree, R. de (2023). Low dose cisplatin weekly versus high dose cisplatin every three weeks in primary chemoradiotherapy in head and neck cancer patients with low skeletal muscle mass: The CISLOW-study protocol. *PLoS ONE*, 18(11), pp.e0294147–e0294147.
- Arutyunyan, I., Enar Jumaniyazova, Makarov, A. and Timur Fatkhudinov (2023). In Vitro Models of Head and Neck Cancer: From Primitive to Most Advanced. *Journal of Personalized Medicine*, 13(11), pp.1575–1575.
- Audebert, M., Salles, B. and Calsou, P. (2004). Involvement of Poly(ADP-ribose) Polymerase-1 and XRCC1/DNA Ligase III in an Alternative Route for DNA Double-strand Breaks Rejoining. *Journal of Biological Chemistry*, 279(53), pp.55117–55126.

- Ayala, A., Muñoz, M.F. and Argüelles, S. (2014). Lipid Peroxidation: Production, Metabolism, and Signaling Mechanisms of Malondialdehyde and 4-Hydroxy-2-Nonenal. *Oxidative Medicine and Cellular Longevity*, 2014(360438), pp.1–31.
- Aykul, S. and Martinez-Hackert, E. (2016). Determination of half-maximal inhibitory concentration using biosensor-based protein interaction analysis. *Analytical Biochemistry*, 508(1), pp.97–103.
- Azarm, K. and Smith, S. (2020). Nuclear PARPs and genome integrity. *Genes & Development*, 34(5-6), pp.285–301.
- Bajrami, I., Kigozi, A., Van Weverwijk, A., Brough, R., Frankum, J., Lord, C.J. and Ashworth, A. (2012). Synthetic lethality of PARP and NAMPT inhibition in triple-negative breast cancer cells. *EMBO molecular medicine*, 4(10), pp.1087–1096.
- Barsouk, A., John Sukumar Aluru, Prashanth Rawla, Kalyan Saginala and Barsouk, A. (2023). Epidemiology, Risk Factors, and Prevention of Head and Neck Squamous Cell Carcinoma. *Medical Sciences*, 11(2), pp.42–42.
- Beli, P., Lukashchuk, N., Wagner, Sebastian A., Weinert, Brian T., Olsen, Jesper V., Baskcomb, L., Mann, M., Jackson, Stephen P. and Choudhary, C. (2012). Proteomic Investigations Reveal a Role for RNA Processing Factor THRAP3 in the DNA Damage Response. *Molecular Cell*, 46(2), pp.212–225.
- Berger, N.D., Stanley, F.K.T., Moore, S. and Goodarzi, A.A. (2017). ATM-dependent pathways of chromatin remodelling and oxidative DNA damage responses. *Philosophical Transactions of the Royal Society B: Biological Sciences*, [online] 372(1731). doi:<https://doi.org/10.1098/rstb.2016.0283>.
- Bernadett Szikriszt, Ádám Póti, Eszter Németh, Kanu, N., Swanton, C. and Dávid Szüts (2020). Cisplatin is more mutagenic than carboplatin or oxaliplatin at equitoxic concentrations. *bioRxiv (Cold Spring Harbor Laboratory)*.
- Bernardes, V.F., Gleber-Netto, F.O., Sousa, S.F., Silva, T.A. and Aguiar, M.C.F. (2010). Clinical significance of EGFR, Her-2 and EGF in oral squamous cell carcinoma: a case control study. *Journal of experimental & clinical cancer research: CR*, [online] 29(1), p.40.
- Bernstein, J.M., Bernstein, C.R., Catharine and Homer, J.J. (2012). Molecular and cellular processes underlying the hallmarks of head and neck cancer. *European Archives of Oto-Rhino-Laryngology*, 270(10), pp.2585–2593.
- Bhowmick, N.A., Neilson, E.G. and Moses, H.L. (2004). Stromal fibroblasts in cancer initiation and progression. *Nature*, 432(7015), pp.332–337.
- Biddlestone-Thorpe, L., Sajjad, M., Rosenberg, E., Beckta, J.M., Valerie, N.C.K., Tokarz, M., Adams, B.R., Wagner, A.F., Khalil, A., Gilfor, D., Golding, S.E., Deb, S., Temesi, D.G., Lau, A., O'Connor, M.J., Choe, K.S., Parada, L.F., Lim, S.K., Mukhopadhyay, N.D. and Valerie, K. (2013). ATM Kinase Inhibition Preferentially Sensitizes p53-Mutant Glioma to Ionizing Radiation. *Clinical Cancer Research*, 19(12), pp.3189–3200.
- Boccia, S., Hashibe, M., Gallì, P., De Feo, E., Asakage, T., Hashimoto, T., Hiraki, A., Katoh, T., Nomura, T., Yokoyama, A., van Duijn, C.M., Ricciardi, G. and Boffetta, P.

- (2009). Aldehyde dehydrogenase 2 and head and neck cancer: a meta-analysis implementing a Mendelian randomization approach. *Cancer Epidemiology, Biomarkers & Prevention: A Publication of the American Association for Cancer Research, Cosponsored by the American Society of Preventive Oncology*, 18(1), pp.248–254.
- Boffetta, P. and Hashibe, M. (2006). Alcohol and cancer. *The Lancet Oncology*, 7(2), pp.149–156.
 - Boudewijn J.M. Braakhuis, Peter J.F. Snijders, Keune, W.-J.H., Chris J.L.M. Meijer, Ruijter-Schippers, H.J., C. René Leemans and Brakenhoff, R.H. (2004). Genetic Patterns in Head and Neck Cancers That Contain or Lack Transcriptionally Active Human Papillomavirus. *Journal of the National Cancer Institute*, 96(13), pp.998–1006.
 - Braný, D., Dvorská, D., Halašová, E. and Škovierová, H. (2020). Cold Atmospheric Plasma: A Powerful Tool for Modern Medicine. *International Journal of Molecular Sciences*, [online] 21(8).
 - Braný, D., Dvorská, D., Strnádel, J., Matáková, T., Halašová, E. and Škovierová, H. (2021). Effect of Cold Atmospheric Plasma on Epigenetic Changes, DNA Damage, and Possibilities for Its Use in Synergistic Cancer Therapy. *International Journal of Molecular Sciences*, 22(22), p.12252.
 - Brown, A., Kumar, S. and Tchounwou, P.B. (2019). Cisplatin-Based Chemotherapy of Human Cancers. *Journal of Cancer Science & Therapy*, 11(4), p.97. Available at: <https://pubmed.ncbi.nlm.nih.gov/32148661/>.
 - Brown, J.S., O’Carrigan, B., Jackson, S.P. and Yap, T.A. (2016). Targeting DNA Repair in Cancer: Beyond PARP Inhibitors. *Cancer Discovery*, 7(1), pp.20–37.
 - Browning, A.P., Sharp, J.A., Murphy, R.J., Gency Gunasingh, Lawson, B., Burrage, K., Haass, N.K. and Simpson, M. (2021). Quantitative analysis of tumour spheroid structure. *eLife*, 10.
 - Bruni, L., Saura-Lázaro, A., Montoliu, A., Brotons, M., Alemany, L., Diallo, M.S., Afsar, O.Z., LaMontagne, D.S., Mosina, L., Contreras, M., Velandia-González, M., Pastore, R., Gacic-Dobo, M. and Bloem, P. (2021). HPV vaccination introduction worldwide and WHO and UNICEF estimates of national HPV immunization coverage 2010–2019. *Preventive Medicine*, 144, p.106399.
 - Brunner, T.F., Probst, F.A., Matthias Troeltzsch, Schwenk-Zieger, S., Zimmermann, J.L., Gregor Morfill, Becker, S., Ulrich Harréus and Welz, C. (2022). Primary cold atmospheric plasma combined with low dose cisplatin as a possible adjuvant combination therapy for HNSCC cells—an in-vitro study. *Head & Face Medicine*, [online] 18(1).
 - Bryant, H.E., Schultz, N., Thomas, H.D., Parker, K.M., Flower, D., Lopez, E., Kyle, S., Meuth, M., Curtin, N.J. and Helleday, T. (2005). Specific killing of BRCA2-deficient tumours with inhibitors of poly(ADP-ribose) polymerase. *Nature*, 434(7035), pp.913–7.

- Cai, B.-H., Hsu, Y.-C., Yeh, F.-Y., Lin, Y.-R., Lu, R.-Y., Yu, S.-J., Shaw, J.-F., Wu, M.-H., Tsai, Y.-Z., Lin, Y.-C., Bai, Z.-Y., Shih, Y.-C., Hsu, Y.-C., Liao, R.-Y., Kuo, W.-H., Hsu, C.-T., Lien, C.-F. and Chen, C.-C. (2022). P63 and P73 Activation in Cancers with p53 Mutation. *Biomedicines*, 10(7), p.1490.
- Caldecott, K.W. (2022). DNA single-strand break repair and human genetic disease. *Trends in Cell Biology*.
- Canady, J., Murthy, K., Zhuang, T., Gitelis, S., Nissan, A., Ly, L., Jones, O., Cheng, X., Adileh, M., Blank, A.T., Colman, M.W., Millikan, K.W., O'Donoghue, C., Stenson, K., Ohara, K., Gal Schtrechman, Keidar, M. and Giacomo Basadonna (2023). The First Cold Atmospheric Plasma Phase I Clinical Trial for the Treatment of Advanced Solid Tumors: A Novel Treatment Arm for Cancer. *Cancers*, 15(14), pp.3688–3688.
- Cancer Research UK (2018). *Head and neck cancers statistics*. Cancer Research UK. Available at: <https://www.cancerresearchuk.org/health-professional/cancer-statistics/statistics-by-cancer-type/head-and-neck-cancers>.
- Caponigro, F., Formato, R., Caraglia, M., Normanno, N. and Iaffaioli, R.V. (2005). Monoclonal antibodies targeting epidermal growth factor receptor and vascular endothelial growth factor with a focus on head and neck tumors. *Current Opinion in Oncology*, 17(3), pp.212–217.
- Carneiro, B.A. and El-Deiry, W.S. (2020). Targeting apoptosis in cancer therapy. *Nature Reviews Clinical Oncology*, 17(7), pp.395–417.
- Castañeda, A.M., Meléndez, C.M., Uribe, D. and Pedroza-Díaz, J. (2022). Synergistic effects of natural compounds and conventional chemotherapeutic agents: recent insights for the development of cancer treatment strategies. *Heliyon*, [online] 8(6), p.e09519. doi:<https://doi.org/10.1016/j.heliyon.2022.e09519>.
- Castorina, P., Martorana, E. and Forte, S. (2022). Dynamical Synergy of Drug Combinations during Cancer Chemotherapy. *Journal of personalized medicine*, [online] 12(11), p.1873. doi:<https://doi.org/10.3390/jpm12111873>.
- Castle, P.E. and Maza, M. (2015). Prophylactic HPV vaccination: past, present, and future. *Epidemiology and Infection*, 144(3), pp.449–468.
- Cepeda, V., Fuertes, M., Castilla, J., Alonso, C., Quevedo, C. and Perez, J. (2007). Biochemical Mechanisms of Cisplatin Cytotoxicity. *Anti-Cancer Agents in Medicinal Chemistry*, 7(1), pp.3–18.
- Chandra, S. (2002). Studies of cell division (mitosis and cytokinesis) by dynamic secondary ion mass spectrometry ion microscopy: LLC-PK1 epithelial cells as a model for subcellular isotopic imaging. *Journal of Microscopy*, 204(2), pp.150–165.
- Chaturvedi, A.K., Graubard, B.I., Broutian, T., Pickard, R.K.L., Tong, Z.-Y., Xiao, W., Kahle, L. and Gillison, M.L. (2018). Effect of Prophylactic Human Papillomavirus (HPV) Vaccination on Oral HPV Infections Among Young Adults in the United States. *Journal of Clinical Oncology*, 36(3), pp.262–267.

- Chaudhary, K., Imam, A.M. and Ali, S.Z.H.R. and J. (2017). *Plasma Kinetic Theory*. www.intechopen.com. IntechOpen. Available at: <https://www.intechopen.com/chapters/57376>.
- Cheng, N., Chytil, A., Shyr, Y., Joly, A. and Moses, H.L. (2008). Transforming Growth Factor- β Signaling-Deficient Fibroblasts Enhance Hepatocyte Growth Factor Signaling in Mammary Carcinoma Cells to Promote Scattering and Invasion. *Molecular Cancer Research*, 6(10), pp.1521–1533.
- Cheong, S.C., Vatanasapt, P., Yi-Hsin, Y., Zain, R.B., Kerr, A.R. and Johnson, N.W. (2017). Oral cancer in South East Asia. *Translational Research in Oral Oncology*, 2, p.2057178X1770292.
- Chinen, T., Yusuke Sasabuchi, Matsui, H., Yamaguchi, H. and Yasunaga, H. (2022). Oxaliplatin- versus cisplatin-based regimens for elderly individuals with advanced gastric cancer: a retrospective cohort study. *BMC cancer*, 22(1).
- Chiu, L.-Y., Sun, Q., Zenke, F.T., Blaukat, A. and Vassilev, L.T. (2023). Selective ATM inhibition augments radiation-induced inflammatory signaling and cancer cell death. *Aging*, 15(2), pp.492–512.
- Choi, S. and Myers, J.N. (2008). Molecular pathogenesis of oral squamous cell carcinoma: implications for therapy. *Journal of dental research*, 87(1), pp.14–32.
- Colevas, A.D. (2006). Chemotherapy Options for Patients With Metastatic or Recurrent Squamous Cell Carcinoma of the Head and Neck. *Journal of Clinical Oncology*, 24(17), pp.2644–2652.
- Crowley, L.C., Scott, A.P., Marfell, B.J., Boughaba, J.A., Chojnowski, G. and Waterhouse, N.J. (2016). Measuring Cell Death by Propidium Iodide Uptake and Flow Cytometry. *Cold Spring Harbor protocols*, 2016(7), p.10.1101/pdb.prot087163.
- Csaba Hegedűs and László Virág (2014). Inputs and outputs of poly(ADP-ribose)ation: Relevance to oxidative stress. *Redox Biology*, 2, pp.978–982.
- Cuneo, K.C., Morgan, M.A., Davis, M.C., Parcels, L.A., Parcels, J., Karnak, D., Ryan, C., Liu, N., Maybaum, J. and Lawrence, T.S. (2016). Wee1 Kinase Inhibitor AZD1775 Radiosensitizes Hepatocellular Carcinoma Regardless of TP53 Mutational Status Through Induction of Replication Stress. *International Journal of Radiation Oncology Biology Physics*, 95(2), pp.782–790.
- Curtin, N.J. and Szabo, C. (2020). Poly(ADP-ribose) polymerase inhibition: past, present and future. *Nature Reviews Drug Discovery*, 19(10), pp.711–736.
- D'Souza, G., Gross, N.D., Pai, S.I., Haddad, R., Anderson, K.S., Rajan, S., Gerber, J., Gillison, M.L. and Posner, M.R. (2014). Oral Human Papillomavirus (HPV) Infection in HPV-Positive Patients With Oropharyngeal Cancer and Their Partners. *Journal of Clinical Oncology*, 32(23), pp.2408–2415.
- D'Souza, G., Kreimer, A.R., Viscidi, R., Pawlita, M., Fakhry, C., Koch, W.M., Westra, W.H. and Gillison, M.L. (2007). Case–Control Study of Human Papillomavirus and Oropharyngeal Cancer. *New England Journal of Medicine*, 356(19), pp.1944–1956.

- Dasari, S. and Bernard Tchounwou, P. (2014). Cisplatin in Cancer therapy: Molecular Mechanisms of Action. *European Journal of Pharmacology*, 740(1), pp.364–378.
- De Bont, R. and van Larebeke, N. (2004). Endogenous DNA damage in humans: a review of quantitative data. *Mutagenesis*, 19(3), pp.169–185.
- De Oliveira, L.R., Ribeiro-Silva, A. and Zucoloto, S. (2007). Prognostic impact of p53 and p63 immunoeexpression in oral squamous cell carcinoma. *Journal of Oral Pathology & Medicine*, 36(4), pp.191–197.
- Deeks, E.D. (2015). Olaparib: First Global Approval. *Drugs*, 75(2), pp.231–240.
- Demuynck, R., Efimova, I., Lin, A., Declercq, H. and Krysko, D.V. (2020). A 3D Cell Death Assay to Quantitatively Determine Ferroptosis in Spheroids. *Cells*, 9(3), p.703.
- Devanabanda, B. and Kasi, A. (2021). *Oxaliplatin*. PubMed. Available at: <https://www.ncbi.nlm.nih.gov/books/NBK557690/>.
- Diab, A., Kao, M., Kehrl, K., Kim, H.Y., Sidorova, J. and Mendez, E. (2019). Multiple Defects Sensitize p53-Deficient Head and Neck Cancer Cells to the WEE1 Kinase Inhibition. *Molecular Cancer Research*, 17(5), pp.1115–1128.
- Dianov, G.L. and Hübscher, U. (2013). Mammalian Base Excision Repair: the Forgotten Archangel. *Nucleic Acids Research*, 41(6), pp.3483–3490.
- Dong, C., Wang, Y., Tu, Z., Yan, J., Jiang, Y., Lu, T., Chen, Y. and Liu, H. (2022). Recent advances in ATM inhibitors as potential therapeutic agents. *Future Medicinal Chemistry*.
- Drew, Y., Zenke, F.T. and Curtin, N.J. (2024). DNA damage response inhibitors in cancer therapy: lessons from the past, current status and future implications. *Nature Reviews Drug Discovery*.
- Drolet, M., Bénard, É., Pérez, N., Brisson, M., Ali, H., Boily, M.-C., Baldo, V., Brassard, P., Brotherton, J.M.L., Callander, D., Checchi, M., Chow, E.P.F., Cocchio, S., Dalianis, T., Deeks, S.L., Dehlendorff, C., Donovan, B., Fairley, C.K., Flagg, E.W. and Gargano, J.W. (2019). Population-level impact and herd effects following the introduction of human papillomavirus vaccination programmes: updated systematic review and meta-analysis. *The Lancet*, 394(10197).
- Duarte, D. and Vale, N. (2022). Evaluation of synergism in drug combinations and reference models for future orientations in oncology. *Current Research in Pharmacology and Drug Discovery*, 3, p.100110.
- Durant, S.T., Zheng, L., Wang, Y., Chen, K., Zhang, L., Zhang, T., Yang, Z., Riches, L., Trinidad, A.G., Fok, J.H.L., Hunt, T., Pike, K.G., Wilson, J., Smith, A., Colclough, N., Reddy, V.P., Sykes, A., Janefeldt, A., Johnström, P. and Varnäs, K. (2018). The brain-penetrant clinical ATM inhibitor AZD1390 radiosensitizes and improves survival of preclinical brain tumor models. *Science Advances*, 4(6).
- Ermolaeva, M.A. and Schumacher, B. (2014). Systemic DNA damage responses: organismal adaptations to genome instability. *Trends in Genetics*, 30(3), pp.95–102.

- Esposito, F., Giuffrida, R., Raciti, G., Puglisi, C. and Forte, S. (2021). Wee1 Kinase: A Potential Target to Overcome Tumor Resistance to Therapy. *International Journal of Molecular Sciences*, 22(19), p.10689.
- Fakhry, C. and D'Souza, G. (2013). Discussing the diagnosis of HPV-OSCC: Common questions and answers. *Oral Oncology*, 49(9), pp.863–871.
- Fang, C. and Kang, Y. (2021). E-Cadherin: Context-Dependent Functions of a Quintessential Epithelial Marker in Metastasis. *Cancer Research*, 81(23), pp.5800–5802.
- Faraji, F., Zaidi, M., Fakhry, C. and Gaykalova, D.A. (2017). Molecular mechanisms of human papillomavirus-related carcinogenesis in head and neck cancer. *Microbes and Infection*, 19(9-10), pp.464–475.
- Farmer, H., McCabe, N., Lord, C.J., Tutt, A.N.J., Johnson, D.A., Richardson, T.B., Santarosa, M., Dillon, K.J., Hickson, I., Knights, C., Martin, N.M.B., Jackson, S.P., Smith, G.C.M. and Ashworth, A. (2005). Targeting the DNA repair defect in BRCA mutant cells as a therapeutic strategy. *Nature*, 434(7035), pp.917–921.
- Fayette, J., Fontaine-Delaruelle, C., Ambrun, A., Clémentine Daveau, Poupart, M., Ramade, A., Philippe Zrounba, Neidhardt, E.-M., Julien Péron, Diallo, A. and Philippe Céruse (2016). Neoadjuvant modified TPF (docetaxel, cisplatin, fluorouracil) for patients unfit to standard TPF in locally advanced head and neck squamous cell carcinoma: a study of 48 patients. *Oncotarget*, 7(24), pp.37297–37304.
- Feng, X., Li, Z., Liu, Y., Chen, D. and Zhou, Z. (2024). CRISPR/Cas9 technology for advancements in cancer immunotherapy: from uncovering regulatory mechanisms to therapeutic applications. *Experimental Hematology and Oncology*, 13(1).
- Ferlay, J., Colombet, M., Soerjomataram, I., Mathers, C., Parkin, D.M., Piñeros, M., Znaor, A. and Bray, F. (2018). Estimating the global cancer incidence and mortality in 2018: GLOBOCAN sources and methods. *International Journal of Cancer*, 144(8).
- Fernald, K. and Kurokawa, M. (2013). Evading apoptosis in cancer. *Trends in Cell Biology*, 23(12), pp.620–633.
- Ferraguti, G., Terracina, S., Petrella, C., Greco, A., Minni, A., Lucarelli, M., Agostinelli, E., Ralli, M., de Vincentiis, M., Raponi, G., Polimeni, A., Ceccanti, M., Caronti, B., Di Certo, M.G., Barbato, C., Mattia, A., Tarani, L. and Fiore, M. (2022). Alcohol and Head and Neck Cancer: Updates on the Role of Oxidative Stress, Genetic, Epigenetics, Oral Microbiota, Antioxidants, and Alkylating Agents. *Antioxidants*, 11(1), p.145.
- Fiebrandt, M., Lackmann, J.-W. and Stapelmann, K. (2018). From patent to product? 50 years of low-pressure plasma sterilization. *Plasma Processes and Polymers*, 15(12), p.1800139.
- Fitzmaurice, C., Allen, C., Barber, R.M., Barregard, L., Bhutta, Z.A., Brenner, H., Dicker, D.J., Chimed-Orchir, O., Dandona, R., Dandona, L., Fleming, T.,

- Forouzanfar, M.H., Hancock, J., Hay, R.J., Hunter-Merrill, R., Huynh, C., Hosgood, H.D., Johnson, C.O., Jonas, J.B. and Khubchandani, J. (2017). Global, Regional, and National Cancer Incidence, Mortality, Years of Life Lost, Years Lived With Disability, and Disability-Adjusted Life-years for 32 Cancer Groups, 1990 to 2015: A Systematic Analysis for the Global Burden of Disease Study. *JAMA Oncology*, 3(4), pp.524–548.
- Fortin, A., Wang, C.S. and Vigneault, E. (2009). Influence of smoking and alcohol drinking behaviors on treatment outcomes of patients with squamous cell carcinomas of the head and neck. *International Journal of Radiation Oncology, Biology, Physics*, 74(4), pp.1062–1069.
 - Frezza, M., Hindo, S., Chen, D., Davenport, A., Schmitt, S., Tomco, D. and Ping Dou, Q. (2010). Novel Metals and Metal Complexes as Platforms for Cancer Therapy. *Current Pharmaceutical Design*, 16(16), pp.1813–1825.
 - Gaschler, M.M. and Stockwell, B.R. (2017). Lipid peroxidation in cell death. *Biochemical and Biophysical Research Communications*, 482(3), pp.419–425.
 - Gaur, N., Kurita, H., Oh, J.-S., Miyachika, S., Ito, M., Mizuno, A., Cowin, A.J., Allinson, S., Short, R.D. and Szili, E.J. (2020). On cold atmospheric-pressure plasma jet induced DNA damage in cells. *Journal of Physics D: Applied Physics*, 54(3), p.035203.
 - Gaur, N., Patenall, B.L., Bhagirath Ghimire, Naing Tun Thet, Gardiner, J.E., Le, K.E., Ramage, G., Short, B., Heylen, R.A., Williams, C., Short, R.D. and Jenkins, T.A. (2023). Cold Atmospheric Plasma-Activated Composite Hydrogel for an Enhanced and On-Demand Delivery of Antimicrobials. *ACS Applied Materials & Interfaces*, 15(16), pp.19989–19996.
 - Geenen, J.J.J. and Schellens, J.H.M. (2017). Molecular Pathways: Targeting the Protein Kinase Wee1 in Cancer. *Clinical Cancer Research*, 23(16), pp.4540–4544.
 - Gelmon, K.A., Tischkowitz, M., Mackay, H., Swenerton, K., Robidoux, A., Tonkin, K., Hirte, H., Huntsman, D., Clemons, M., Gilks, B., Yerushalmi, R., Macpherson, E., Carmichael, J. and Oza, A. (2011). Olaparib in patients with recurrent high-grade serous or poorly differentiated ovarian carcinoma or triple-negative breast cancer: a phase 2, multicentre, open-label, non-randomised study. *The Lancet Oncology*, 12(9), pp.852–861.
 - Gjika, E., Pal-Ghosh, S., Kirschner, M.E., Lin, L., Sherman, J.H., Stepp, M.A. and Keidar, M. (2020). Combination therapy of cold atmospheric plasma (CAP) with temozolomide in the treatment of U87MG glioblastoma cells. *Scientific Reports*, 10(1).
 - Goel, B., Tiwari, A.K., Pandey, R.K., Singh, A.P., Kumar, S., Sinha, A., Jain, S.K. and Khattri, A. (2022). Therapeutic approaches for the treatment of head and neck squamous cell carcinoma—An update on clinical trials. *Translational Oncology*, 21, p.101426.

- Golan, T., Hammel, P., Reni, M., Van Cutsem, E., Macarulla, T., Hall, M.J., Park, J.-O., Hochhauser, D., Arnold, D., Oh, D.-Y., Reinacher-Schick, A., Tortora, G., Algül, H., O'Reilly, E.M., McGuinness, D., Cui, K.Y., Schlienger, K., Locker, G.Y. and Kindler, H.L. (2019). Maintenance Olaparib for Germline BRCA-Mutated Metastatic Pancreatic Cancer. *New England Journal of Medicine*, 381(4), pp.317–327.
- Gonzalez, V.M., Fuertes, M.A., Alonso, C. and Perez, J.M. (2001). Is Cisplatin-Induced Cell Death Always Produced by Apoptosis? *Molecular Pharmacology*, 59(4), pp.657–663.
- Goodman, M.F. and Woodgate, R. (2013). Translesion DNA Polymerases. *Cold Spring Harbor Perspectives in Biology*, 5(10), pp.a010363–a010363.
- Gormley, M., Creaney, G., Schache, A., Ingarfield, K. and Conway, D.I. (2022). Reviewing the epidemiology of head and neck cancer: definitions, trends and risk factors. *British Dental Journal*, [online] 233(9), pp.780–786.
- Goto, N., Bazar, G., Kovacs, Z., Kunisada, M., Morita, H., Kizaki, S., Sugiyama, H., Tsenkova, R. and Nishigori, C. (2015). Detection of UV-induced cyclobutane pyrimidine dimers by near-infrared spectroscopy and aquaphotomics. *Scientific Reports*, 5(1).
- Grandis, J.R., Drenning, S.D., Qing Liang Zeng, Watkins, S.C., Melhem, M.F., Endo, S., Johnson, D., Huang, L., He, Y. and Jae Nyoung Kim (2000). Constitutive activation of Stat3 signaling abrogates apoptosis in squamous cell carcinogenesis *in vivo*. 97(8), pp.4227–4232.
- Guler, S., DiPoto, M.C., Crespo, A., Caldwell, R., Doerfel, B., Grossmann, N., Ho, K., Huck, B., Jones, C.C., Lan, R., Musil, D., Potnick, J., Schilke, H., Sherer, B., Simon, S., Sirrenberg, C., Zhang, Z. and Liu-Bujalski, L. (2023). Selective Wee1 Inhibitors Led to Antitumor Activity *In Vitro* and Correlated with Myelosuppression. *ACS Medicinal Chemistry Letters*, 14(5), pp.566–576.
- Gupta, A.K., Tulsyan, S., Thakur, N., Sharma, V., Sinha, D.N. and Mehrotra, R. (2020). Chemistry, metabolism and pharmacology of carcinogenic alkaloids present in areca nut and factors affecting their concentration. *Regulatory Toxicology and Pharmacology*, 110, p.104548.
- Gupta, T., Kannan, S., Ghosh-Laskar, S. and Agarwal, J.P. (2022). Concurrent chemoradiotherapy with cisplatin given once-a-week versus every-three weekly in head and neck squamous cell carcinoma: Non-inferior, equivalent, or superior? *Oral Oncology*, 134, p.106130.
- Hakem, R. (2008). DNA-damage repair; the good, the bad, and the ugly. *The EMBO Journal*, [online] 27(4), pp.589–605.
- Hanahan, D. (2022). Hallmarks of Cancer: New Dimensions. *Cancer Discovery*, [online] 12(1), pp.31–46. doi:<https://doi.org/10.1158/2159-8290.cd-21-1059>.
- Hanahan, D. and Weinberg, Robert A. (2011). Hallmarks of cancer: the next Generation. *Cell*, 144(5), pp.646–674.

- Hananya, N., Daley, S.K., Bagert, J.D. and Muir, T.W. (2021). Synthesis of ADP-Ribosylated Histones Reveals Site-Specific Impacts on Chromatin Structure and Function. *Journal of the American Chemical Society*, 143(29), pp.10847–10852.
- HAPANI, N., D’Cruz, S., Dimri, K. and Kaur, D. (2022). POS-016 Incidence Of Acute Kidney Injury In Patients Receiving Cisplatin And Carboplatin And To Evaluate Associated Risk Factors For Acute Kidney Injury. *Kidney International Reports*, 7(2), pp.S6–S7.
- Hatcher, J.L., Sterba, K.R., Tooze, J.A., Day, T.A., Carpenter, M.J., Alberg, A.J., Sullivan, C.A., Fitzgerald, N.C. and Weaver, K.E. (2015). Tobacco use and surgical outcomes in patients with head and neck cancer. *Head & Neck*, 38(5), pp.700–706.
- Helleday, T. (2011). The underlying mechanism for the PARP and BRCA synthetic lethality: Clearing up the misunderstandings. *Molecular Oncology*, 5(4), pp.387–393.
- Hezel, A.F. and Bardeesy, N. (2008). LKB1; linking cell structure and tumor suppression. *Oncogene*, 27(55), pp.6908–6919.
- Humans, I.W.G. on the E. of C.R. to (2007). *Molecular Mechanisms of HPV-induced Carcinogenesis*. www.ncbi.nlm.nih.gov. International Agency for Research on Cancer. Available at: <https://www.ncbi.nlm.nih.gov/books/NBK321762/>.
- IARC Working Group on the Evaluation of Carcinogenic Risks to Humans (2010). Alcohol consumption and ethyl carbamate. *IARC monographs on the evaluation of carcinogenic risks to humans*, 96, pp.3–1383. Available at: <https://www.ncbi.nlm.nih.gov/pmc/articles/PMC4781168/>.
- Im, K., Mareninov, S., Diaz, M.F.P. and Yong, W.H. (2019). An introduction to Performing Immunofluorescence Staining. *Methods in molecular biology (Clifton, N.J.)*, 1897(2), pp.299–311.
- Ishida, S., Lee, J., Thiele, D.J. and Herskowitz, I. (2002). Uptake of the anticancer drug cisplatin mediated by the copper transporter Ctr1 in yeast and mammals. *Proceedings of the National Academy of Sciences*, 99(22), pp.14298–14302.
- Jeong, H.-G., Cho, H.-J., Chang, I.-Y., Yoon, S.-P., Jeon, Y.-J., Chung, M.-H. and You, H.J. (2002). Rac1 prevents cisplatin-induced apoptosis through down-regulation of p38 activation in NIH3T3 cells. *FEBS letters*, 518(1-3), pp.129–34.
- Jethwa, A.R. and Khariwala, S.S. (2017). Tobacco-related carcinogenesis in head and neck cancer. *Cancer and Metastasis Reviews*, 36(3), pp.411–423.
- Jiang, H., Reinhardt, H.C., Bartkova, J., Tommiska, J., Blomqvist, C., Nevanlinna, H., Bartek, J., Yaffe, M.B. and Hemann, M.T. (2009a). The combined status of ATM and p53 link tumor development with therapeutic response. *Genes & Development*, [online] 23(16), pp.1895–1909.
- Jiang, Y., Rabbi, M., Kim, M., Ke, C., Lee, W., Clark, R.L., Mieczkowski, P.A. and Marszalek, P.E. (2009b). UVA Generates Pyrimidine Dimers in DNA Directly. *Biophysical Journal*, [online] 96(3), pp.1151–1158.

- Jin, M., Ande, A., Kumar, A. and Kumar, S. (2013). Regulation of cytochrome P450 2e1 expression by ethanol: role of oxidative stress-mediated pkc/jnk/sp1 pathway. *Cell Death & Disease*, 4(3), pp.e554–e554.
- Johnson, D.E., Burtness, B., Leemans, C.R., Lui, V.W.Y., Bauman, J.E. and Grandis, J.R. (2020). Head and neck squamous cell carcinoma. *Nature reviews. Disease primers*, 6(1), p.92.
- Kao, M., Green, C., Sidorova, J. and Méndez, E. (2017). Strategies for Targeted Therapy in Head and Neck Squamous Cell Carcinoma Using WEE1 Inhibitor AZD1775. *JAMA Otolaryngology–Head & Neck Surgery*, 143(6), p.631.
- Kaprio, J. (2022). Twin studies of smoking and tobacco use. *Twin Research for Everyone*, pp.371–384.
- Kato, S., Schwaederle, M., Daniels, G.A., Piccioni, D., Kesari, S., Bazhenova, L., Shimabukuro, K., Parker, B.A., Fanta, P. and Kurzrock, R. (2015). Cyclin-dependent kinase pathway aberrations in diverse malignancies: clinical and molecular characteristics. *Cell cycle (Georgetown, Tex.)*, [online] 14(8), pp.1252–9.
- Kelland, L. (2007). The resurgence of platinum-based cancer chemotherapy. *Nature Reviews Cancer*, 7(8), pp.573–584.
- Keshavarzi, M., Darijani, M., Momeni, F., Moradi, P., Ebrahimnejad, H., Masoudifar, A. and Mirzaei, H. (2017). Molecular Imaging and Oral Cancer Diagnosis and Therapy. *Journal of Cellular Biochemistry*, 118(10), pp.3055–3060.
- Kessel, S., Cribbes, S., Déry, O., Kuksin, D., Sincoff, E., Qiu, J. and Chan, L.L.-Y. (2016). High-Throughput 3D Tumor Spheroid Screening Method for Cancer Drug Discovery Using Celigo Image Cytometry. *SLAS TECHNOLOGY: Translating Life Sciences Innovation*, 22(4), pp.454–465.
- Khalid, A., Hussain, T., Manzoor, S., Saalim, M. and Khaliq, S. (2017). PTEN: A potential prognostic marker in virus-induced hepatocellular carcinoma. *Tumor Biology*, 39(6), p.101042831770575.
- Khariwala, S.S., Hatsukami, D. and Hecht, S.S. (2011). Tobacco carcinogen metabolites and DNA adducts as biomarkers in Head and Neck cancer: Potential screening tools and prognostic indicators. *Head & Neck*, 34(3), pp.441–447.
- Kim, J.W., Park, Y., Roh, J.-L., Cho, K.-J., Choi, S.-H., Nam, S.Y. and Kim, S.Y. (2016). Prognostic value of glucosylceramide synthase and P-glycoprotein expression in oral cavity cancer. *International Journal of Clinical Oncology*, 21(5), pp.883–889.
- Kines, R.C., Thompson, C.D., Lowy, D.R., Schiller, J.T. and Day, P.M. (2009). The initial steps leading to papillomavirus infection occur on the basement membrane prior to cell surface binding. *Proceedings of the National Academy of Sciences*, 106(48), pp.20458–20463.
- Koboldt, D.C., Fulton, R.S., McLellan, M.D., Schmidt, H., Kalicki-Veizer, J., McMichael, J.F., Fulton, L.L., Dooling, D.J., Ding, L., Mardis, E.R., Wilson, R.K., Ally, A., Balasundaram, M., Butterfield, Y.S.N., Carlsen, R., Carter, C., Chu, A., Chuah, E.,

- Chun, H.-J.E. and Coope, R.J.N. (2012). Comprehensive molecular portraits of human breast tumours. *Nature*, [online] 490(7418), pp.61–70.
- Kolev, V., Mandinova, A., Guinea-Viniegra, J., Hu, B., Lefort, K., Lambertini, C., Neel, V., Dummer, R., Wagner, E.F. and Dotto, G.P. (2008). EGFR signalling as a negative regulator of Notch1 gene transcription and function in proliferating keratinocytes and cancer. *Nature Cell Biology*, 10(8), pp.902–911.
 - Kong, M.G., Kroesen, G., Morfill, G., Nosenko, T., Shimizu, T., van Dijk, J. and Zimmermann, J.L. (2009). Plasma medicine: an introductory review. *New Journal of Physics*, 11(11), p.115012.
 - Konstantinos Karakostis, Malbert-Colas, L., Aikaterini Thermou, Borek Vojtesek and Fähræus, R. (2024). The DNA damage sensor ATM kinase interacts with the p53 mRNA and guides the DNA damage response pathway. *Molecular Cancer*, 23(1).
 - Kops, G.J.P.L., Weaver, B.A.A. and Cleveland, D.W. (2005). On the road to cancer: aneuploidy and the mitotic checkpoint. *Nature Reviews Cancer*, 5(10), pp.773–785.
 - Kozakiewicz, P. and Grzybowska-Szatowska, L. (2018). Application of molecular targeted therapies in the treatment of head and neck squamous cell carcinoma. *Oncology Letters*, [online] 15(5), pp.7497–7505.
 - Ku, B.M., Bae, Y.-H., Koh, J., Sun, J.-M., Lee, S.-H., Ahn, J.S., Park, K. and Ahn, M.-J. (2017). Mutational status of TP53 defines the efficacy of Wee1 inhibitor AZD1775 in KRAS-mutant non-small cell lung cancer. *Oncotarget*, 8(40), pp.67526–67537.
 - Kumar, S. and Tchounwou, P.B. (2015). Molecular mechanisms of cisplatin cytotoxicity in acute promyelocytic leukemia cells. *Oncotarget*, 6(38).
 - Kuo, L.J. and Yang, L.-X. (2008). Gamma-H2AX - a novel biomarker for DNA double-strand breaks. *In Vivo (Athens, Greece)*, [online] 22(3), pp.305–309. Available at: <https://pubmed.ncbi.nlm.nih.gov/18610740/>.
 - Kurasawa, Y., Shiiba, M., Nakamura, M., Fushimi, K., Ishigami, T., Bukawa, H., Yokoe, H., Uzawa, K. and Tanzawa, H. (2008). PTEN expression and methylation status in oral squamous cell carcinoma. *Oncology Reports*, 19(6), pp.1429–1434. Available at: <https://pubmed.ncbi.nlm.nih.gov/18497947/> [Accessed 20 Mar. 2024].
 - Lafontaine, J., Boisvert, J.-S., Glory, A., Coulombe, S. and Wong, P. (2020). Synergy between Non-Thermal Plasma with Radiation Therapy and Olaparib in a Panel of Breast Cancer Cell Lines. *Cancers*, 12(2), p.348.
 - Langie, S.A.S., Koppen, G., Desaulniers, D., Al-Mulla, F., Al-Temaimi, R., Amedei, A., Azqueta, A., Bisson, W.H., Brown, D., Brunborg, G., Charles, A.K., Chen, T., Colacci, A., Darroudi, F., Forte, S., Gonzalez, L., Hamid, R.A., Knudsen, L.E., Leyns, L. and Lopez de Cerain Salsamendi, A. (2015). Causes of genome instability: the effect of low dose chemical exposures in modern society. *Carcinogenesis*, [online] 36(Suppl 1), pp.S61–S88. doi:<https://doi.org/10.1093/carcin/bgv031>.

- Langmuir, I. (1928). Oscillations in Ionized Gases. *Proceedings of the National Academy of Sciences*, 14(8), pp.627–637.
- Laroussi, M. (2020). Cold Plasma in Medicine and Healthcare: The New Frontier in Low Temperature Plasma Applications. *Frontiers in Physics*, 8.
- Laverty, D.J., Gupta, S.K., Bradshaw, G.A., Hunter, A.S., Carlson, B.L., Nery Matias Calmo, Chen, J., Tian, S., Sarkaria, J.N. and Nagel, Z.D. (2024). ATM inhibition exploits checkpoint defects and ATM-dependent double strand break repair in TP53-mutant glioblastoma. *Nature Communications*, 15(1).
- Lei, L., Bai, Y., Qin, X., Liu, J., Huang, W. and Lv, Q. (2022). Current Understanding of Hydrogel for Drug Release and Tissue Engineering. *Gels*, 8(5), p.301.
- Lemmon, M.A. and Schlessinger, J. (2010). Cell Signaling by Receptor Tyrosine Kinases. *Cell*, [online] 141(7), pp.1117–1134.
- Levine, A.J. and Oren, M. (2009). The first 30 years of p53: growing ever more complex. *Nature Reviews Cancer*, 9(10), pp.749–758.
- Li, G.-M. (2007). Mechanisms and Functions of DNA Mismatch Repair. *Cell Research*, 18(1), pp.85–98. doi:<https://doi.org/10.1038/cr.2007.115>.
- Li, Q., Qian, W., Yang, Z., Hu, L., Chen, S. and Xia, Y. (2023a). A new wave of innovations within the DNA damage response. *Signal Transduction and Targeted Therapy*, 8(1).
- Li, S., Wang, L., Wang, Y., Zhang, C., Hong, Z. and Han, Z. (2022). The synthetic lethality of targeting cell cycle checkpoints and PARPs in cancer treatment. *Journal of Hematology & Oncology*, 15(1).
- Li, X., Xu, X., Xu, M., Geng, Z., Ji, P. and Liu, Y. (2023b). Hydrogel systems for targeted cancer therapy. *Frontiers in Bioengineering and Biotechnology*, 11.
- Lim, Y.C., Han, J.H., Kang, H.J., Kim, Y.S., Lee, B.H., Choi, E.C. and Kim, C.-H. (2012). Overexpression of c-Met promotes invasion and metastasis of small oral tongue carcinoma. *Oral Oncology*, 48(11), pp.1114–1119.
- Lionnel Geoffrois, Martin, L., Pascal Garaud, Raucourt, D.D., Miny, J., Philippe Maingon, Lafond, C., Tuchais, C., Sire, C., Babin, E., Alexandre Coutte, Tao, Y., Rolland, F., Girard-Calais, M.H. and Bourhis, J. (2016). Induction docetaxel platinum 5-FU (TPF) followed by cetuximab-radiotherapy (cetux-RT) versus concurrent chemo-radiotherapy (CT/RT) in patients with N2b/c-N3 non operated stage III-IV squamous cell cancer of the head and neck (SCCHN): Results of the GORTEC 2007-02 phase III randomized trial. *Journal of Clinical Oncology*, 34(15_suppl), pp.6000–6000.
- Liu, X., Fan, L., Lu, C., Yin, S. and Hu, H. (2020). Functional Role of p53 in the Regulation of Chemical-Induced Oxidative Stress. *Oxidative Medicine and Cellular Longevity*, 2020, pp.1–10.
- Lomonosov, M. (2003). Stabilization of stalled DNA replication forks by the BRCA2 breast cancer susceptibility protein. *Genes & Development*, 17(24), pp.3017–3022.

- Louie, K.S., Mehanna, H. and Sasieni, P. (2015). Trends in head and neck cancers in England from 1995 to 2011 and projections up to 2025. *Oral Oncology*, 51(4), pp.341–348.
- Lu, S.-L. . (2006). Loss of transforming growth factor-beta type II receptor promotes metastatic head-and-neck squamous cell carcinoma. *Genes & Development*, 20(10), pp.1331–1342.
- Macha, M.A., Matta, A., Kaur, J., Chauhan, S.S., Thakar, A., Shukla, N.K., Gupta, S.D. and Ralhan, R. (2011). Prognostic significance of nuclear pSTAT3 in oral cancer. *Head & Neck*, [online] 33(4), pp.482–489.
- Marechal, A. and Zou, L. (2013). DNA Damage Sensing by the ATM and ATR Kinases. *Cold Spring Harbor Perspectives in Biology*, [online] 5(9), pp.a012716–a012716.
- Marin, V.P., Pytynia, K.B., Langstein, H.N., Dahlstrom, K.R., Wei, Q. and Sturgis, E.M. (2008). Serum Cotinine Concentration and Wound Complications in Head and Neck Reconstruction. *Plastic and Reconstructive Surgery*, 121(2), pp.451–457.
- Marron, M., Boffetta, P., Zhang, Z.-F. ., Zaridze, D., Wunsch-Filho, V., Winn, D.M., Wei, Q., Talamini, R., Szeszenia-Dabrowska, N., Sturgis, E.M., Smith, E., Schwartz, S.M., Rudnai, P., Purdue, M.P., Olshan, A.F., Eluf-Neto, J., Muscat, J., Morgenstern, H., Menezes, A. and McClean, M. (2009). Cessation of alcohol drinking, tobacco smoking and the reversal of head and neck cancer risk. *International Journal of Epidemiology*, 39(1), pp.182–196.
- Marteiijn, J.A., Lans, H., Vermeulen, W. and Hoeijmakers, J.H.J. (2014). Understanding nucleotide excision repair and its roles in cancer and ageing. *Nature Reviews Molecular Cell Biology*, 15(7), pp.465–481.
- Marur, S. and Forastiere, A.A. (2016). Head and Neck Squamous Cell Carcinoma: Update on Epidemiology, Diagnosis, and Treatment. *Mayo Clinic Proceedings*, 91(3), pp.386–396. doi:<https://doi.org/10.1016/j.mayocp.2015.12.017>.
- Mateo, J., Carreira, S., Sandhu, S., Miranda, S., Mossop, H., Perez-Lopez, R., Nava Rodrigues, D., Robinson, D., Omlin, A., Tunariu, N., Boysen, G., Porta, N., Flohr, P., Gillman, A., Figueiredo, I., Paulding, C., Seed, G., Jain, S., Ralph, C. and Protheroe, A. (2015). DNA-Repair Defects and Olaparib in Metastatic Prostate Cancer. *New England Journal of Medicine*, 373(18), pp.1697–1708.
- Matthews, H.K., Bertoli, C. and de Bruin, R.A.M. (2021). Cell cycle control in cancer. *Nature Reviews Molecular Cell Biology*, 23.
- Middleton, F., Pollard, J. and Curtin, N. (2018). The Impact of p53 Dysfunction in ATR Inhibitor Cytotoxicity and Chemo- and Radiosensitisation. *Cancers*, 10(8), p.275.
- Milad Ashrafizadeh, Ahmadi, Z., Tahereh Farkhondeh and Saeed Samarghandian (2019). Autophagy as a molecular target of quercetin underlying its protective effects in human diseases. *Archives of Physiology and Biochemistry*, 128(1), pp.200–208.

- Miller-Pinsler, L. and Wells, P.G. (2014). Deficient DNA repair exacerbates ethanol-initiated DNA oxidation and embryopathies in *ogg1* knockout mice: gender risk and protection by a free radical spin trapping agent. *Archives of Toxicology*, 90(2), pp.415–425.
- Min, H.-Y. and Lee, H.-Y. (2022). Molecular targeted therapy for anticancer treatment. *Experimental & Molecular Medicine*, [online] 54(10), pp.1670–1694. doi:<https://doi.org/10.1038/s12276-022-00864-3>.
- Mishina, Y., Duguid, E.M. and He, C. (2006). Direct Reversal of DNA Alkylation Damage. *Chemical Reviews*, 106(2), pp.215–232.
- Moghtaderi, H., Sadeghian, G., Abiri, H., Khan, F., Rahman, M.M., Al-Harrasi, A. and Rahman, S.M. (2024). Electric cell-substrate impedance sensing in cancer research: An in-depth exploration of impedance sensing for profiling cancer cell behavior. *Sensors and Actuators Reports*, 7, p.100188.
- Montagnani, F., Turrisi, G., Marinozzi, C., Aliberti, C. and Fiorentini, G. (2011). Effectiveness and safety of oxaliplatin compared to cisplatin for advanced, unresectable gastric cancer: a systematic review and meta-analysis. *Gastric Cancer*, 14(1), pp.50–55.
- Monteiro, L., Ricardo, S., Delgado, M., Garcez, F., do Amaral, B. and Lopes, C. (2013). Phosphorylated EGFR at tyrosine 1173 correlates with poor prognosis in oral squamous cell carcinomas. *Oral Diseases*, 20(2), pp.178–185.
- Mordes, D.A. and Cortez, D. (2008). Activation of ATR and related PIKKs. *Cell Cycle*, 7(18), pp.2809–2812. doi:<https://doi.org/10.4161/cc.7.18.6689>.
- Moreira, J., Tobias, A., O'Brien, M.P. and Agulnik, M. (2017). Targeted Therapy in Head and Neck Cancer: An Update on Current Clinical Developments in Epidermal Growth Factor Receptor-Targeted Therapy and Immunotherapies. *Drugs*, 77(8), pp.843–857.
- Murillo, D., Huergo, C., Gallego, B., Rodríguez, R. and Tornín, J. (2023). Exploring the Use of Cold Atmospheric Plasma to Overcome Drug Resistance in Cancer. *Biomedicines*, 11(1), p.208.
- Napp, J., Daeschlein, G., Napp, M., von Podewils, S., Gumbel, D., Spitzmueller, R., Fornaciari, P., Hinz, P. and Jünger, M. (2015). On the history of plasma treatment and comparison of microbiostatic efficacy of a historical high-frequency plasma device with two modern devices. *GMS Hygiene and Infection Control*, 10.
- National Cancer Institute (2021). *Head and Neck Cancers*. [online] National Cancer Institute. Available at: <https://www.cancer.gov/types/head-and-neck/head-neck-fact-sheet>.
- Neskey, D.M., Osman, A.A., Ow, T.J., Katsonis, P., McDonald, T., Hicks, S.C., Hsu, T.-K., Pickering, C.R., Ward, A., Patel, A., Yordy, J.S., Skinner, H.D., Giri, U., Sano, D., Story, M.D., Beadle, B.M., El-Naggar, A.K., Kies, M.S., William, W.N. and Caulin, C. (2015). Evolutionary Action Score of TP53 Identifies High-Risk Mutations Associated with Decreased Survival and Increased Distant Metastases in Head and Neck Cancer. *Cancer Research*, 75(7), pp.1527–1536.

- Ngoi, N.Y.L., Leo, E., O'Connor, M.J. and Yap, T.A. (2021). Development of Next-Generation Poly(ADP-Ribose) Polymerase 1–Selective Inhibitors. *The Cancer Journal*, 27(6), pp.521–528.
- Nijman, S.M.B. (2010). Synthetic lethality: General principles, utility and detection using genetic screens in human cells. *FEBS Letters*, 585(1), pp.1–6.
- Nikitaki, Z., Pariset, E., Sudar, D., Costes, S.V. and Georgakilas, A.G. (2020). In Situ Detection of Complex DNA Damage Using Microscopy: A Rough Road Ahead. *Cancers*, 12(11), p.3288.
- Nitsch, A., Strakeljahn, S., Jacoby, J.M., Sieb, K.F., Mustea, A., Sander Bekeschus, Axel Ekkernkamp, Stope, M.B. and Lyubomir Haralambiev (2022). New Approach against Chondrosoma Cells—Cold Plasma Treatment Inhibits Cell Motility and Metabolism, and Leads to Apoptosis. *Biomedicines*, 10(3), pp.688–688.
- Noël, G., Godon, C., Fernet, M., Giocanti, N., Mégnin-Chanet, F. and Favaudon, V. (2006). Radiosensitization by the poly(ADP-ribose) polymerase inhibitor 4-amino-1,8-naphthalimide is specific of the S phase of the cell cycle and involves arrest of DNA synthesis. *Molecular Cancer Therapeutics*, 5(3), pp.564–574.
- Norris, R.E., Adamson, P.C., Nguyen, V.T. and Fox, E. (2013). Preclinical evaluation of the PARP inhibitor, olaparib, in combination with cytotoxic chemotherapy in pediatric solid tumors. *Pediatric Blood & Cancer*, 61(1), pp.145–150.
- O'Neil, N.J., Bailey, M.L. and Hieter, P. (2017). Synthetic lethality and cancer. *Nature Reviews Genetics*, 18(10), pp.613–623.
- Osman, A.A., Neskey, D.M., Katsonis, P., Patel, A.A., Ward, A.M., Hsu, T.-K., Hicks, S.C., McDonald, T.O., Ow, T.J., Alves, M.O., Pickering, C.R., Skinner, H.D., Zhao, M., Sturgis, E.M., Kies, M.S., El-Naggar, A., Perrone, F., Licitra, L., Bossi, P. and Kimmel, M. (2015). Evolutionary Action Score of *TP53* Coding Variants Is Predictive of Platinum Response in Head and Neck Cancer Patients. *Cancer Research*, 75(7), pp.1205–1215.
- Paal, J.V. der, Neyts, E.C., Verlackt, C.C.W. and Bogaerts, A. (2015). Effect of lipid peroxidation on membrane permeability of cancer and normal cells subjected to oxidative stress. *Chemical Science*, 7(1), pp.489–498.
- Padhi, S.S., Roy, S., Kar, M., Saha, A., Roy, S., Adhya, A., Baisakh, M. and Banerjee, B. (2017). Role of CDKN2A/p16 expression in the prognostication of oral squamous cell carcinoma. *Oral Oncology*, 73, pp.27–35.
- Parker, A.J.R., Marshall, E.J. and Ball, D.M. (2008). Diagnosis and management of alcohol use disorders. *BMJ*, 336(7642), pp.496–501.
- Partanen, J.I., Nieminen, A.I. and Klefstrom, J. (2009). 3D view to tumor suppression: lkb1, polarity and the arrest of oncogenic c-myc. *Cell Cycle*, 8(5), pp.716–724.
- Partecke, L.I., Evert, K., Haugk, J., Doering, F., Normann, L., Diedrich, S., Weiss, F.-U., Evert, M., Huebner, N.O., Guenther, C., Heidecke, C.D., Kramer, A., Bussiahn, R., Weltmann, K.-D., Pati, O., Bender, C. and von Bernstorff, W. (2012). Tissue

Tolerable Plasma (TTP) induces apoptosis in pancreatic cancer cells in vitro and in vivo. *BMC Cancer*, 12(1).

- Pastore, M.N., Kalia, Y.N., Horstmann, M. and Roberts, M.S. (2015). Transdermal patches: history, development and pharmacology. *British Journal of Pharmacology*, 172(9), pp.2179–2209.
- Patel, A.G., Sarkaria, J.N. and Kaufmann, S.H. (2011). Nonhomologous end joining drives poly(ADP-ribose) polymerase (PARP) inhibitor lethality in homologous recombination-deficient cells. *Proceedings of the National Academy of Sciences*, [online] 108(8), pp.3406–3411.
- Perfettini, J.-L., Castedo, M., Nardacci, R., Ciccocanti, F., Boya, P., Roumier, T., Larochette, N., Piacentini, M. and Kroemer, G. (2005). Essential role of p53 phosphorylation by p38 MAPK in apoptosis induction by the HIV-1 envelope. *Journal of Experimental Medicine*, 201(2), pp.279–289.
- Petrova, Y.I., Schecterson, L. and Gumbiner, B.M. (2016). Roles for E-cadherin cell surface regulation in cancer. *Molecular Biology of the Cell*, 27(21), pp.3233–3244.
- Pilié, P.G., Tang, C., Mills, G.B. and Yap, T.A. (2018). State-of-the-art strategies for targeting the DNA damage response in cancer. *Nature Reviews Clinical Oncology*, 16(2), pp.81–104.
- Poeta, M.L., Manola, J., Goldwasser, M.A., Forastiere, A., Benoit, N., Califano, J.A., Ridge, J.A., Goodwin, J., Kenady, D., Saunders, J., Westra, W., Sidransky, D. and Koch, W.M. (2007). TP53 Mutations and Survival in Squamous-Cell Carcinoma of the Head and Neck. *New England Journal of Medicine*, 357(25), pp.2552–2561. doi:<https://doi.org/10.1056/nejmoa073770>.
- Posner, M.R., Hershock, D.M., Blajman, C.R., Mickiewicz, E., Winkquist, E., Gorbounova, V., Tjulandin, S., Shin, D.M., Cullen, K., Ervin, T.J., Murphy, B.A., Racz, L.E., Cohen, R.B., Spaulding, M., Tishler, R.B., Roth, B., Viroglio, R. del C., Venkatesan, V., Romanov, I. and Agarwala, S. (2007). Cisplatin and Fluorouracil Alone or with Docetaxel in Head and Neck Cancer. *New England Journal of Medicine*, 357(17), pp.1705–1715.
- Potash, A.E., Karnell, L.H., Christensen, A.J., Vander Weg, M.W. and Funk, G.F. (2009). Continued alcohol use in patients with head and neck cancer. *Head & Neck*, p.NA-NA.
- Preta, G. (2020). New Insights Into Targeting Membrane Lipids for Cancer Therapy. *Frontiers in Cell and Developmental Biology*, 8.
- Pucci, C., Martinelli, C. and Ciofani, G. (2019). Innovative approaches for cancer treatment: current perspectives and new challenges. *Ecancermedicalscience*, 13(1).
- Pujade-Lauraine, E., Ledermann, J.A., Selle, F., Gebski, V., Penson, R.T., Oza, A.M., Korach, J., Huzarski, T., Poveda, A., Pignata, S., Friedlander, M., Colombo, N., Harter, P., Fujiwara, K., Ray-Coquard, I., Banerjee, S., Liu, J., Lowe, E.S., Bloomfield, R. and Pautier, P. (2017). Olaparib tablets as maintenance therapy in patients with platinum-sensitive, relapsed ovarian cancer and a BRCA1/2 mutation

(SOLO2/ENGOT-Ov21): a double-blind, randomised, placebo-controlled, phase 3 trial. *The Lancet Oncology*, 18(9), pp.1274–1284.

- Qian, J., Liao, G., Chen, M., Peng, R.-W., Yan, X., Du, J., Huang, R., Pan, M., Lin, Y., Gong, X., Xu, G., Zheng, B., Chen, C. and Yang, Z. (2024). Advancing cancer therapy: new frontiers in targeting DNA damage response. *Frontiers in Pharmacology*, [online] 15. doi:<https://doi.org/10.3389/fphar.2024.1474337>.
- Ramírez-Gamboa, D., Ana Laura Díaz-Zamorano, Edgar Ricardo Meléndez-Sánchez, Reyes-Pardo, H., Karen Rocio Villaseñor-Zepeda, López-Arellanes, M.E., Juan Eduardo Sosa-Hernández, Coronado-Apodaca, K.G., Ana Maria Gámez-Méndez, Samson Afewerki, Hafiz M.N. Iqbal, Parra-Saldívar, R. and Martínez-Ruiz, M. (2022). Photolyase Production and Current Applications: A Review. *Molecules*, 27(18), pp.5998–5998.
- Raúl González-García, Naval-Gías, L., F.J. Rodríguez-Campo, Jesús Sastre-Pérez, M.F. Muñoz-Guerra and J.L. Gil-Díez Usandizaga (2008). Contralateral Lymph Neck Node Metastasis of Squamous Cell Carcinoma of the Oral Cavity: A Retrospective Analytic Study in 315 Patients. *Journal of Oral and Maxillofacial Surgery*, 66(7), pp.1390–1398.
- Redza-Dutordoir, M. and Averill-Bates, D.A. (2016). Activation of apoptosis signalling pathways by reactive oxygen species. *Biochimica et Biophysica Acta (BBA) - Molecular Cell Research*, [online] 1863(12), pp.2977–2992.
- Roden, R.B.S. and Stern, P.L. (2018). Opportunities and challenges for human papillomavirus vaccination in cancer. *Nature Reviews Cancer*, 18(4), pp.240–254.
- Rudolph, J., Roberts, G. and Luger, K. (2021). Histone Parylation factor 1 contributes to the inhibition of PARP1 by cancer drugs. *Nature Communications*, 12(1).
- Sablina, A.A., Budanov, A.V., Ilyinskaya, G.V., Agapova, L.S., Kravchenko, J.E. and Chumakov, P.M. (2005). The antioxidant function of the p53 tumor suppressor. *Nature Medicine*, 11(12), pp.1306–1313.
- Sabrin, S., Hong, S.-H., Karmokar, D.K., Habibullah, H., Fitridge, R., Short, R.D. and Szili, E.J. (2024). Healing wounds with plasma-activated hydrogel therapy. *Trends in Biotechnology*.
- Salaspuro, M. (2020). Local Acetaldehyde: Its Key Role in Alcohol-Related Oropharyngeal Cancer. *Visceral Medicine*, 36(3), pp.167–174.
- Sale, J.E. (2013). Translesion DNA Synthesis and Mutagenesis in Eukaryotes. *Cold Spring Harbor Perspectives in Biology*, 5(3), pp.a012708–a012708.
- Saleh-Gohari, N., Bryant, H.E., Schultz, N., Parker, K.M., Cassel, T.N. and Helleday, T. (2005). Spontaneous Homologous Recombination Is Induced by Collapsed Replication Forks That Are Caused by Endogenous DNA Single-Strand Breaks. *Molecular and Cellular Biology*, 25(16), pp.7158–7169.
- Samra, B., Tam, E., Baseri, B. and Shapira, I. (2018). Checkpoint inhibitors in head and neck cancer: current knowledge and perspectives. *Journal of Investigative Medicine*, 66(7), pp.1023–1030.

- Sandulache, V.C., Michikawa, C., Kataria, P., Gleber-Netto, F.O., Bell, D., Trivedi, S., Rao, X., Wang, J., Zhao, M., Jasser, S., Myers, J.N. and Pickering, C.R. (2018). High-Risk TP53 Mutations Are Associated with Extranodal Extension in Oral Cavity Squamous Cell Carcinoma. *Clinical Cancer Research: An Official Journal of the American Association for Cancer Research*, 24(7), pp.1727–1733.
- Sasahira, T. and Kirita, T. (2018). Hallmarks of Cancer-Related Newly Prognostic Factors of Oral Squamous Cell Carcinoma. *International Journal of Molecular Sciences*, 19(8), p.2413. doi:<https://doi.org/10.3390/ijms19082413>.
- Semmler, M.L., Bekeschus, S., Schäfer, M., Bernhardt, T., Fischer, T., Witzke, K., Seebauer, C., Rebl, H., Grambow, E., Vollmar, B., Nebe, J.B., Metelmann, H.-R., Woedtke, T. von, Emmert, S. and Boeckmann, L. (2020). Molecular Mechanisms of the Efficacy of Cold Atmospheric Pressure Plasma (CAP) in Cancer Treatment. *Cancers*, 12(2), p.269.
- Setton, J., Zinda, M., Riaz, N., Durocher, D., Zimmermann, M., Koehler, M., Reis-Filho, J.S. and Powell, S.N. (2021). Synthetic Lethality in Cancer Therapeutics: The Next Generation. *Cancer Discovery*, 11(7), pp.1626–1635.
- Shaw, P., Kumar, N., Privat-Maldonado, A., Smits, E. and Bogaerts, A. (2021). Cold Atmospheric Plasma Increases Temozolomide Sensitivity of Three-Dimensional Glioblastoma Spheroids via Oxidative Stress-Mediated DNA Damage. *Cancers*, 13(8), p.1780.
- Shaw, R. and Beasley, N. (2016). Aetiology and risk factors for head and neck cancer: United Kingdom National Multidisciplinary Guidelines. *The Journal of Laryngology & Otology*, 130(S2), pp.S9–S12.
- Shaw, R.J. (2009). Tumor Suppression by LKB1: SIK-ness Prevents Metastasis. *Science Signaling*, 2(86).
- Silva, S.D., Alaoui-Jamali, M.A., Hier, M., Soares, F.A., Graner, E. and Kowalski, L.P. (2014). Cooverexpression of ERBB1 and ERBB4 receptors predicts poor clinical outcome in pN+ oral squamous cell carcinoma with extranodal spread. *Clinical & Experimental Metastasis*, 31(3), pp.307–316.
- Snezhkina, A.V., Kudryavtseva, A.V., Kardymon, O.L., Savvateeva, M.V., Melnikova, N.V., Krasnov, G.S. and Dmitriev, A.A. (2019). ROS Generation and Antioxidant Defense Systems in Normal and Malignant Cells. *Oxidative Medicine and Cellular Longevity*, 2019, pp.1–17.
- Song, G., Liu, J., Tang, X., Zhong, J., Zeng, Y., Zhang, X., Zhou, J., Zhou, J., Cao, L., Zhang, Q. and Li, Y. (2024). Cell cycle checkpoint revolution: targeted therapies in the fight against malignant tumors. *Frontiers in Pharmacology*, 15. doi:<https://doi.org/10.3389/fphar.2024.1459057>.
- Sosa, V., Moliné, T., Somoza, R., Paciucci, R., Kondoh, H. and LLeonart, M.E. (2013). Oxidative stress and cancer: An overview. *Ageing Research Reviews*, [online] 12(1), pp.376–390. doi:<https://doi.org/10.1016/j.arr.2012.10.004>.
- Sreedevi, P.R. and Suresh, K. (2023). Cold atmospheric plasma mediated cell membrane permeation and gene delivery-empirical interventions and

- pertinence. *Advances in Colloid and Interface Science*, [online] 320, p.102989. doi:<https://doi.org/10.1016/j.cis.2023.102989>.
- Stenvall, A., Larsson, E., Holmqvist, B., Strand, S.-E. and Jönsson, B.-A. (2020). Quantitative γ -H2AX immunofluorescence method for DNA double-strand break analysis in testis and liver after intravenous administration of $^{111}\text{InCl}_3$. *EJNMMI Research*, 10(1). doi:<https://doi.org/10.1186/s13550-020-0604-8>.
 - Stransky, N., Egloff, A.M., Tward, A.D., Kostic, A.D., Cibulskis, K., Sivachenko, A., Kryukov, G.V., Lawrence, M.S., Sougnez, C., McKenna, A., Shefler, E., Ramos, A.H., Stojanov, P., Carter, S.L., Voet, D., Cortes, M.L., Auclair, D., Berger, M.F., Saksena, G. and Guiducci, C. (2011). The Mutational Landscape of Head and Neck Squamous Cell Carcinoma. *Science*, [online] 333(6046), pp.1157–1160. doi:<https://doi.org/10.1126/science.1208130>.
 - Sung, H., Ferlay, J., Siegel, R.L., Laversanne, M., Soerjomataram, I., Jemal, A. and Bray, F. (2021). Global Cancer Statistics 2020: GLOBOCAN Estimates of Incidence and Mortality Worldwide for 36 Cancers in 185 Countries. *CA: a Cancer Journal for Clinicians*, 71(3), pp.209–249. doi:<https://doi.org/10.3322/caac.21660>.
 - Suraj Kumar Singh, Abbas, S., Ajit Kumar Saxena, Tiwari, S., Lokendra Kumar Sharma and Tiwari, M. (2020). Critical role of three-dimensional tumorsphere size on experimental outcome. 69(5), pp.333–338. doi:<https://doi.org/10.2144/btn-2020-0081>.
 - Sykora, P., Witt, K.L., Revanna, P., Smith-Roe, S.L., Dismukes, J., Lloyd, D.G., Engelward, B.P. and Sobol, R.W. (2018). Next generation high throughput DNA damage detection platform for genotoxic compound screening. *Scientific Reports*, [online] 8(1), p.2771. doi:<https://doi.org/10.1038/s41598-018-20995-w>.
 - Szlasa, W., Zendran, I., Zalesińska, A., Tarek, M. and Kulbacka, J. (2020). Lipid composition of the cancer cell membrane. *Journal of Bioenergetics and Biomembranes*, 52(5), pp.321–342. doi:<https://doi.org/10.1007/s10863-020-09846-4>.
 - Tanaka, N., T Odajima, Ogi, K., Ikeda, T. and M Satoh (2003). Expression of E-cadherin, α -catenin, and β -catenin in the process of lymph node metastasis in oral squamous cell carcinoma. *British Journal of Cancer*, 89(3), pp.557–563. doi:<https://doi.org/10.1038/sj.bjc.6601124>.
 - Tanaka, T.I. and Alawi, F. (2018). Human Papillomavirus and Oropharyngeal Cancer. *Dental Clinics of North America*, [online] 62(1), pp.111–120. doi:<https://doi.org/10.1016/j.cden.2017.08.008>.
 - Tang, M.W., Oakley, R., Dale, C., Purushotham, A., Møller, H. and Gallagher, J.E. (2014). A surgeon led smoking cessation intervention in a head and neck cancer centre. *BMC Health Services Research*, 14(1). doi:<https://doi.org/10.1186/s12913-014-0636-8>.
 - Tchounwou, P.B., Dasari, S., Noubissi, F.K., Ray, P. and Kumar, S. (2021). Advances in Our Understanding of the Molecular Mechanisms of Action of Cisplatin in

Cancer Therapy. *Journal of Experimental Pharmacology*, Volume 13, pp.303–328. doi:<https://doi.org/10.2147/jep.s267383>.

- Tero, R., Suda, Y., Kato, R., Tanoue, H. and Hirofumi Takikawa (2014). Plasma irradiation of artificial cell membrane system at solid–liquid interface. *Applied Physics Express*, 7(7), pp.077001–077001. doi:<https://doi.org/10.7567/apex.7.077001>.
- Tezal, M., Sullivan, M.A., Hyland, A., Marshall, J.R., Stoler, D., Reid, M.E., Loree, T.R., Rigual, N.R., Merzianu, M., Hauck, L., Lillis, C., Wactawski-Wende, J. and Scannapieco, F.A. (2009). Chronic Periodontitis and the Incidence of Head and Neck Squamous Cell Carcinoma. *Cancer Epidemiology Biomarkers & Prevention*, 18(9), pp.2406–2412. doi:<https://doi.org/10.1158/1055-9965.epi-09-0334>.
- Thannickal, V.J. and Fanburg, B.L. (2000). Reactive oxygen species in cell signaling. *American Journal of Physiology-Lung Cellular and Molecular Physiology*, 279(6), pp.L1005–L1028. doi:<https://doi.org/10.1152/ajplung.2000.279.6.l1005>.
- Torgovnick, A. and Schumacher, B. (2015). DNA repair mechanisms in cancer development and therapy. *Frontiers in Genetics*, [online] 6(157). doi:<https://doi.org/10.3389/fgene.2015.00157>.
- Torre, L.A., Bray, F., Siegel, R.L., Ferlay, J., Lortet-Tieulent, J. and Jemal, A. (2015). Global cancer statistics, 2012. *CA: A Cancer Journal for Clinicians*, [online] 65(2), pp.87–108. doi:<https://doi.org/10.3322/caac.21262>.
- Ueda, N., Kaushal, G.P. and Shah, S.V. (2000). Apoptotic mechanisms in acute renal failure. *The American Journal of Medicine*, [online] 108(5), pp.403–415. doi:[https://doi.org/10.1016/S0002-9343\(00\)00311-9](https://doi.org/10.1016/S0002-9343(00)00311-9).
- Urashima, M., Hama, T., Suda, T., Suzuki, Y., Ikegami, M., Sakanashi, C., Akutsu, T., Amagaya, S., Horiuchi, K., Imai, Y., Mezawa, H., Noya, M., Nakashima, A., Mafune, A., Kato, T. and Kojima, H. (2013). Distinct Effects of Alcohol Consumption and Smoking on Genetic Alterations in Head and Neck Carcinoma. *PLoS ONE*, 8(11), p.e80828. doi:<https://doi.org/10.1371/journal.pone.0080828>.
- Valentin-Vega, Y.A., Barboza, J.A., Chau, G.P., El-Naggar, A.K. and Lozano, G. (2007). High levels of the p53 inhibitor MDM4 in head and neck squamous carcinomas. *Human Pathology*, [online] 38(10), pp.1553–1562. doi:<https://doi.org/10.1016/j.humpath.2007.03.005>.
- Van der Paal, J., Verheyen, C., Neyts, E.C. and Bogaerts, A. (2017). Hampering Effect of Cholesterol on the Permeation of Reactive Oxygen Species through Phospholipids Bilayer: Possible Explanation for Plasma Cancer Selectivity. *Scientific Reports*, 7(1). doi:<https://doi.org/10.1038/srep39526>.
- Vanhaesebroeck, B., Stephens, L. and Hawkins, P. (2012). PI3K signalling: the path to discovery and understanding. *Nature Reviews Molecular Cell Biology*, [online] 13(3), pp.195–203. doi:<https://doi.org/10.1038/nrm3290>.
- Wang, G.-F., Dong, Q., Bai, Y., Yuan, J., Xu, Q., Cao, C. and Liu, X. (2017). Oxidative stress induces mitotic arrest by inhibiting Aurora A-involved mitotic spindle

formation. *Free Radical Biology and Medicine*, 103, pp.177–187.

doi:<https://doi.org/10.1016/j.freeradbiomed.2016.12.031>.

- Wang, Y., Sreekanth Chanickal Narayanapillai, Hu, Q., Fujioka, N. and Xing, C. (2019). Detection and quantification of 4-hydroxy-1-(3-pyridyl)-1-butanone (HPB) from smoker albumin and its potential as a surrogate biomarker of tobacco-specific nitrosamines exposure and bioactivation. *Toxicology Letters*, [online] 311, pp.11–16. doi:<https://doi.org/10.1016/j.toxlet.2019.04.020>.
- Warnakulasuriya, S. and Chen, T.H.H. (2022). Areca Nut and Oral Cancer: Evidence from Studies Conducted in Humans. *Journal of Dental Research*, 101(10), pp.1139–1146. doi:<https://doi.org/10.1177/00220345221092751>.
- Watanya Trakarnphornsombat and Kimura, H. (2023). Live-cell tracking of γ -H2AX kinetics reveals the distinct modes of ATM and DNA-PK in the immediate response to DNA damage. *Journal of cell science*, 136(8). doi:<https://doi.org/10.1242/jcs.260698>.
- Westra, W.H. (2012). The Morphologic Profile of HPV-Related Head and Neck Squamous Carcinoma: Implications for Diagnosis, Prognosis, and Clinical Management. *Head and Neck Pathology*, 6(S1), pp.48–54. doi:<https://doi.org/10.1007/s12105-012-0371-6>.
- Wheate, N.J., Walker, S., Craig, G.E. and Oun, R. (2010). The status of platinum anticancer drugs in the clinic and in clinical trials. *Dalton Transactions*, 39(35), p.8113. doi:<https://doi.org/10.1039/c0dt00292e>.
- Wilson, Z., Odedra, R., Wallez, Y., Wijnhoven, P.W.G., Hughes, A.M., Gerrard, J., Jones, G.N., Bargh-Dawson, H., Brown, E., Young, L.A., O'Connor, M.J. and Lau, A. (2022). ATR Inhibitor AZD6738 (Ceralasertib) Exerts Antitumor Activity as a Monotherapy and in Combination with Chemotherapy and the PARP Inhibitor Olaparib. *Cancer Research*, [online] 82(6), pp.1140–1152. doi:<https://doi.org/10.1158/0008-5472.CAN-21-2997>.
- Witsch, E., Sela, M. and Yarden, Y. (2010). Roles for growth factors in cancer progression. *Physiology (Bethesda, Md.)*, 25(2), pp.85–101. doi:<https://doi.org/10.1152/physiol.00045.2009>.
- Woedtke, T.V., Schmidt, A., Bekeschus, S., Wende, K. and Weltmann, K.-D. (2019). Plasma Medicine: A Field of Applied Redox Biology. *In Vivo*, [online] 33(4), pp.1011–1026. doi:<https://doi.org/10.21873/invivo.11570>.
- Wright, G., Golubeva, V., Remsing Rix, L.L., Berndt, N., Luo, Y., Ward, G.A., Gray, J.E., Schonbrunn, E., Lawrence, H.R., Monteiro, A.N.A. and Rix, U. (2017). Dual Targeting of WEE1 and PLK1 by AZD1775 Elicits Single Agent Cellular Anticancer Activity. *ACS Chemical Biology*, 12(7), pp.1883–1892. doi:<https://doi.org/10.1021/acscchembio.7b00147>.
- Ye, H., Zhang, X., Chen, Y., Liu, Q. and Wei, J. (2016). Ranking novel cancer driving synthetic lethal gene pairs using TCGA data. *Oncotarget*, 7(34), pp.55352–55367. doi:<https://doi.org/10.18632/oncotarget.10536>.

- Yeh, S.-A. (2010). Radiotherapy for Head and Neck Cancer. *Seminars in Plastic Surgery*, 24(02), pp.127–136. doi:<https://doi.org/10.1055/s-0030-1255330>.
- Yusupov, M., Van der Paal, J., Neyts, E.C. and Bogaerts, A. (2017a). Synergistic effect of electric field and lipid oxidation on the permeability of cell membranes. *Biochimica et Biophysica Acta (BBA) - General Subjects*, [online] 1861(4), pp.839–847. doi:<https://doi.org/10.1016/j.bbagen.2017.01.030>.
- Yusupov, M., Wende, K., Kupsch, S., Neyts, E.C., Reuter, S. and Bogaerts, A. (2017b). Effect of head group and lipid tail oxidation in the cell membrane revealed through integrated simulations and experiments. *Scientific Reports*, 7(1). doi:<https://doi.org/10.1038/s41598-017-06412-8>.
- Zandarashvili, L., Langelier, M.-F., Velagapudi, U.K., Hancock, M.A., Steffen, J.D., Billur, R., Hannan, Z.M., Wicks, A.J., Krastev, D.B., Pettitt, S.J., Lord, C.J., Talele, T.T., Pascal, J.M. and Black, B.E. (2020). Structural basis for allosteric PARP-1 retention on DNA breaks. *Science (New York, N.Y.)*, [online] 368(6486), p.eaax6367. doi:<https://doi.org/10.1126/science.aax6367>.
- Zaqout, S., Becker, L.-L. and Kaindl, A.M. (2020). Immunofluorescence Staining of Paraffin Sections Step by Step. *Frontiers in Neuroanatomy*, 14. doi:<https://doi.org/10.3389/fnana.2020.582218>.
- Zevallos, J.P., Mallen, M.J., Lam, C.Y., Karam-Hage, M., Blalock, J., Wetter, D.W., Garden, A.S., Sturgis, E.M. and Cinciripini, P.M. (2009). Complications of radiotherapy in laryngopharyngeal cancer. *Cancer*, 115(19), pp.4636–4644. doi:<https://doi.org/10.1002/cncr.24499>.
- Zhang Mingbin, Jiang, L., Wang, L., Tian, Z., Zhang, P., Xu, Q., Zhang, C., Fang, W. and Chen, W. (2013). Prognostic significance of p21, p27 and survivin protein expression in patients with oral squamous cell carcinoma. *Oncology Letters*, 6(2), pp.381–386. doi:<https://doi.org/10.3892/ol.2013.1381>.
- Zhang, C., Peng, K., Liu, Q., Huang, Q. and Liu, T. (2024). Adavosertib and beyond: Biomarkers, drug combination and toxicity of WEE1 inhibitors. *Critical Reviews in Oncology/Hematology*, 193, pp.104233–104233. doi:<https://doi.org/10.1016/j.critrevonc.2023.104233>.
- Zhang, J., Wang, X., Vikash, V., Ye, Q., Wu, D., Liu, Y. and Dong, W. (2016). ROS and ROS-Mediated Cellular Signaling. *Oxidative Medicine and Cellular Longevity*, 2016, pp.1–18.
- Zhang, X.-Y. and Zhang, P.-Y. (2016). Combinations in multimodality treatments and clinical outcomes during cancer. *Oncology Letters*, 12(6), pp.4301–4304.
- Zhao, J., Chi, J., Gao, M., Zhi, J., Li, Y. and Zheng, X. (2017). Loss of PTEN Expression Is Associated With High MicroRNA 24 Level and Poor Prognosis in Patients With Tongue Squamous Cell Carcinoma. *Journal of Oral and Maxillofacial Surgery: Official Journal of the American Association of Oral and Maxillofacial Surgeons*, 75(7), pp.1449.e1–1449.e8.
- Zheng, F., Zhang, Y., Chen, S., Weng, X., Rao, Y. and Fang, H. (2020). Mechanism and current progress of Poly ADP-ribose polymerase (PARP) inhibitors in the

treatment of ovarian cancer. *Biomedicine & Pharmacotherapy*, 123, p.109661.
doi:<https://doi.org/10.1016/j.biopha.2019.109661>.

- Zhou, J.Z., Jou, J. and Cohen, E. (2021). Vaccine Strategies for Human Papillomavirus-Associated Head and Neck Cancers. *Cancers*, 14(1), p.33.
- Zong, C., Zhu, T., He, J., Huang, R., Jia, R. and Shen, J. (2022). PARP mediated DNA damage response, genomic stability and immune responses. *International Journal of Cancer*, 150(11), pp.1745–1759.